The Effects of HIV-1 Infection on Subcortical Brain Structures in Children Receiving ART: A Structural MRI Study

By

Steven Ronald Randall

RNDSTE002

SUBMITTED TO THE UNIVERSITY OF CAPE TOWN

In fulfilment of the requirements for the degree

M.Sc (Med) - ANATOMY

Faculty of Health Sciences

UNIVERSITY OF CAPE TOWN

Date of Submission

Supervisors: Prof .Ernesta Meintjes[1, 2], Dr Christopher Warton[2]

[1]MRC/UCT Medical Imaging Research Unit

[2]Department of Human Biology, University of Cape Town

DECLARATION

I, *Steven Ronald Randall*, hereby declare that the work on which this dissertation/thesis is based is my original work (except where acknowledgements indicate otherwise) and that neither the whole work nor any part of it has been, is being, or is to be submitted for another degree in this or any other university.

I empower the university to reproduce for the purpose of research either the whole or any portion of the contents in any manner whatsoever.

Signature:

Signature removed
Steven Randall

Date: 19/04/2015

ABSTRACT

INTRODUCTION This project investigated volumetric differences in certain subcortical structures as measured on high-resolution structural Magnetic Resonance Imaging (MRI) scans traced manually. The sample comprised 79 5-year old children, 52 with HIV and 27 uninfected controls. Infected children were all stable on antiretroviral therapy (ART) and were from the Children with HIV early antiretroviral (CHER) cohort who have been followed since birth. The study aimed to investigate the long-term effects of HIV and ART on the developing brain. While high-resolution structural data has been analysed using automated FreeSurfer to determine volume and cortical thickness, manual tracing remains the gold standard. Thus, manual tracing was used to validate automated measures and investigate subtle group differences in selected regions of interest.

METHODS Extensive clinical data were available for all participants in the study. MR images were AC-PC transformed and converted to analyse format. Structures were traced using MultiTracer software. Structures selected included the caudate, nucleus accumbens (NA), putamen (Pu), globus pallidus (GP) and corpus callosum (CC). Four of these structures occur bilaterally. Tracing was performed in 79 subjects. Three subjects were excluded due to poor quality images or pathology; 5 HIV-1 infected children were excluded as they were not randomized between treatment groups. Certain subjects were retraced for inter and intrarater reliabilities. The effect and association of ethnicity, age, birthweight and sex as possible confounders were investigated. As the groups were not well matched for ethnicity, all Cape Coloured children were excluded from further analyses. Analysis of variance was used to test the effect on structure size between HIV-1 infected children and controls, as well as between 3 treatment arms (ART deferred until clinical criteria were met, early ART for 40 weeks, early ART for 96 weeks) and uninfected controls. Analysis of covariance was used to control for the possible confounding effects of sex and age. Each structure was tested for possible association with clinical variables (CD4, CD8, CD4/CD8 ratio and CD4%) both at enrolment and time of scanning. Linear regressions were modelled using clinical variables that showed significant correlation with structure size whilst controlling for covariates. Congruence between automated FreeSurfer and manual segmentation were evaluated via Bland-Altman, Pearson *r* and Cronbach's alpha.

RESULTS Uninfected controls were marginally older (5.6±0.5Yrs) than HIV-1 infected children (5.4±0.4Yrs) ($F(1,61)=3.05, p=0.04$). Bilateral NA and putamen were larger in HIV-1 infected children, whilst the CC was smaller. The largest differences were between children in the deferred treatment arm and uninfected controls. There were no differences between deferred and early treatment arms. Regression showed that age at scan was a greater predictor of size than other clinical measures, next to age at ART initiation and CD4/CD8 ratio at time of scan. While automated volumes correlated significantly with manual volumes in all grey matter regions, separate analyses within groups revealed significant differences between manual and automated segmentation in all structures except the left GP amongst infected children.

DISCUSSION Affected grey matter structures were larger in infected children, but decreased with age. This concurs with global atrophy observed in adults. This also suggests that damage occurs before 5 years of age in HIV-1 infected children, causing the volume to initially be larger than in controls. The difference in effect size between early and deferred treatment arms suggests that early ART mitigates HIV-1's effects on the affected structures. Since volumes in the left NA and bilateral putamen differed between the deferred treatment arm and controls, perturbations to motor learning, planning sequences and performance is expected in these children. This is substantiated by a previous study in the same cohort that reported lower general Griffiths and locomotor scores in the ART deferred group compared to children receiving early ART (Laughton et al. 2012). Although there were no differences between manual and automated volumes bilaterally in the caudate and GP, or CC, amongst uninfected children, automated and manual volumes differed in all regions except the left GP in infected children, indicating that subtle pathology may introduce bias between manual and automated measures in infected children.

CONCLUSION Early ART mitigates the effect of HIV-1 infection in select structures, however atrophy still occurs with time. FreeSurfer may introduce bias into subcortical structure volumes in Xhosa children at, or around, 5 years of age. Caution should be employed when using automated segmentation to assess volume differences as a result of pathology in children.

ACKNOWLEDGEMENTS

I would like to acknowledge the parents and children who participated in the study.

I offer my sincerest gratitude to my supervisor and PI, Prof Ernesta Meintjes, for her patience and guidance during these past few years. I am forever grateful for the skills that I have learned under her guidance. I cannot overstate my gratitude to my co-supervisor, Dr Christopher Warton, with whom I have worked for almost four years, during which I gained an immeasurable amount of knowledge. His wisdom and support will always be appreciated. I feel privileged to have worked with them and been part of this study.

Dr Barbara Laughton and Prof Andre van der Kouwe principal investigators of the neuroimaging study. Prof Mark Cotton and the CIPRA study for access to the clinical and demographic data from infancy and to the cohort. I further extend our gratitude to Kennedy Otwombe from the Perinatal HIV Research Unit and CIPRA-SA and Christie Heiberg formerly of the Desmond Tutu HIV Foundation for assisting with clinical data requests; the CUBIC radiographers Marie-Louise de Villiers and Nailah Maroof; research staff Thandiwe Hamana, Rosy Khethelo and Anita Janse van Rensburg of Stellenbosch University for assisting with data collection, the study paediatrician Dr Els Dobbels, and Shabir A Madhi for facilitating the study.

A thank you to all students and postdoctoral fellows in the MRI laboratory who have been involved in data acquisition, data management and image processing. A special thank you to Kenneth Mbugua who ran the FreeSurfer analyses. Dr Martha Holmes who is the postdoctoral fellow working on the CHER Neuorimaging study. I would also like to thank my colleagues, Dr Coenraad Hattingh for his neuroanatomical consultation, Dr Natalie Strickland for her immunological expertise, Dr Jacqueline Dimatelis for statistical and physiological guidance and Stevie Biffen, for her involvement in interrater reliabilities and support.

A further personal thank you to Greg and Theresa Randall for their steadfast support throughout. In memorial of Trooroy Carlos.

Support for this study was provided by NRF/DST South African Research Chairs Initiative; US National Institute of Allergy and Infectious Diseases (NIAID) through the CIPRA network, Grant U19 AI53217; NIH grants R01HD071664 and R21MH096559; NRF grant CPR20110614000019421, and the Medical Research Council (MRC). As well as my personal NRF Innovation Master's Scholarship. The content of this thesis does not reflect the views or policies of NIAID, nor does mention of trade names, commercial projects, or organizations imply endorsement by any Government.

Table of Contents

List of Figures

List of Tables

LIST OF ABBREVIATIONS

Abbreviation	-	Full Term

General

SA	-	South Africa
SSA	-	Sub-Saharan Africa

AIDS	-	Acquired Immunodeficiency Syndrome
HIV	-	Human Immunodeficiency Virus
ART	-	Antiretroviral Therapy
ART-40W	-	ART Initiated Immediately And Interrupted After 40 Weeks
ART-96W	-	ART Initiated Immediately And Interrupted After 96 Weeks
ART-Def	-	ART Deferred
ARV	-	Antiretroviral
HAART	-	Highly Active Antiretroviral Therapy
CHER	-	Children With HIV Early Antiretroviral Therapy
CIPRA	-	Comprehensive International Program For Research On AIDS In South Africa
CUBIC	-	Cape Universities Brain Imaging Centre
GMDS	-	Griffiths Mental Development Scales
HPE	-	HIV-Associated Progressive Encephalopathy Of Childhood
KID-CRU	-	Children's Infectious Diseases Clinical Research Unit
MeSH	-	Medical Subject Headings
MTCT	-	Mother-To-Child Transmission
PMTCT	-	Prevention Of Mother-To-Child Transmission

Immunological

APOBEC3	-	Apolipoprotein B Mrna-Eliciting Enzyme Catalytic Polypeptide-Like 3
ATP	-	Adenosine Triphosphate
B-Cell	-	Bone Marrow Cell
CAF	-	CD8 Antiviral Factors
CCL#	-	Chemokine Ligands Eg. CCL2, CCL3, CCL5
CCR#	-	C-C Chemokine Receptor Type # Eg. CCR3, CCR5
CD#	-	Cluster Of Differentiation (4) E.G. CD4, CD8 T-Cells
CD4%	-	CD4 Percentage
CXCR4	-	C-X-C Chemokine Receptor Type 4
DNA	-	Deoxyribonucleic Acid
gp	-	Glycoprotein
HLA	-	Human Leukocyte Antigens
LTR	-	Long Terminal Repeats
MHC	-	Major Histocompatibility Complex
M-tropic	-	Macrophage Tropic
PCR	-	Polymerase Chain Reaction
PVL	-	Plasma Viral Load
RNA	-	Ribonucleic Acid
mRNA	-	Messenger RNA
ssRNA	-	Single Stranded RNA
vRNA	-	Viral RNA
RT	-	Reverse Transcriptase
T-Cell	-	Thymus Cell
TRIM5α	-	Tripartite-Motif-Containing 5 alpha
VL	-	Viral Load

Imaging

3T	-	3 Tesla
AAM	-	Auto-Assisted Manual
aparc	-	Automatic Parcellation
aseg	-	Automatic Subcortical Segmentation
BOLD	-	Blood Oxygen Level Dependent
CT	-	Computerized Tomography
EPI	-	Echo-Planar Imaging
IBASPM	-	Individual Brain Atlases Using Statistical Parametric Mapping
MEMPRAGE	-	Multi Echo Magnetization Prepared Rapid Gradient Echo
MR	-	Magnetic Resonance
MRI	-	Magnetic Resonance Imaging
MRS	-	Magnetic Resonance Spectroscopy
fMRI	-	Functional Magnetic Resonance Imaging
PET	-	Positron Emission Tomography
PIU	-	Pixel Intensity Units

Neuroanatomical

AC-PC	-	Anterior and Posterior Commissure
BBB	-	Blood-Brain-Barrier
Caud	-	Caudate
CC	-	Corpus Callosum
CNS	-	Central Nervous System
CSF	-	Cerebrospinal Fluid
GM	-	Grey Matter
GP	-	Globus Pallidus
ICV	-	Intracranial Volume
L	-	Left
R	-	Right
NA	-	Nucleus Accumbens
Pu	-	Putamen
ROI	-	Region Of Interest
WM	-	White Matter

Statistical

ANCOVA	-	Analysis Of Covariance
ANOVA	-	Analysis Of Variance
FDR	-	False Discovery Rate
ICC	-	Intraclass Correlation
LSD	-	Least Significant Difference
n	-	Sample Size
p.a.	-	Per Annum
s.e.	-	Standard Error
SD	-	Standard Deviation
Wks	-	Weeks
Yrs	-	Years

CHAPTER 1 INTRODUCTION

1.1 Research Rationale and Motivation

Southern Africa is home to some of the most alarming statistics regarding HIV's effect on humanity. The UNAIDS census conducted in South Africa in 2011, indicated that approximately 5100 000 adults and 460 000 children are living with HIV/AIDS (WHO-UNAIDS 2013). The HIV/AIDS epidemic in 2003 accounted for around 5% of child mortalities within the Southern African region (Mahy 2003). Since the advent of highly active antiretroviral treatment (HAART), HIV is no longer necessarily a fatal disease but more a chronic condition in which there may be ongoing damage to the body and central nervous system (CNS), especially in the developing brain of the fetus, infant and young child (van Rie et al. 2007; WHO-UNAIDS 2010).

Tardieu and colleagues (2000) conducted a study on data collected in a French cohort of 426 perinatally infected children and 1516 adults (Tardieu et al. 2000). They found that the incidence of HIV associated encephalopathy was higher in children under the age of 5 years (9.9%) compared to adults (0.3%) in their first year post-infection (Tardieu et al. 2000). In the second year, the incidence decreased to 4.2% in children while adults dropped to 0%, after which both groups showed incidences of encephalopathy of less than 1% per year (Mitchell, W 2001; Tardieu et al. 2000).

Neurosis affects children differently and more dramatically than adults (Mitchell, W 2001). Neurological disease can occur before systemic immunodeficiency. It has been shown that CNS maturation is impaired and language functions are affected more in infected children than in adults (van Rie et al. 2007). Significant brain development in the first few years of life puts infected children at greater risk of neurological impairment as opposed to individuals infected later in life (Mitchell, W 2001; Tardieu et al. 2000). Furthermore, HAART or other factors may cause neurodevelopmental impairment despite virological suppression in the CNS (van Rie et al. 2007; Tardieu et al. 2005).

As CNS penetration by antiretroviral therapy (ART) is limited, the brain becomes a reservoir for the virus, and few drugs are available that impact these reservoirs (van Rie et al. 2007). It is necessary to investigate the impact of HIV-1 infection on the developing brain and evaluate the extent to which damage to the CNS is mitigated by HAART. Certain therapies have been flagged to have particular negative effects on brain development in children (Tardieu et al. 2005), it is thus also necessary to investigate whether the drugs used

in HAART may have any impact on brain development themselves in conjunction with HIV-1 infection.

Although automated image analysis tools such as FreeSurfer provide accurate cortical and subcortical segmentations, manual tracing still remains the gold standard and may have greater sensitivity to detect subtle morphometric differences. Studies that have investigated similar research questions have made use of automated and semi-automated segmentation techniques to evaluate structural volume differences in the brains of HIV-1 infected individuals (Dewey et al. 2010; Heaps et al. 2012). Automated measures are far less time consuming, less subjective, and more cost effective than manual tracing (Dewey et al. 2010). However, very little research has been done to investigate if the results from these automated techniques are reliable in measuring subcortical structural volumes in children, especially in children infected with HIV-1.

Since neuroimaging studies of children with HIV are rare, even in developed countries, and often span a wide age range, very little is known about the effects of antiretrovirals (ARV) and HIV on the developing brain (Hoare et al. 2013; Laughton et al. 2012; van Rie et al. 2007; Tamula et al. 2003). Hoare and colleagues (2013) compiled an extensive systematic review of relevant neuroimaging studies pertaining to the effects of vertically transmitted HIV on children and adolescents (Hoare et al. 2013). The review took the form of a database search and a critical analysis of the search results (the review was submitted for publication on 3 September 2013). The databases searched were Pubmed, Medline, and Scopus. The search criteria was a formation of keywords and included all possible combinations of words and phrases as both text and MeSH terms relating to HIV/AIDS, the brain and neuroimaging (Hoare et al. 2013). The two investigators assigned to the task systematically evaluated the titles, abstracts, and keywords associated with each individual article and assessed their relevance. Of 904 search results, 258 were found to be irrelevant to the scope of their review. Of the remaining 646 journal article results, 427 included only HIV or neuroimaging separately, and 219 included both HIV and neuroimaging together (Hoare et al. 2013). The inclusion criteria for further review and consideration were that the studies had to be original scientific outputs with a minimum of five subjects (0 to 18 years of age). The subjects had to be diagnosed with HIV and either naïve to, or on ART or HAART. They commented on the lack of literature pertaining to the subject, as well as the large assortment of imaging modalities employed to investigate the research topics, which made it impossible to compile a meta-analysis. Few studies were found to be statistically relevant, if statistical methods were used at all. There was a lack of descriptive variables and insufficient controls across

most studies. The literature was too sparse to assess the changes the brain undergoes with increasing age in the presence of HIV infection (Hoare et al. 2013).

At the time of writing, there have been no imaging studies that have comprehensively assessed using manual tracing structural brain changes in children vertically infected with HIV-1 and stable on ART (Hoare et al. 2013).

Lindsey and colleagues (Lindsey et al. 2007 pp e681) have identified the need for this type of research on a large cohort followed from birth: “Additional longitudinal research is needed to better understand the role of antiretroviral therapy as well as the impact of genetic and environmental factors on neurodevelopmental functioning in children affected by HIV.”

Similarly van Rie et al. (2007)highlighted the need for this type of research. As taken from Tamula et al. (2003): “It is therefore important to better understand the evolution of the child’s neurodevelopment following initiation of ART and to document the prevalence of and risk factors for discordance between control of HIV disease in the periphery versus the CNS.”

Laughton et al. (2013) stated that little is known about the complex nature of brain recovery following ART initiation and reaffirmed that longitudinal research is needed to assess the long-term effects of ART and timing of ART initiation on neurodevelopmental outcomes in perinatally HIV-infected adolescents by gender, particularly in resource-constrained settings.

1.2 Background

The Children with HIV early antiretroviral therapy (CHER) trial investigated new approaches and strategies for treating HIV-infected children (Cotton et al. 2013; Laughton et al. 2009, 2012; Violari et al. 2008). The CHER trial is supported under the umbrella of the Comprehensive International Program for Research on AIDS in South Africa (CIPRA-SA). The CHER trial compared outcomes and prognosis in infants with perinatally acquired HIV-1 infection, diagnosed between 6 and 12 weeks of age, who had been randomised into three treatment arms (Cotton et al. 2013; Violari et al. 2008). The study postulated that starting ART earlier (before 12 weeks of age), followed by interruption of therapy, would show a long-term benefit by preventing immunological and clinical progression of HIV-1 when compared with children in whom treatment was deferred until certain immunological criteria were met (Violari et al. 2008).

The CHER study was an open-label randomised controlled trial comprising 377 HIV-1 infected asymptomatic infants born to seropositive mothers (Cotton et al. 2013). Pregnant women were recruited from the public prevention of mother-to-child transmission (PMTCT) programmes in the Western Cape and Gauteng provinces. In the Western Cape province, Zidovudine (ZDV, AZT, Retrovir®) was administered to mothers from 34 weeks gestation and to neonates for 7 days. Additionally, a single dose Nevirapine (NVP, Viramune®) was given to mothers in labour and to infants shortly after birth. HIV infection was confirmed by a positive polymerase chain reaction (PCR) test for HIV-1 DNA and plasma viral load (PVL) > 1000 HIV-1 RNA copies/ml. The timing of administration of PMTCT treatment is vital as it reduces the risk of mother-to-child transmission and takes into consideration the known complications of zidovudine treatment at an early gestational age. Treatment of zidovudine at an early gestational age has been linked to increased risk of mitochondrial dysfunction and neurological disorders in neonates (Tardieu et al. 2005).

Infants between 6-12 weeks of age testing positive for HIV-1 infection with a percentage of CD4+ T-lymphocytes (CD4%) higher than 25%, were randomly allocated to one of three treatment arms (Cotton et al. 2013):

- ART-Def (ART deferred until CD4% < 25% in first year or CD4% < 20% thereafter, or if clinical disease progression criteria presented)
- ART-40W (ART initiated early – i.e., as close as possible to age 6 weeks – and interrupted after 40 weeks), and
- ART-96W (ART initiated early and interrupted after 96 weeks).

Re-initiation of treatment occurred if CD4% dropped below 25% or CD4+ T-lymphocyte count fell below 1000cells/mm^3. Secondary criteria for re-initiation of treatment were certain severe clinical events (refer to Cotton et al. 2013-appendix pp 131-133). The CHER study showed that early HIV diagnosis and early ART reduce early infant mortality by 76% and HIV progression by 75% (Violari et al. 2008). Early time-limited ART resulted in better clinical and immunological outcomes than deferred ART (Cotton et al. 2013).

A neurodevelopmental sub study of the CHER trial evaluated the effect of early versus deferred ART on the neurodevelopmental outcomes in children from the CHER trial residing in Cape Town (Laughton et al. 2009). These children have undergone regular clinical and immunological follow-up, including comprehensive neurodevelopmental testing at the Children's Infectious Diseases Clinical Research Unit (KID-CRU) at Tygerberg Hospital. The children all returned to KID-CRU at age 5 for their final neurodevelopmental assessment. At this time, a subset of the participants received high-resolution neuroimaging using custom developed sequences that have been optimized for paediatric imaging and that include real-time motion correction in order to investigate the effects of HAART and HIV on the developing brain.

1.3 Overview of HIV-1 Infection

1.3.1 Human Immunodeficiency Virus – 1

Human immunodeficiency virus-1 (HIV-1) is a complex retrovirus within the Lentivirus genus (Cullen 1992). The genomic organization and viral gene expression, which is controlled by interactions between cis-acting viral RNA (vRNA) sequences and host cell trans-acting factors, gives HIV-1 its complexity, while its ability to reverse the process of transcription (RNA to DNA) makes it a retrovirus (Cullen 1992). HIV-1 is a linear single stranded RNA (ssRNA) virus that is composed of nine genes that encode for viral gene products that are involved in structural or enzymatic functions. These genes are divided into three standard genes in the retrovirus family, namely *gag, pol,* and *env,* which is flanked by long terminal repeats (LTRs) and six accessory genes*, vif, vpr, tat, rev, vpu,* and *nef* (in the form: 5' LTR-*gag-pol-vif-vpr-tat-rev-vpu-env-nef*-LTR 3') (Cullen 1992; Ochsenbauer et al. 2012). The 5' LTR region promotes viral transcription by coding for enhancer and promoter elements that are necessary for transcription to occur (Cullen 1991, 1992). The 3' LTR region contains sequences that allow for polyadenylation of the messenger RNA (mRNA) (Cullen 1991, 1992).

The *gag* gene encodes for virion structural proteins, the *pol* gene encodes for various enzymes, the *env* gene encodes for the precursor envelope glycoprotein (gp) 160, which is later cleaved into gp120 and gp41 that function in host tropism and membrane merging, respectively (Ashkenazi & Shai 2011; Cullen 1992). Both *tat* and *rev* genes regulate gene expression and replication by acting in trans against the normally cis isoform of genes. The *tat* gene is associated with increased viral gene expression and is regulated by its gene products, while the *rev* gene is necessary for the generation of structural proteins by inducing splice mechanisms of vRNA and has been linked as a transport molecule for pre-mRNA from the nucleus to the cytoplasm (Fischer et al. 1995). The Nef and Vpu proteins downregulate the surface expression of the CD4 receptor and major histocompatibility complex (MHC) class I, while Nef further causes T-cell activation (Kirchhoff 2010; Malim & Bieniasz 2012). The *vif* and *vpu* genes are essential for viral maturation and release of virion particles. The final gene product, Vpr, is a structural protein found in the virion and its gene *vpr* has been found to enhance replication rates of HIV-1 in culture (Cullen 1992).

1.3.2 HIV-1 Life Cycle

The genes and their products play an important role in the life cycle and even the evolution of the virus (Cullen 1991). Infection of the host cell occurs when the viral surface glycoprotein, gp120, directly binds to a CD4 receptor on the surface of mammalian target cell types (T-cells, macrophages/monocytes, and microglia) as well as a coreceptor, either CCR5 or CXCR4 (Musich et al. 2011). This binding leads to conformational changes and exposure of the gp120-associated fusion protein, gp41, to the external environment. The N-terminus of the gp41 fusion protein then undergoes structural changes, which facilitates the insertion of the protein into the cell membrane of the host cell (Berger, Murphy & Farber 1999; Lawless et al. 1996). Fusion of viral and host cell membranes allows for the viral nucleocapsid (the viral genome inclusive of the protein coat) to enter the host cell cytoplasm (Pollard & Malim 1998). Viral linear ssRNA is reverse-transcribed into linear double-stranded (ds) DNA by the viral enzyme reverse transcriptase (RT) and enters the host nucleus as the preintegration complex (nucleic acid-protein complex) (Pollard & Malim 1998). The complex is then incorporated into the host cell's genome by another virally encoded enzyme, intergrase, thereby forming the provirus, the viral transcriptional template (Brik & Wong 2003; Pollard & Malim 1998).

Viral transcription and translation (viral replication) occurs when the host cell is activated (Brik & Wong 2003). The 5' LTR region contains two binding sites for the inducible host transcription factor, NF-κB that is involved in cellular response to infection by activating cytokines and cytokine receptors, and acute phase protein genes. HIV-1 activates host T-cells via nef proteins and utilizes the activated NF-κB to enhance viral gene expression; therefore viral replication occurs at sites of inflammation (Cullen 1991). Viral replication is divided into two phases based on the mRNA produced: the early regulatory phase, consisting of multiple splice (~2kb) regulatory mRNA for proteins nef, rev, and tat; and the late structural phase, consisting of unspliced (~9kb) and singly spliced (~4kb) mRNA for structural proteins. The *tat* gene product regulates the increase in viral gene expression, which in turn causes the increased expression of the rev protein that is required for the switch between these two phases (Cullen 1991). The final virally encoded enzyme, HIV protease, cleaves the polyprotein precursors into mature proteins, which are assembled at the cell surface forming new virions (Brik & Wong 2003). The gag and pol proteins assemble around two copies of the full length vRNA to form the immature nucleocapsid. The outer capsular layer is formed during budding where the host cell membrane containing Env proteins surrounds the nucleocapsid (Pollard & Malim 1998).

1.3.3 HIV-1 Tropism

HIV-1 tropism has been linked to the gp120 subunit of the env protein (Feng et al. 2011). The concept of tropism is used to reflect the preference of env's activity to specific coreceptors that are expressed on specific target cell types (Berger, Murphy & Farber 1999). These coreceptors are (C-X-C chemokine receptor type 4) and CCR5 (C-C chemokine receptor type 5), where T-cell lines [(TCL)-tropic] have a preference for CXCR4, macrophage (M)-tropic have a preference for CCL5, and dual-tropic have a preference for both coreceptors. However, it is important to note that this preference is not the rule, i.e. there are cells, other than macrophages, that have a preference for CCR5 (Berger, Murphy & Farber 1999). CCR5 has been associated with early disease progression, HIV-1 transmission, and spreading capacity, while CXCR4 has been associated with late disease progression, especially in adults, and a rapid decline in CD4 T-cells leading to death (Mariani et al. 2012; Musich et al. 2011).

Macrophages express low levels of CD4, which is required for HIV-1 infection of these cell lines. M-tropism has been linked to protein changes in the CD4 binding site, which can directly impact CD4 affinity or affect exposure residues to CD4 (Musich et al. 2011). The study of macrophages are becoming increasingly important, especially when they become infected, because they have a long-lifespan and have access to immunoprivileged sites such as the brain; therefore, they are important cellular reservoirs (Mlcochova et al. 2014).

1.3.4 Host Defence Mechanisms and Susceptibility

The response and susceptibility of the host cell to infection is largely based on the host genetic and immunological factors (Mackelprang et al. 2008), and the mutational adaptation of the virus to evade host responses (Kirchhoff 2010; Malim & Bieniasz 2012).

Mammalian cells have developed innate defence mechanisms in response to viral infection, by utilizing proteins, termed restriction factors, to suppress viral replication (Malim & Bieniasz 2012). These intrinsic factors include the apolipoprotein B mRNA-eliciting enzyme catalytic polypeptide-like 3 (APOBEC3) family (especially APOBEC3G), tetherin, and tripartite-motif-containing 5α (TRIM5α) (Kirchhoff 2010; Malim & Bieniasz 2012). APOBEC3G protein is widely expressed in human cell types, and becomes incorporated into the *gag* region of the nucleocapsid of the assembling virion. During viral replication, it causes positive strand guanine to adenine hypermutations, leading to a decrease in genetic integrity, which may also lead to viral diversity and evolution, especially if it results in immune escape or drug resistance (Malim & Bieniasz 2012). The cytoplasmic protein, TRIM5α, is associated with

failure in viral dsDNA synthesis via premature viral uncoating and cross-species transition of HIV-1 (Kirchhoff 2010; Malim & Bieniasz 2012). Another restriction factor, tetherin, allows for the maturation of virions but does not allow the matured virions to be released from the cell surface of infected cells (Kirchhoff 2010). However, HIV-1 has developed mechanisms to evade these host intrinsic factors with the protein associated as the accessory genes, namely *vif* (inhibits APOBEC3G) and *vpu* (inhibits tetherin) (Malim & Bieniasz 2012).

Host acquired immunity, especially CD8 T-cells, play an important role in controlling viral replication and in viral suppression (Zhang et al. 2002). CD8 T-cells have the ability to directly kill infected cells (Kirchhoff 2010) and secrete soluble factors, CD8 antiviral factors (CAF), which have been shown to inhibit non-specific tropic viral replication (Zhang et al. 2002). CD8 T-cells further secrete β-chemokines (CCL5/RANTES and the macrophage inflammatory proteins MIP-1α and MIP-1β), which block M-tropic HIV-1 infection (Zhang et al. 2002).

The final component conferring protection from disease progression to a susceptible host cell is the genetic make-up of the individual, since human variation is an important indicator of disease progression (Fellay et al. 2007). Fellay and colleagues (2007) identified polymorphisms in the MHC or human leukocyte antigens (HLA) class I genes that explain variation in viral load and HIV disease progression amongst HIV-1 infected individuals (Fellay et al. 2007). These polymorphisms result in variation in antigen presentation or increase the likelihood of viral escape, and, therefore, can be used as determinants of disease progression and susceptibility (Farquhar et al. 2004). This is due to the fact that different HLAs lead to the activation of cellular immune responses towards a specific HIV-1 epitope. This immune response exerts immune pressure on HIV-1, leading to viral mutations that increase the chance of immune escape (Mackelprang et al. 2008). Genetic polymorphism in the CCR5 promoter region and increased chemokine SDF-1 levels have been linked to delayed disease progression but not transmissibility. CCR5 polymorphisms may lead to varying regulation in the CCR5 gene transcript, while increased SDF-1 levels are thought to block its ligand, CXCR4, thereby preventing the attachment of HIV-1 to the coreceptor (McDermott et al. 1998).

1.3.5 Viral Load, CD4 and CD8 T-cell Count Monitoring

Upon initial diagnosis of a positive HIV infection in adults, the relative stage of disease progression is determined by CD4 T-cell count and viral load (VL). However, further monitoring of these biomarkers in the presence of ART initiation is controversial.

Monitoring of VL has been indicated as a biomarker for treatment efficacy (Reynolds et al. 2014). This in turn also aids in reducing the risk of genotypic resistance and of morbidity associated with advanced immune suppression (Reynolds et al. 2014). VL is also a tool to improve adherence to ART, indicating patients with the need for enhanced adherence support, thereby providing an additional benefit to treatment programs/trials (Bonner et al. 2013; Reynolds et al. 2014). Immune activation and expansion of CD8 T-cell populations are also caused by HIV infection (Shearer et al. 2007).

The necessity of sustained CD4 T-cell count monitoring has been questioned in the era of viral load suppression resulting from ART (Gale et al. 2013; Girard et al. 2013; Reynolds et al. 2014). It has been reported that individuals with virologic suppression (VL ≤ 400 RNA/mL) and an immunological response to ART, have a very low risk of CD4 T-cell count below 200 cells/μL (Reynolds et al. 2014). This finding by Reynolds and colleagues (2014) on 1553 adult Ugandan patients is in accordance with that described in North America (Gale et al. 2013; Girard et al. 2013). CD4 T-cell count also tends to fluctuate throughout the day. Children have a naturally high CD4 T-cell count, which decreases with age, and thus differs greatly from that of adults (Shearer et al. 2007). As MTCT occurs around the time of birth, or during breastfeeding, the initial CD4 T-cell count in HIV positive infants is often equivalent to that of HIV negative infants(Shearer et al. 2003, 2007). Studies on untreated adults show that CD8 T-cell activation occurs early after primary infection, whereas CD4 T-cell count decreases over time (Deeks et al. 2004). It should be noted that a subpopulation of CD8 T-lymphocytes, CD38+, linked to immaturity and recent thymic emigrants is also high in infancy and decreases with time (Paul et al. 2005). High CD8 T-cell count has been associated with more advanced disease progression in HIV-infected children (Paul et al. 2005). Either CD4 percentage (CD4%) or CD4/CD8 ratio are suggested as more reliable predictive biomarkers of HIV-1 infection and disease progression in children than CD4 T-cell count. CD4% is the relative percentage of lymphocytes that are CD4 cells within a given blood sample. CD4/CD8 ratio is the amount of CD4 T-cells relative to a single CD8 T-cell. In infants, CD4/CD8 ratio has been described as a more reliable diagnostic marker than CD4 T-cell count alone (Shearer et al. 2007).

1.3.6 Mother to Child Transmission

Mother to child transmission (MTCT) has been linked to HIV-1 tropism and genetic variation (Cavarelli & Scarlatti 2011; Mariani et al. 2012). Mother to child transmission occurs during gestation, intrapartum, through the placenta or breast milk by ingesting infected fluids (Cavarelli & Scarlatti 2011; Mackelprang et al. 2008).

The tropism of the HIV-1 strain of the mother plays an important role in the transmission from mother to child. Mothers having CXCR4-tropic or dual-tropic HIV-1 strains have been found to have an increased likelihood of MTCT than those with CCR5-tropic strains, and if MTCT does occur, the CCR5-tropic strain is most likely the cause of infection in the fetus (Mariani et al. 2012). In children, infection with the CXCR4-tropic HIV-1 strain usually result from the evolution of the initial infected CCR5-tropic strain to the CXCR4-tropic strain, as seen in adults during disease progression (Cavarelli & Scarlatti 2011; Mariani et al. 2012).

HLA variation between mother and child further influence the susceptibility of the fetus to MTCT (MacDonald et al. 1998; Mackelprang et al. 2008). The more genetically identical (concordant) the HLA alleles are between mother and child, the higher the risk of perinatal infection in the absence of prophylaxis (Mackelprang et al. 2008). In HLA concordance, viruses that have evaded maternal responses will also evade fetal responses because they are genetically similar in immunity (MacDonald et al. 1998; Mackelprang et al. 2008). The more alleles the mother shares with the fetus the more rapid HIV-1 disease progression in the fetus. Genetic differences in the HLA alleles (discordant) between the mother and child are thought to play a protective role against perinatal transmission because the immune response of the fetus can act against infected maternal cells or free virions (Mackelprang et al. 2008). It would thus follow that the more genetically different and discordant the HLA alleles between any two individuals the more protected the recipient is against transmission, and if infected it leads to slow disease progression. That is if the dissimilar HLA alleles in the recipient provide enough immune pressure on the incoming HIV-1 variant. Whether the principle stated above can be extrapolated upon to that of different genetic population groups (such as transmission between Xhosa and Cape Coloured populations) is still a matter of further research and debate (Abubakar et al. 2008; Gray et al. 2013; Hoare et al. 2012; Violari et al. 2008).

1.3.7 HIV-1 Outcomes in Children versus Adults

HIV-1 infection outcomes in perinatally infected children is highly variable and is largely based on the gestational period of fetal HIV-1 infection, immunocompetent status of the child or mother (HLA concordance), viral load, and biological phenotype (Cavarelli & Scarlatti 2011). Large differences in HIV-1 infection rate and progression have been identified between children and adults (Mariani et al. 2012; Tardieu et al. 2000). Firstly, approximately 50-70% of HIV-infected adults present with mononucleosis-like symptoms, compared to approximately 75% of infants (Cavarelli & Scarlatti 2011; Mariani et al. 2012). These mononucleosis-like symptoms extend to that of fever, acute pharyngitis, swollen glands, fatigue, malaise, and body pains. Secondly, infants have a higher plasma viral load in their first month of life than adults, and the decrease in viral load takes years (in the absence of combination antiretroviral therapy) rather than months leading to a longer viral exposure time in infants (Cavarelli & Scarlatti 2011; Mariani et al. 2012). Thirdly, adults remain clinically asymptomatic after primary exposure compared to approximately 25% of infants that become symptomatic and progress to acquired immunodeficiency syndrome (AIDS) within the first year of life (Cavarelli & Scarlatti 2011; Mariani et al. 2012).

1.3.8 Summary of the Mechanism of HIV-1 Infection

Upon initial entry of HIV into the human body it infects immune cells carrying CD4 receptors, thereby evading the immune response designed to eliminate it. The virus enters the immune cell and utilises the immune cell's infrastructure to replicate. This results in the release of toxins and cytokines, by both the virus and immune cell respectively, causing inflammation. This activates more immune cells carrying CD4 receptors that are recruited in response to the infection. These recruited immune cells in turn become infected allowing the cycle to continue. Additional immune pressures exerted upon HIV by the immune cells allow it to mutate which increase the chance of viral immune escape.

1.4 ARV Drugs and Their Action: CHER Trial (Cotton et al. 2013)

First Line ART

First line ART includes the following drugs:

- Zidovudine (Esposito, Corona & Tramontano 2012; Ghodke et al. 2012)

Zidovudine is a member of the nucleoside analogue reverse transcriptase inhibitor (NRTI) family. It competes with thymidine triphosphate, a nucleotide that is utilised by reverse transcriptase during conversion from ssRNA to dsDNA. Incorporation of zidovudine (which lacks the 3' hydroxyl group) instead of thymidine triphosphate causes chain termination and thus inhibits HIV-1 replication.

- Lamivudine (Esposito, Corona & Tramontano 2012)

Lamivudine is similar to zidovudine, but it competes with cytosine triphosphate instead of thymidine triphosphate. It also inhibits the replication of HIV-1 by causing chain termination.

- Lopinavir-ritonavir (Bazzoli et al. 2010)

Lopinavir-ritonavir are protease inhibitors, which prevent the cleavage of the precursor proteins by HIV proteases to form activated proteins required in the construction of new virions.

Second Line ART

Second line ART includes:

- Didanosine (Esposito, Corona & Tramontano 2012)

Didanosine is also an NRTI, but is an adenine analogue instead of thymidine triphosphate. It inhibits the replication of HIV-1 by causing chain termination.

- Abacavir (Esposito, Corona & Tramontano 2012)

Same as Zidovudine but is a guanosine analogue instead of thymidine triphosphate. It inhibits the replication of HIV-1 by causing chain termination.

- Nevirapine and Efavirenz (Esposito, Corona & Tramontano 2012)

Both nevirapine and efavirenz are part of the non-nucleoside reverse transcriptase inhibitor (NNRTI) family. This group noncompetitively binds to a hydrophobic pocket in the reverse transcriptase structure. The pocket is located near the polymerase active site and binding leads to conformational (structural) changes in reverse transcriptase, which in turn inhibits the elongation of DNA during DNA synthesis.

1.4.1 Adverse Effects of HAART

The possibility of curing the HIV epidemic via current therapy regimens seems unlikely (Carr & Cooper 2000). Indefinite use of antiretroviral therapy is needed to preserve clinical benefits. Due to the rapid spread of the HIV epidemic there was an increased need for initiation of treatment, so that licencing of antiretroviral agents were accelerated (Carr & Cooper 2000). The increased rate of pharmaceutical licencing meant the possible negation of studying long-term effects to such treatments. When HIV-1 infected individuals initiate HAART, they often take at least three drugs to manage their condition (Carr & Cooper 2000). With the number of drugs on the market the possible number of HAART combinations is large. As HIV has progressed from a terminal disease to a chronic illness, drug-related toxicity is becoming increasingly common.

Common acute side effects to ARVs, which could occur in both adults and children, include hypersensitivity reactions, impaired concentration/CNS function, fatigue, myaligia, distal pain, anaemia, nausea, abdominal pain, vomiting, and diarrhoea (Ammassari et al. 2001; Carr & Cooper 2000). Hypersensitivity reactions usually manifests after 1-3 weeks of therapy, as an erythematous, maculopapular, pruritic and confluent rash (Carr & Cooper 2000). Adverse effects linked to efavirenz, nevirapine, and sometimes delavirdine, manifest mostly within the CNS (Carr & Cooper 2000). The side effects often present clinically as dizziness, insomnia, somnolence, impaired concentration, vivid dreams, nightmares, and mania in about 40% of patients in the first few days to weeks of treatment (Ammassari et al. 2001; Carr & Cooper 2000). Women receiving nelfinavir or nevirapine are at increased risk of hyperglycaemia, hepatoxicity and gastrointestinal symptoms during pregnancy (Timmermans et al. 2005).

Mitochondrial toxicity, a major adverse effect resultant from NRTIs (and NNRTIs), is not necessarily reversed over time (Mitchell, Wendy 2001; Tardieu et al. 2005; Venerosi, Calamandrei & Alleva 2002). This involves inhibition of DNA polymerase γ. The result is impaired synthesis of mitochondrial enzymes which generate adenosine triphosphate (ATP) by oxidative phosphorylation (Carr & Cooper 2000). Mid to long-term adverse effects from such mitochondrial toxicities may include myopathy, neuropathy, hepatic steatosis, lactic acidaemia, pancreatitis, and possibly peripheral lipoatrophy (Carr & Cooper 2000). A group of French scientists conducted a study to assess the effects of prenatal exposure to Zidovudine in uninfected children born to seropositive mothers (Tardieu et al. 2005). Of the 49 children in the cohort, 22 had mitochondrial dysfunction. Fourteen without

mitochondrial dysfunction had unexplained neurological symptoms, and only 6 children were completely asymptomatic (Tardieu et al. 2005). The images showed global antiretroviral-induced mitochondrial dysfunction in many of the brains within the cohort, mimicking that of congenital mitochondrial disease; the exception being that the mitochondrial dysfunction was confined to the CNS of the children, with none of the children showing signs of systemic mitochondrial dysfunction (Tardieu et al. 2005).

Ramos-Sanchez and colleagues (2014) examined the side effects of Indinavir (a potent protease inhibitor often used in conjunction with NRTIs) in vivo in a hamster model receiving both normal or high-fat diets (Ramos-Sanchez et al. 2014). They observed that with increasing dosage of Indinavir survival rates of hamsters diminished significantly. Histology revealed that the drug caused serious perturbations in both cardiac and renal areas (Ramos-Sanchez et al. 2014).

Knowledge of the adverse effects of ART drugs is imperative to treatment planning and management of disease progression. This is especially true since these adverse effects contribute significantly to non-adherence (Ammassari et al. 2001). Especially in children, who initiate treatment soon after birth and will remain on ART life-long, it is important to study the long-term consequences of extended ART on neurodevelopment.

1.5 HIV-1 Infection in the Brain

General neurodegeneration is a hallmark of HIV-1 infection in adults (Berger & Arendt 2000). In adults antiretroviral therapy has been shown to reverse neurodegeneration in the presence of HIV-1 infection as well as slow the progression to AIDS (Tamula et al. 2003). By contrast, very little is known about the effects of ART and HIV on the developing brain. An article reviewing all studies in Sub-Saharan Africa (SSA), evaluating as their primary outcomes development, cognition and behaviour in HIV-positive children, highlighted the paucity of data in this field (Abubakar et al. 2008). Highly active antiretroviral therapy (HAART) improves some of the neurological pathology seen in HIV positive children (Laughton et al. 2009). However, most studies have been conducted in developed countries and the data is scarce for children living in SSA where the dominant genetic clade (and possible neurotoxicity) of the virus varies from that of North America (Abubakar et al. 2008; Hoare et al. 2012; Violari et al. 2008). From the literature the patterns of CNS pathology in HIV-infected children that have been highlighted previously are:

- HIV related encephalopathy, both progressive and static.
- HIV related CNS compromise, characterized by global cognitive functioning within normal limits, but with significant impairments in select neurodevelopmental functions.
- Non-HIV related CNS impairment, which is related to these children's complex medical histories (metabolic, endocrine, systemic illnesses, toxic side effects of drugs, secondary CNS infections)

(Brouwers et al. 1995).

1.5.1 Neuropathogenesis of HIV-1 Infection

HIV-1 invades the CNS early on in infection, usually within the first 10 days post-infection (Ivey, MacLean & Lackner 2009). The predominant mechanism of invasion is via infected monocytes, macrophages and CD4+ T lymphocytes (Ivey, MacLean & Lackner 2009; van Rie et al. 2007). In fact, M-tropic forms of HIV-1 tend to favour infecting the CNS (Aquaro et al. 2002; van Rie et al. 2007). Autopsied brain tissue showed that higher concentrations of HIV-1 are found primarily in specific cells associated with CD4 and chemokine coreceptors (mainly CCR5 and CCR3) which are necessary for the progression of HIV-1 infection (Medders & Kaul 2011; van Rie et al. 2007; Schnell et al. 2011; Wiley et al. 1986). These cells include that of perivascular macrophages and microglia (Aquaro et al. 2002; van Rie et al. 2007; Wiley et al. 1986). It is also known that HIV-1 has a particular affinity for infection of astrocytes (Blumberg, Gelbard & Epstein 1994; van Rie et al. 2007; Tornatore et al. 1994). Astrocytes are the most numerous of the glial cells in the CNS (Kandel, Schwartz & Jessell 2000). They have a star-like shape with broad end-feet on their processes. The projections with terminal end-feet projecting out from the main cell body centre, place the cell in contact with numerous other cells and structures, mainly capillaries and neurons (Kandel, Schwartz & Jessell 2000). Astrocytes are thought to have a nutritive function, as well as playing an important role in forming the blood brain barrier (BBB) (Kandel, Schwartz & Jessell 2000). The BBB is an impermeable lining in the capillaries and venules of the brain that act to prevent toxic substances in the blood from entering the CNS. Infection of astrocytes within the CNS may thus cause loss of supporting growth factors causing neuronal dysfunction, dysregulating the reuptake of neurotransmitters causing localised neurotoxicity, and loosening of the BBB permitting further seeding of HIV-1 and other opportunistic infections (Blumberg, Gelbard & Epstein 1994). Blumberg and colleagues (1994) have proposed two main pathways causing neuronal damage during HIV-1 infection in children. The first being widespread active and latent HIV-1 infection of astrocytes (Blumberg, Gelbard & Epstein 1994). The second major pathway is via HIV-1-infected macrophages. These macrophages initiate inflammatory responses which are amplified through cell-cell interactions with astrocytes (Blumberg, Gelbard & Epstein 1994). Macrophage-astrocyte interactions in the advent of HIV-1 infection produce arachidonic metabolites and potentially neurotoxic cytokines (TNF-α and IL-1β) (Blumberg, Gelbard & Epstein 1994). These neurotoxic events thus lead to further astrocyte and macrophage activation and proliferation which expectedly amplifies these cellular processes (Blumberg, Gelbard & Epstein 1994). Ultimately, the findings presented by Blumberg and colleagues (1994) are important as they show how a

small number of HIV-1 infected cells indirectly cause widespread tissue pathology. This could in turn elicit profound neurological impairment. The infection of glial cells within the CNS is of particular worry as certain viral proteins, pro-inflammatory cytokines and nitric oxide that are released by these infected cells could lead to neurotoxic events (Epstein & Gelbard 1999; van Rie et al. 2007). It is hypothesized that fetal astrocytes as well as the developing CNS are particularly susceptible to perturbations in astrocyte function (van Rie et al. 2007). This is the primary concern when dealing with perinatally infected children, as viral interactions on the glial cells may play a significant role in paediatric HIV-associated progressive encephalopathy. While it is still not clear whether neurons are specifically infected by HIV, a study has shown some directly infected neurons in children, albeit a negligible number (Cantó-nogués et al. 2005).

The unique CNS environment allows neurotropic HIV-1 to develop distinct genetic patterns characterized by their specificity in cell infection (Misra et al. 2003; Pillai et al. 2006). Genetic variation develops in the viral *env*, especially in gp120, which leads to changes in the CD4 binding domain, either by increasing the efficiency of gp120 and CD4 interaction or by increasing glycoprotein affinity for CCR5 (Salimi et al. 2013). This is an important finding as it shows that due to the unique compartmentalization of the viral populations via the BBB we are faced with added problems of a possible unique genetic sequence, which may itself be drug resistant. Genetic mutation allowing for compartmentalisations has been confirmed in adults by evidence of differences in HIV-1 genetic sequences or drug resistance via tests between blood and CSF (Lanier et al. 2001; Ritola et al. 2005; Strain et al. 2005). Similar findings of unique viral populations in the CNS have also been reported in children (McCoig et al. 2002; van Rie et al. 2007).

The effects of ART are hampered by the limited ability of the ARVs to pass the BBB; the variable perfusion of these drugs into the CNS could further result in drug resistant populations (Letendre et al. 2004; Yazdanian 1999). Another concern is the longer lifespan of macrophages, microglia and astrocytes as compared to CD4 T-cells; this does not allow for swift eradication of infected cells and thus these unique viral populations would have a longer period to produce the virus, vRNA, and neurotoxic viral proteins (Env and Tat) (Aquaro et al. 2002; Medders & Kaul 2011; Perelson et al. 1997).

1.5.2 Progressive Encephalopathy

"HIV-associated progressive encephalopathy of childhood" (HPE) is a term used to denote the clinical and pathological occurrence of progressive encephalopathy in children (Cantó-nogués et al. 2005; Rosenfeldt, Valerius & Paerregaard 2000). The presentation of HPE is characterised by impaired brain growth, cognitive decline, and an overall dysfunction in global neurological abilities (Rosenfeldt, Valerius & Paerregaard 2000). HPE progression is monitored by neurological tests, combined with computed tomography (CT) scanning or magnetic resonance imaging (MRI). These techniques are also used to gauge the efficacy of certain drugs and ARTs. Used as a clinical tool the researcher is able to test drug efficacy in hampering the progression of the encephalopathy (Johann-Liang et al. 1998; Rosenfeldt, Valerius & Paerregaard 2000). MRI has been found to be more sensitive in exposing abnormalities of periventricular white matter than CT scans (Rosenfeldt, Valerius & Paerregaard 2000). High viral load and low CD4 T-cell count has been linked to an increased risk of children presenting with HPE (Rosenfeldt, Valerius & Paerregaard 2000). This said, in a study conducted on 128 perinatally HIV-infected children, 21% showed characteristic evidence of HIV infection induced encephalopathy despite at least 74% of children having viral load suppression at the time of diagnosis (Cooper et al. 1998). Findings of viral load suppression in the systemic blood supply may not be representative of the compartmentalised and unique viral reservoirs in the CNS (Pillai et al. 2006; Strain et al. 2005). One need also understand that the findings of sometimes aggressive encephalopathy in children infected with HIV were gathered in a time where there were few ARTs available and little was known as to their effects on infants both pre- and post-natally (Johann-Liang et al. 1998). Johann-Liang and colleagues (1998) performed neuroradiographic imaging in 33 children infected with HIV. They showed that apart from gross cerebral atrophy, there was also presence of calcification of the basal ganglia (Johann-Liang et al. 1998). Calcifications within the basal ganglia appear to be a common finding in HIV-1 infected children (Chiriboga et al. 2005; Epstein et al. 1986; Mitchell, Wendy 2001; Nozyce et al. 2006; Rosenfeldt, Valerius & Paerregaard 2000; Shah et al. 1996) and adults (Berger & Arendt 2000; McArthur, Brew & Nath 2005; Walot et al. 1996).

Additional alterations that have been linked to HIV in children include reactive gliolisis, neuronal loss, ventricular dilation, periventricular white matter abnormalities, as well as calcifications of other areas of the brain (Ernst, Chang & Arnold 2003; George et al. 2009; Johann-Liang et al. 1998; Rosenfeldt, Valerius & Paerregaard 2000). Certain magnetic resonance spectroscopy (MRS) studies have indicated that glial cell activation in the white

matter and subcortical grey matter occurs early on in infection rather than immediate neuronal cell loss (Chang et al. 2002; Ernst, Chang & Arnold 2003).

It has been suggested that the increased calcifications seen in some studies may have been as a result of increased viral load within the CNS (Rosenfeldt, Valerius & Paerregaard 2000). Combination therapy may be able to slow the encephalopathic progression due to the ability of the protease inhibitors to lower the viral load and increase the CD4 T-cell count (Bazzoli et al. 2010). With the decreased viral load, it follows that the level of calcification as well as rate of global atrophy will decrease.

1.5.3 Biomarkers Linked to HIV-1 Infection and ART Administration

There is a need for objective biomarkers that diagnose and predict HIV-related brain disease. Such biomarkers would contribute to individual treatment plans and drug trials.

Autopsy Studies

Findings via autopsy samples have shown significant localised differences of HIV-1 vRNA in various brain regions. The caudate nucleus is one of the affected areas. Given the caudate's close proximity to the ventricles and thus CSF, it is particularly susceptible to HIV-1 attack (McClernon et al. 2001). McClernon (2001) observed individuals, all of whom on ART, experiencing high levels of dementia had presence of significantly higher VL within the CNS compared to mild to non-demented individuals; whilst no significant differences between their plasma viral loads were observed, peripherally. This is in concordance with previous studies mentioning the unique compartmentalized nature of HIV infection in the CNS (Lanier et al. 2001; Ritola et al. 2005; Strain et al. 2005). It was necessary to investigate such HIV-infected autopsy patients stereologically to gain insight into the relative volume and morphological changes that accompany HIV infection (Oster et al. 1993). Since the study was of a formalin fixed cadaver sample and are representative of very sick subjects, findings may be biased. The primary cause of death was pneumonia (84%). Oster found that there was a vast increase in ventricular size of up to 55% in HIV-infected subjects compared to the controls. Oster et al. also observed a global decrease in tissue mass in the HIV-infected individuals (Oster et al. 1993). It was further identified that there was significant atrophy in central brain nuclei, mainly in the striatum and thalamus (Oster et al. 1993). Eleven of nineteen (58%) had perturbations to glial cells, whilst seven (37%) had presence of reactive gliosis.

Adult Studies

MRI and volumetric analysis has found a significant decrease in the volume of the basal ganglia in HIV-1 infected homosexual males with dementia as compared to those without dementia as well as HIV negative controls (Aylward et al. 1993). This is a finding already well documented in adults (Becker et al. 2011; Cohen et al. 2010; Sarma et al. 2014). Chiang and colleagues (2007) conducted a study on adults involving 26 HIV-1 infected individuals and 14 HIV-1 seronegative controls. Their study used 3D T1-weighted brain MR images and showed that even before the development of AIDS dementia or infections within the CNS, severe brain atrophy occurs within the corpus striatum, cingulate gyrus and callosal fibres, as well as other sensorimotor areas (Chiang et al. 2007). Chiang et al. (2007) found that caudate atrophy was not readily detectable via tensor-based morphometry, however, detection and significance was found via surface-based anatomical modelling methods (Chiang et al. 2007). They attributed this discrepancy in findings to the lack of contrast between the caudate and surrounding tissue, making it difficult to profile the caudate accurately when using automated segmentation techniques (Chiang et al. 2007). Arguably this study, as well as that of Aylward et al. (1993) and others, may contain a sample bias as the studies only included males (Aylward et al. 1993; Chiang et al. 2007). However, the results may be applicable to the general population as, to date, no differences have been found in the progression of HIV in the CNS between males and females (McArthur 2004; Safriel et al. 2000; Xia et al. 2011).

Along with the perturbations to deep grey matter structures, white matter has also been indicated to be affected by HIV infection (Andronikou et al. 2014; Chiang et al. 2007; Pomara et al. 2001; Thompson et al. 2006). Thinning of the corpus callosum and ventricular expansion is associated with increased viral load (Thompson et al. 2006). An increase in HIV-1 vRNA within the CNS is associated with increased levels of HIV associated dementia (McClernon et al. 2001; Rosenfeldt, Valerius & Paerregaard 2000). However, overall white matter thinning may not necessarily be as a direct result of viral load and may occur in response to grey matter damage, and thus neuronal cell death projecting from deep grey matter areas (Tate et al. 2011).

Von Giesen and colleagues (2000) found, using MRI in conjunction with electrophysiological motor testing at the time of PET, that HIV-1 infected males receiving ART showed hypermetabolism in the basal ganglia. The men had PVL ranging upward from undetectable levels to 30000 RNA/ml, with 6 of 19 (32%) having PVL above 1000 RNA/ml(von Giesen et al. 2000). This finding could be due to the recruitment of glial cells to the site of the localised inflammatory response (Ernst, Chang & Arnold 2003; McClernon et al. 2001;

Sacktor et al. 2004; Silverstein & Kumar 2013). The authors suggested a time course occurring in these adults, where, initially, hypermetabolism within the basal ganglia of these patients is associated with normal motor performance. However, with time there is a shift to decreased motor performance once hypermetabolism converts to hypometabolism (von Giesen et al. 2000). The more widespread the hypometabolism within the basal ganglia the more severe the deficit and pathologic slowing of motor performance. Ernst and colleagues (2003) conducted similar research involving 14 HIV-1 positive males (age 37.8±7.1 years) using MRS and fMRI. The mean PVL of the patients was 8318±20 RNA/ml. The research indicated that increased concentrations of glial markers (choline-containing compounds, myo-inositol, and total creatine) in the frontal white matter and basal ganglia were associated with increased Blood-oxygen-level dependent (BOLD) activation during working memory tasks as compared to controls (Ernst et al., 2003). These findings suggest that working memory deficits in HIV patients are modulated by inflammation occurring in the white matter and basal ganglia (Ernst, Chang & Arnold 2003). Working memory deficits observed via Ernst et al. (2003) coupled with motor deficits observed by von Giesen, indicate pathology to the entire corpus striatum's functional areas, in response to HIV infection.

Chang and colleagues presented a study involving 18 seronegative controls and 24 HIV positive subjects. Within the HIV-infected group, 12 were receiving ARV treatment with PVL <50 RNA/ml, whilst the 12 individuals not on treatment had PVL 28964±12009 RNA/ml (Chang et al. 2008). Each participant performed a set of visual attention tasks with increasing load during fMRI. Although the HIV-infected group showed greater load-dependent increases in brain activation than seronegative controls, subjects receiving ARV treatment had more activation in the bilateral superior frontal regions, compounded with a lower percent accuracy with increasing load (Chang et al. 2008). Seronegative controls also showed less activation following repeated trials, whilst HIV positive individuals showed increased activation for repeated trials with increasing load. Chang et al. (2008) thus concluded that ARV treatment may lead to higher neurocognitive recruitment and greater demand on the attentional network reserve, as well as less efficient usage of the neural networks and less practice effects. The exhaustion of such reserve capacity in individuals receiving HAART would lead to additive decline in performance, compared to seronegative controls and those not receiving ART (Chang et al. 2008). These findings are strongly contrasted by other adult studies reporting positive and sustained effect on neurocognitive impairment in the presence of HAART in adults (von Giesen et al. 2002; Tozzi et al. 1999). i.e. VL suppression is associated with regression of neuropsychological test abnormalities (Tozzi et al. 1999).

Child Studies

It is not clear whether the findings from adult studies can be extrapolated to the developing brain of children. There is little research that has actively followed and imaged a cohort of children stable on long term HAART since birth. Most studies are of a cross-sectional nature with small sample sizes, and large age ranges (Andronikou et al. 2014; Depas et al. 1995; von Giesen et al. 2003; Langerak et al. 2014; Sei et al. 1996; Tornatore et al. 1994). The atrophy and perturbations to brain tissue may correlate with the initial depletion of CD4 T-cells signifying that brain atrophy may accompany immunosuppression by HIV (Chiang et al. 2007; Rosca et al. 2011). However, significant differences have been observed between CNS and plasma VL in previous studies; for example in a sample of vertically infected children (6 months to 18 years of age) disturbances to the CNS were associated with VL within the CSF but not with Plasma VL (McClernon et al. 2001; Sei et al. 1996). Damage to the corpus striatum appears to occur despite treatment and is possibly related to the rate of initial insult, following initial penetration of HIV into the CNS (Andronikou et al. 2014; Becker et al. 2011).

Anatomical changes that accompany development in healthy children are well documented (Bendersky et al. 2006; Caviness et al. 1996; Dowker 2006; Fan et al. 2011; Giedd et al. 1999; Rapoport et al. 2001). Some studies that have attempted to conduct longitudinal research in HIV have not accurately described the effect of HAART given at or around birth (Koekkoek et al. 2006). Although structural imaging studies of HIV-1 infected children are relatively scarce, one may expect that along with the global atrophy and encephalopathy observed in many HIV-1 infected children, some of the alterations in the subcortical brain structures observed in adults would also be found in children (Safriel et al. 2000).

One study took a unique approach looking at some pre-BBB manifestations of HIV infection in children (Shah et al. 1996). Using MR images, CT scans, as well as autopsy findings, they showed that HIV-1 infected children had certain cerebrovascular abnormalities (Shah et al. 1996). The abnormalities included subacute infarction, fusiform dilation in major vessels of the circle of Willis, as well as some other ischaemic lesions and arteriopathy (Shah et al. 1996). This study, however, comprised only five individuals with ages spanning 9 to 18 years, and thus carries little statistical power. These pathological changes to the arterial supply and lining of vessels of the CNS may result in increased penetration of HIV through the BBB.

Using PET with 18F-labeled fluorodeoxyglucose in a group of 8 children (ranging from 2.5 - 5.5 years of age) born to seropositive mothers and receiving AZT therapy it was found that diffuse hypometabolism and subcortical hypermetabolism was common to individuals with already severe neurological symptoms (n=3) (Depas et al. 1995). Bilateral hypermetabolism was also present in the caudate nuclei of two children, as well as parietal hypermetabolism, while the lenticular nuclei were found to be abnormal in the same two children (Depas et al. 1995). The study showed functional cerebral abnormalities in children without neurological signs, who also had normal morphological images (Depas et al. 1995). Therefore, functional cerebral abnormalities may precede the clinical and neurological signs and symptoms in the brains of HIV-1 infected children (Arendt et al. 1994; Depas et al. 1995; von Giesen et al. 2003; Sacktor et al. 1996). Von Giesen et al. (2003) in a study of 17 HIV-infected children (mean age 12.5±3.4 years, 12 vertically infected,14 receiving HAART, 10 with PVL between 50 and 30000 RNA/ml)observed that CNS pathology in children is mainly centred on the basal ganglia, with major perturbations in cerebral white and deep grey matter (von Giesen et al. 2003). Contrary to most findings observed in adults (von Giesen et al. 2002, 2003; Tozzi et al. 1999), motor performance is slowed leading to an increased recruitment of neural networks in children treated effectively with HAART (von Giesen et al. 2003), a finding supported by Chang et al. (2008) in adults receiving ART. A longitudinal study conducted on 34 children between 4 to 12 years of age (16 HAART naïve initiating HAART, 7 HAART naïve not receiving treatment, and 11 who had already received treatment for over a year) (Koekkoek et al. 2006). Psychomotor tests were administered 0, 4 and 12 months after enrolment. Psychomotor performances were equal between groups at baseline and decreased significantly in the newly treated and untreated groups by 12 months (Koekkoek et al. 2006). Although both groups showed decreased performance over time, the treated group had lower performance in shape tracking, finger tapping and reaction time. Notably the newly treated group had significantly lower CD4% at baseline with high PVL, however all were stable and below 100 RNA/ml at 12 months, whilst untreated had VL between 1000 and 31500 RNA/ml at 12 months. This study raises questions as to the optimal timing of ART initiation and long-term effects of different treatment strategies. To date, no studies have in a systematic way examined long-term effects of HIV and HAART in children, stable on ART, who initiated treatment at different times in infancy/early childhood.

1.5.4 Cognitive-Behavioural Biomarkers of Interest.

Atrophy or pathology of the areas discussed above may result in associated neuropsychological impairment. As stated, HIV dementia is one of the most frequently studied topics with regard to the effects of HIV on the brain (Aylward et al. 1993; Berger & Arendt 2000; Duyckaerts & Litvan 2008; McArthur 2004; Ritola et al. 2005; Sacktor et al. 2004; Xia et al. 2011). Since dementia is mainly linked to the formation and retrieval of memories, the limbic system is of special importance (Leon et al. 2001). Studies of HIV encephalopathy in children show some surprising similarities as well as important differences with HIV-1 neuropathogenesis in adults. It was reported that HIV-1 caused certain delays in neurological development because of calcifications and atrophy of brain areas. Developmental deficits associated with HIV infection in children include impaired language and motor skills, cognitive deficits, impaired visuospatial integration ability, and impaired executive functions (Epstein et al. 1986; van Rie, Mupuala & Dow 2008), with the prevalence of functional deficits increasing with increasing age (van Rie et al. 2007).

Findings regarding behavioural problems associated with HIV infection have been inconsistent. Certain studies showed increased behavioural problems in HIV-infected children (Nozyce et al. 2006), whilst others documented decreased or equivalent behavioural problems in HIV-infected children compared to HIV-exposed, uninfected and control groups (Bachanas et al. 2001; Laughton et al. 2012; Mellins et al. 2003). It has thus been hypothesised that behavioural problems may be as a result of biological or environmental factors as opposed to the direct influence of HIV infection (Mellins et al. 2003).

Deficits in mental development present as a global cognitive deficit later on in infancy (Epstein et al. 1986; van Rie, Mupuala & Dow 2008). The most strongly affected functional domains seem to be that of gross motor skill and function. This is mainly seen when comparing HIV-infected with uninfected children (1 to 11years) (Abubakar et al. 2008; Epstein et al. 1986; Parks & Danoff 1999; Raskino et al. 1999; van Rie, Mupuala & Dow 2008). To date, no studies have systematically investigated differences in specific brain areas linked to cognitive impairments in children infected with HIV-1 (van Rie et al. 2007). Poor language development, most notably deficits in expressive language, is the second most common finding in HIV-infected children (Wolters et al. 1997).

Hyperreflexia and hypotonia have been widely reported (Bagenda et al. 2006; Govender et al. 2011; Laughton et al. 2012) and are both signs of a possible upper motor neuron (premotor) lesion (Kandel, Schwartz & Jessell 2000). Upper motor neuron lesions can occur

in a number of motor pathways originating above the anterior horn of the spinal cord, within the CNS (Kandel, Schwartz & Jessell 2000, p. 600).

Laughton and colleagues (2012) sought to investigate the possible neurodevelopmental effects of early antiretroviral therapy in infants. The children were from the CHER trial; the same cohort from which the children in this study was derived. The authors performed neurological examination and Griffiths Mental Development Scales (GMDS) on the children when they were between 10-16 months of age (Laughton et al. 2012). The sample comprised 26 ART deferred, 64 early ART, 28 HIV-exposed uninfected, and 34 HIV-unexposed uninfected children. All GMDS scores were lower in the deferred treatment arm as compared to children who initiated ART early. General Griffiths and Locomotor scores were significantly lower in the ART deferred group compared to early ART: GQ Score: mean(SD)=100.1(13.8) vs. 106.3(10.6) p=0.02; and Locomotor score: 88.9(16.3) vs. 97.7(12.5), p<0.01, respectively. Early ART children performed as well as uninfected controls except in the Locomotor subscale. The fact that early treatment as well as deferred treatment had lower scores compared to that of uninfected controls in Locomotor scores may be as a result of HAART itself and not merely HIV infection of the CNS alone (Chang et al. 2008; von Giesen et al. 2003; Koekkoek et al. 2006). It needs to be established whether scores for all subscales of HIV-infected as well as uninfected groups fell within the normal range on the GMDS (Laughton et al. 2012). In 2013 Laughton and colleagues highlighted the lack of longitudinal studies of such perinatally infected children from birth through adolescent years (Laughton et al. 2013).

1.6 Standardising Terminology

Terminology and definition of structures is important. Certain atlases and texts avoid clarification of the nucleus accumbens, within the basal ganglia. Certain texts include the cerebellum as part of the basal ganglia, however, negate the inclusion of the substantia nigra and subthalamic nuclei; often contradicting themselves mid-text (Joseph 2000). In other texts the striatum is defined as including only the caudate and putamen (Netter 2002). It is unclear in such texts whether the inclusion of the nucleus accumbens is inferred. The term corpus striatum is used interchangeably with dorsal striatum, however the term 'dorsal striatum' does not include the nucleus accumbens which is part of the ventral striatum (Netter 2002). Due to many incongruences and lack of standardisation, of both physiological and anatomical terms the definition of structures in this study are in line with that defined in:

- Barr's The Human Nervous System: An Anatomical Viewpoint By John Kiernan, Raj Rajakumar, 10th edition (Kiernan & Rajakumar 2013); and
- Principles of Neural Science By Eric Kandel, James H. Schwartz, and Thomas Jessell: Chapter 43: The Basal Ganglia (DeLong 2000).

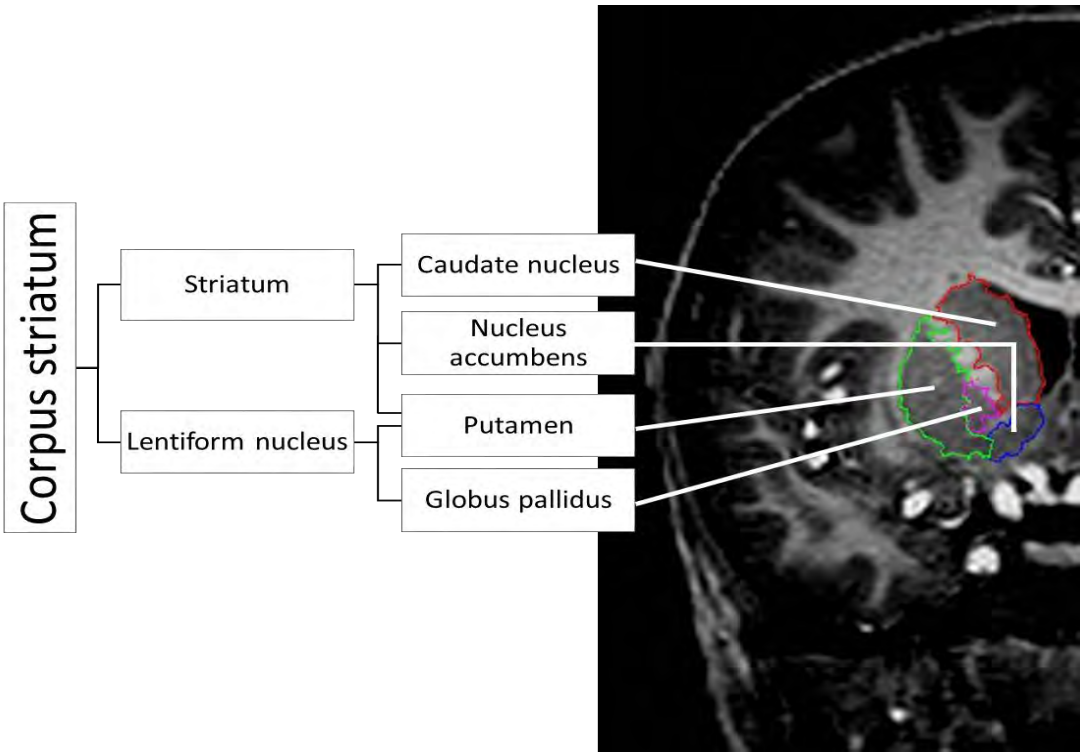

Figure 1.1 Hierarchical structure of the corpus striatum

The basal ganglia refers to a grouping of four subcortical grey matter nuclei, the striatum, globus pallidus, substantia nigra, the subthalamic nucleus (DeLong 2000). These grey matter nuclei are highly connected to the cortex and subcortical motor areas forming complex pathways involved with movement, cognition, affect, motivation and procedural learning (DeLong 2000).

The striatum comprises two main bodies, the caudate nucleus and putamen. The ventral portion (ventral striatum) comprises the nucleus accumbens and olfactory tubercle. The putamen coupled to the globus pallidus is known as the lentiform nucleus. The addition of the globus pallidus to the striatum amends the terminology to corpus striatum (Also referred to as the striated body).

The caudate nucleus lies superiorly to the thalamus and medially to the internal capsule. On the medial surface it is closely associated with the lateral ventricle as well as white matter tracts of the respective hemisphere. Anteriorly the head of the caudate nucleus (the caudate head referred to from here as the caudate (Cd)) is well defined and protuberant. The caudate nucleus begins to taper off gradually as it is viewed posteriorly, this region is known as the caudate tail. The caudate tail terminates in the amygdala.

Together the putamen (Pu) and globus pallidus (GP) form the lenticular nucleus(LN) (Otherwise known as the Lentiform nucleus). The LN is bound laterally by the external capsule and medially by the thalamus and caudate nucleus. Its most antero-medial surface is continuous with the infero-lateral portion of the nucleus accumbens.

The caudate nucleus, Pu, and GP play a role in the planning and modulation of movement pathways. Most findings in the literature have highlighted locomotor deficits in perinatally HIV-infected children (Bagenda et al. 2006; von Giesen et al. 2003; Govender et al. 2011; Laughton et al. 2009, 2013).

The nucleus accumbens (NA) lies anteriorly to the amygdala and inferiorly to the caudate nucleus. The caudate is continuous anteriorly and has projections to and from the nucleus accumbens, which in turn is fused to the inferior portion of the putamen. The NA is a part of the mesolimbic dopamine pathway. It is activated in the presence of a reward and in turn transmits signals to the cortex to acknowledge the incentive; further stimuli are directed to the GP and orbitofrontal cortex eliciting a pleasurable response. This area is thought to be responsible for goal-related activities, and plays an important role in both learning and addiction (Bernier, Whitaker & Morikawa 2011; Berridge 2007; Doya 2000).

The corpus callosum (CC) is the major inter-hemispheric connection. It consists of a wide, flat bundle of neural fibres (axons) located in the midline at the longitudinal fissure (Kandel, Schwartz & Jessell 2000). It connects and allows communication between the left and right cerebral hemispheres, via callosal fibres.

1.7 Manual versus Automated Segmentation

For an accurate study of the effects of pathology on the brain, a large cohort of autopsy patients would be ideal, however when dealing with HIV-1 infection in children, death caused by opportunistic co-infections is a definite confounding factor (Wrzolek et al. 1995). Neuroimaging via MRI is non-invasive. As such, MRI is a solution to viewing the brain of individuals, as opposed to exploratory surgery, which is impossible when dealing with a living individual (Morey et al. 2009). In light of the above, MRI in conjunction with manual segmentation remains the gold standard in estimating the volumes of brain regions (Barnes et al. 2008; Boccardi et al. 2011; Dewey et al. 2010; Hasan & Pedraza 2009; Morey et al. 2009; Sánchez-Benavides et al. 2010; Tae et al. 2008).

As image acquisition has become faster, cheaper and more detailed, the need for answers to pertinent questions, involving the brain and the effects of various pathologies on the brain, has become more apparent. As such, large databases of MR images are being accumulated at a hurried rate. The accumulation of such large databases allows more researchers to delve into quantitative assessments to examine subtle relationships between various brain areas and disease progression, efficacy of treatment regimens, and other factors that may not have been able to be distinguished in smaller samples (Morey et al. 2009; Powell et al. 2008). Manual tracing has been an excellent mode of investigation, however, as the size of datasets has increased the demand on the individual, tracing by hand, as well as the labour cost to the research team has increased to the point where it is no longer a feasible option. With the advent of automated segmentation techniques and fast developing improvements to their accuracy, manual tracing has evolved into a tool to test the reliability of automated techniques, on a small subset of the sample in question, rather than the primary mode of investigation.

1.7.1 Shortcomings of Manual segmentation

Albeit the preferred more accurate mode, manual tracing is thwarted with shortcomings. The first major drawback, alluded to before, is time. An experienced neuroanatomist may require two hours to trace the Pu and GP, and up to ten hours to trace all structures within the basal ganglia, for a single dataset. Even an experienced individual would find it an extremely taxing experience (physically) to spend such extended periods of time in front of a backlit display. To counteract this issue, one could employ more researchers to trace the regions of Interest (ROIs), dividing the workload. However, differences in knowledge between researchers regarding borders of ROIs and subtle differences in subjective thinking (and thus judgement calls for approximate borders of ROIs) may lead to systematically different volume estimates (Morey et al. 2009). Thus, the highest consistency and reliability is achieved by employing a single researcher to delineate all ROIs within a dataset (Morey et al. 2009). To combat this problem, training would need to be established for all manual tracers. Although costly and time consuming, this would occur where the primary researcher has sessions with fellow researchers and guides them through the tracing protocol for each ROI, slice-by-slice, for a number of scanned participants, such that judgement calls and criteria for borders of ROIs are more standardised and established.

Even veteran experts introduce inter-rater and intra-rater variability via criteria drift and bias to the manual outlines which are suggested to be absent in automated computer generated techniques (Boccardi et al. 2011; Mulder et al. 2014; Powell et al. 2008). That being said, inter-rater reliabilities via retracing a subset of the sample by an independent tracer is often employed to gauge the reliability of the single rater. Intra-rater reliabilities are obtained by retracing a subset of images at a later time.

As a result of the shortcomings listed above automated segmentation and parcellation has gained substantial attention over the past few years. Automated techniques provide fairly consistent repeatable results (Morey et al. 2009). Updated software and improvements to segmentation and parcellation algorithms, as well as improvements to atlases are readily accommodated (Han & Fischl 2007; Morey et al. 2009).

1.7.2 Automated Segmentation using FreeSurfer

During automatic subcortical segmentation, each voxel in the normalized brain volume is assigned one of about 40 labels. Automatic subcortical segmentation (aseg) of a brain volume is based upon an atlas containing probabilistic information on the location of structures (Fischl et al. 2002). The atlas was generated from a large training set of manually traced measurements (Fischl et al. 2002). The automatic subcortical segmentation can take over 11 hours to complete (http://ftp.nmr.mgh.harvard.edu/fswiki/SubcorticalSegmentation).

As stated before, it was suggested that inter-rater and intra-rater variability and bias may be absent in automated computer generated techniques (Boccardi et al. 2011; Mulder et al. 2014). However, a paper published in 2012 shed light on some factors that may contribute to varying results obtained via the FreeSurfer software (Gronenschild et al. 2012). In the results of segmented volumes gathered from a group of 30 T1-weighted 3T MRI scans the group showed significantly different results between FreeSurfer version, as well as between type and version of operating system and workstation specifications (Gronenschild et al. 2012). Another two variables which may affect the accuracy of segmentation techniques, are datasets that originate from either a different scanner platform or pulse sequence than that of the original dataset from which the training atlas was derived (Han & Fischl 2007). This could relate to MR scanners of different make or model, or even the same scanner from which the original dataset was acquired that has had software or hardware upgrades. As international collaboration and multicenter clinical research has become easier with the advent of high bandwidth internet and cloud-based datasets archiving the need for standardised outputs has become a necessity (Han & Fischl 2007). Not all research groups or hospitals would have a standardised MR scanner platform. However, some investigators have addressed this problem by introducing an intensity renormalization procedure that automatically adjusts the atlas intensity model (derived from the training set of manually traced measurements) to new input data (Han & Fischl 2007). The new procedure was tested using 27 subjects. The results indicated little to no effect on the performance of automated segmentation, if no contrast change was expected. However, average Dice coefficients improved by over 10% for numerous structures, compared to the non-renormalized model, when data was gathered via a different scanner platform (Han & Fischl 2007). This approach caters for data acquired across different scanner platforms, as well as rendering the tools largely insensitive to scanner upgrades and variations in pulse parameters (Han & Fischl 2007).

Regardless of numerous sophisticated software packages, with algorithms capable of powerful automated segmentation, there is still a lack of comprehensive published research comparing automated software to manual tracing (Barnes et al. 2008; Dewey et al. 2010; Morey et al. 2009; Powell et al. 2008). That being said, certain investigators have sought to gauge the efficacy of various modes of segmentation techniques. Not only did they investigate the similarity of the volumetric measurements, but they also investigated their reliability in highlighting the effects of certain pathologies on the brain (Dewey et al. 2010; Hsu et al. 2002; Morey et al. 2009; Tae et al. 2008). To gauge the efficacy of certain atlases, as well as segmentation software, researchers often opt for areas such as the hippocampus or amygdala (Barnes et al. 2008; Hsu et al. 2002; Morey et al. 2009; Mulder et al. 2014; Sánchez-Benavides et al. 2010; Tae et al. 2008). These structures bear large contrast and are already easily distinguishable compared to surrounding tissues.

1.7.3 Comparison of Segmentation Techniques in HIV Cohorts

The only comprehensive study on an HIV cohort (n=120; mean age 47.3±7.2 yrs) and the efficacy of various segmentation techniques was performed by Dewey et al. (2010). They too highlighted the vastness of literature pertaining to testing the reliability of automated segmented volume versus manual tracing of the hippocampus and relative scarcity of research pertaining to other subcortical structures (Dewey et al. 2010). They compared three segmentation techniques, two automated software packages and one auto-assisted manual (AAM) measurement, to gauge the accuracy and consistency of the techniques. The automated software used were FreeSurfer and Individual Brain Atlases using Statistical Parametric Mapping (IBASPM). Their AAM measurements were acquired from a customised version of the FreeSurfer software and via manually correcting the outputs (Dewey et al. 2010). The main reasoning behind the usage of an auto-assisted technique was to save time, as exclusive manual tracing is exceptionally time consuming (Dewey et al. 2010). The use of AAM to gauge accuracy and consistency could arguably introduce bias to analyses, as correlations with the FreeSurfer software would naturally be higher, as was found to be the case, as the AAM technique is derived from the FreeSurfer software and atlases. Following manual correction, the volumes gained are not entirely mutually exclusive from the automated FreeSurfer derived volumes and the results of this process may be somewhat confounded. Dewey and colleagues addressed this issue by manually tracing a subset of their sample and correlating the manually segmented volumes with that of the AAM measurements (Dewey et al. 2010). They observed an extremely strong correlation between manual and AAM techniques in all structures measured (Cronbach's $\alpha>0.90$) (Dewey et al.

2010). A significant Cronbach's $\alpha>0.90$ falls within the range of what can be expected when correlating inter-rater reliabilities between manual tracers (Dewey et al. 2010; Morey et al. 2009; Tae et al. 2008).

There is very little literature pertaining to the reliability of automated segmentation in the developing brain, let alone the efficacy of these techniques in the developing brain with presence of pathology.

1.8 Research Aims and Objectives

1.8.1 Selection of Regions of Interest

As reported the basal ganglia and surrounding structures are of particular interest when studying the effects of HIV-1 infection on the brain. Previous studies have revealed calcifications, abnormalities in metabolism and function of the basal ganglia in both children and adults. Perturbations in white matter have also been found, specifically in the corpus callosum of HIV-1 infected children. In this study, we have chosen to examine brain volumes in areas that relate to specific functional and cognitive domains where impairment has been reported, specifically with regard to functional deficits reported in the CHER cohort (Laughton et al. 2012).

1.8.2 Aims:

The primary aim of this study is to assess differences in the volumes of selected regions of interest in the developing brain of 5-year old children, with HIV and receiving HAART compared to uninfected controls, using high-resolution structural MRI and manual tracing. Results from manual tracing will be compared with findings from automated segmentation using FreeSurfer.

CHAPTER 2 MATERIALS AND METHODS

2.1 Study Participants

This study included fifty-one 5 year old children from the Children with HIV Early Antiretroviral Therapy (CHER) trial (Cotton et al. 2013) and 30 uninfected control children who were either recruited specifically for this study (n=6) or from an interlinking vaccine trial (n=24).

Children with HIV-1 infection belonged to one of three treatment arms: ART-Def (ART was deferred unless CD4% < 25% in first year or CD4% < 20% from second year onwards, or if a selection of other immunological/clinical criteria presented), ART-40W (ART initiated immediately and interrupted after 40 weeks), and ART-96W (ART initiated immediately and interrupted after 96 weeks) (Cotton et al. 2013).

2.2 Data Collection and Data Transformation

2.2.1 Neuroimaging Protocol

All children received MRI scanning on a 3T Allegra MRI (Siemens, Erlangen, Germany) at the Cape Universities Brain Imaging Centre (CUBIC) according to protocols that had been approved by the Human Research Ethics Committees of the Universities of Cape Town and Stellenbosch. All parents provided written informed consent and all children provided oral assent.

High-resolution T1 weighted images were acquired using a volumetric echo-planar imaging (EPI) navigated (Tisdall et al. 2012) multi echo magnetization prepared rapid gradient echo (MEMPRAGE) sequence (van der Kouwe et al. 2008) Imaging parameters were: FOV: 224 x 224 mm^2; 144 sagittal slices, TR: 2530 ms; TE: 1.53/3.19/4.86/6.53 ms; TI: 1160 ms; Flip angle: 7°; voxel size: 1.3 x 1.0 x 1.0 mm^3, scan time 5:20. The 3D EPI navigator provided real-time motion tracking and correction which served to substantially reduce the presence of any motion artefacts in the structural imaging data, despite significant subject motion.

Data of three uninfected control children were excluded from the analyses: two due to incomplete scanning data and poor image quality; one due to the presence of pathology. As such, scans for 78 children (51 HIV-1 infected/27 uninfected controls; 11 Cape Coloured/67 Xhosa) were traced.

2.2.2 Data Pre-processing

Each subject had a pre-assigned participant ID to ensure anonymity. Each scan's DICOM files were manually transformed into the AC-PC plane and rotated for hemispherical symmetry using BrainVoyager QX software (Brain Innovation, Maastricht). The DICOM files were exported in analyse format (*.img; *.hdr).

2.2.3 Manual Tracing Protocol

Summary of the Manual Tracing Protocol

All structures were manually traced using MultiTracer software (http://bishopw.loni.ucla.edu/MultiTracer/) on a Lenovo ThinkPad X200 tablet and integrated active digitizer stylus. Dr Christopher Warton, a neuroanatomist from the Department of Human Biology at the University of Cape Town developed the protocol used to trace and delineate the structures of interest.

All tracings were performed at 4X magnification. Magnifications greater than this resulted in visible pixelation of the images. In Multitracer software it is possible to adjust the contrast and brightness (Woods 2005). The contrast is adjusted by manipulating a threshold value where any pixels with image intensity values below a chosen threshold appear black (Woods 2005). The range of prescribed voxel intensities range from 0 to 65535 pixel intensity units (PIU) in the Multitracer software (Woods 2005). Image files loaded into the program are scaled accordingly to fit this pixel intensity range (Woods 2005). The contrast used in this study ranged from PIU of 13000 to 18000 depending on the structures measured. Screen brightness for the tracing tablet was set to 100%. Brightness of images loaded into the software was set to 1.34 (49% of a maximum unadjusted default scale value of 2.72) for most structures, however adjusted accordingly depending on structures of interest and ambient lighting (Woods 2005).

MultiTracer allows one to trace the brain structure in each of the three orthogonal planes: sagittal, horizontal and coronal. The tracings of selected brain structures were completed by manually outlining the structures on MR images, slice by slice. Once the subcortical structures were fully outlined in the respective plane for multiple contiguous slices, MultiTracer software computes the area of the contour on each slice and calculates the overall volume of the structure. The frust volumes calculated by MultiTracer were used in the present study. Frust volume is calculated by assuming that the structure extends from the centre of the first plane on which it was drawn to the centre of the last plane on which

it was drawn with the square root of areas varying linearly when moving from the centre of one plane to the centre of the next (Woods 2005). For standardisation purposes, tracing of all subcortical grey matter structures were performed in the coronal plane. Other planes (sagittal or horizontal) were employed as reference planes assisting with tracing in the primary plane. Contours created in other planes appear as a formation of dots forming the outline of the structure in the primary plane. These reference points aided tracing of the contour in the primary plane.

Reliability of Manual Segmentation

Inter-rater and intra-rater reliabilities were assessed for each structure using independent measurements for 10 participants who were randomly selected by an expert neuroanatomist and primary researcher, respectively, and assessed via Pearson and intra-class correlation.

2.2.4 *Specific Tracing Protocol for Regions of Interest*

Due to its frequency in the HIV literature, the basal ganglia was the primary subcortical region of interest (ROI). All grey matter structures within the basal ganglia were traced, with the exception of the substantia nigra and subthalamic nuclei.

Caudate and Nucleus accumbens

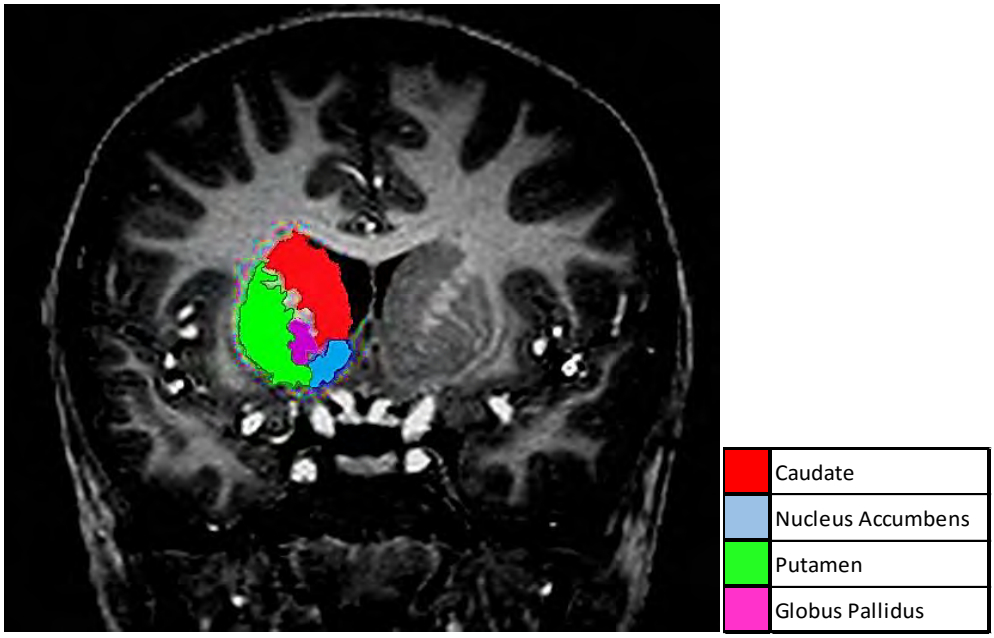

Figure 2.1 Coronal view of an MRI scan showing the four different structures that were traced in the right basal ganglia

Both the caudate and nucleus accumbens were traced in the coronal view. Contrast was set so that PIU less than 13000 appeared as black and brightness to 1.34.

The caudate was traced from the anterior tip of the structure moving posteriorly. The caudate gradually decreases in size to the point where it becomes indistinguishable from surrounding tissues at the posterior end and curves infero-posteriorly toward the thalamus. We completed the tracing for this structure at this point. It is important to note that the caudate is continuous anteriorly and has projections to and from the nucleus accumbens, which in turn is fused to the inferior portion of the putamen. The exact borders between these aforementioned structures are not clearly defined on MR images. The true borders of these structures can only truly be found cytoarchitectonically. It is for this reason that both the caudate (caudate head) and nucleus accumbens were initially traced as a single unit. The lateral border of the nucleus accumbens associated with the putamen was demarcated by a single vertical line (in each slice) arising from the inferior border of the lateral limb of the internal capsule downward to the lower boundary of the ventral striatum. The volume of

the full structure was calculated including both the caudate and the nucleus accumbens. Subsequently, the nucleus accumbens was partitioned away and removed from the current trace. This was achieved by an oblique line (in all slices) from the inferior limb of the lateral ventricle to the inferior border of the internal capsule. The new volume thus derived was that of the caudate alone, while the difference between the two measurements was that of the nucleus accumbens.

Putamen and Globus pallidus

Both the putamen and globus pallidus were traced in the coronal view. Contrast was set so that PIU less than 18000PIU appeared as black and brightness to 1.34. The junction between the putamen and globus pallidus is readily seen in the horizontal plane. A few traces in the horizontal plane acted as reference to the borders between the two structures when tracing in the coronal plane. The coronal plane is still the optimal plane for measurement as it allows one to distinguish superior and inferior borders of both structures from surrounding tissues. Much like the caudate and nucleus accumbens, both structures were traced as a single entity. The volume for the combined structure was calculated. The globus pallidus was then partitioned away and removed. This was done by making use of the reference points created in the horizontal plane and drawing a line (in each slice) following the reference points along the medial border of the putamen. The volume for the new structure would thus be that of the putamen alone. The difference between the volumes of the two structures is that of the globus pallidus.

Corpus Callosum

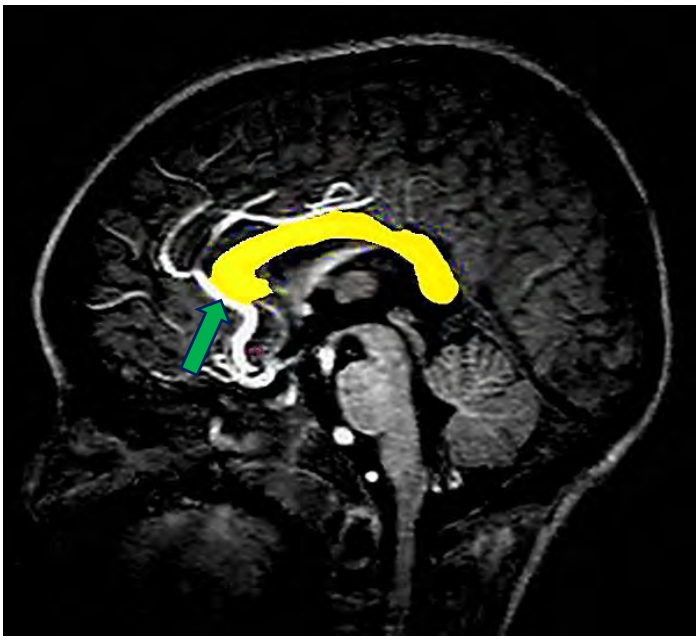

Figure 2.2 Sagittal view of an MRI scan showing the corpus callosum in yellow

The corpus callosum was traced in the sagittal view. Contrast was set so that PIU less than 13000PIU appeared as black and brightness adjusted accordingly to optimally highlight the structure of interest. The blood vessel indicated with a green arrow (Fig2.2) often occluded the view of the corpus callosum and thus frequent adjustment of the brightness was necessary to adequately view the structure.

The tracing of the corpus callosum involved finding the midline of the subject's brain, in the sagittal plane. As the MRI scans were AC-PC transformed and rotated, the midline often fell between the middle few slices of the scan (approximately slice 128/256). The exact midline was found by visually inspecting slices adjacent to slice 128 in order to identify the slice where the thalamus appeared to be the smallest in size. This midpoint of the thalamus marks the midline of the midbrain and is known as the massa intermedia. The corpus callosum was then traced in adjacent slices, either side of the midline, in the sagittal plane. The volume of a single slice was calculated by dividing the volume for both slices by the number of slices traced (two).

2.2.5 Automated Volumetric Measurements

Brains of each subject were automatically segmented by an independent researcher into cortical and subcortical regions using FreeSurfer software (http://surfer.nmr.mgh.harvard.edu/). The atlas used in this study was aseg+aparc a2009. The outcome of the segmentation process is a labelled volume comprising 175 white matter (WM), grey matter (GM) and cerebrospinal fluid (CSF) regions. Segmentations were checked for errors and manually corrected where needed, after which automatic reconstruction was repeated. This process was repeated in an iterative way.

2.3 Data handling and Statistical Analyses

The primary researcher was blinded to all participant demographic data and automated results pending the completion of manual tracing.

Statistical analyses were managed and performed in Statistica 11 (StatSoft Inc. 2012) and IBM SPSS Statistics 22 (IBM Corp. 2013). Descriptive statistics were compiled for all variables. A Shapiro-Wilk test was used to test for normality of continuous variables (Shapiro & Wilk 1965). Appropriate results were displayed and relevant tests performed depending whether the variables in question were parametric or nonparametric. The Grubbs' Test was used to test for any possible outliers in the sample (Grubbs 1969).

2.3.1 Standardization for Brain Size

A reduction of total brain size and underlying structure, as a result of HIV-1 infection has been reported in adults (von Giesen et al. 2000; Lawrence & Major 2002). Thus, controlling and standardising for total brain size in adults may be necessary. Over and above the expected global atrophy, resultant from HIV-1 infection, controlling for brain size would allow one to determine pathology. In children it is uncertain whether global atrophy or hypertrophy would be expected. As such, structural volumes were not normalised for total brain volume in this study.

2.3.2 Testing for Confounders

Sex, age at scan, birthweight, and ethnicity were investigated as possible confounders of the effects of HIV and ART on brain volumes. Possible sampling bias was investigated.

Categorical Confounders

A Chi squared test was used to examine associations within categorical confounding variables (sex and ethnicity) and their distribution across treatment groups. Univariate analysis of variance (ANOVA) was performed to test for possible volumetric differences resulting from the potential confounding effects of each categorical confounding factor.

Continuous Confounders

The association of continuous variables (age at scan and birthweight) were examined via univariate ANOVA to assess differences in the means between treatment groups. A Pearson or Spearman rank ordered correlation was used to test the correlation of continuous variables with structural volumes.

Subset Removal

Ethnicity was found to be a major confounding factor (Appendix A). Significant volume differences between Xhosa and Cape Coloured individuals were observed. The distribution of children across treatment groups were also found to be not well matched within the Cape Coloured group. As such, the Cape Coloured subset (n=11) was removed from the sample, leaving 67 Xhosa children (49 HIV-1 infected and 18 uninfected controls).

Five HIV-1 infected children were symptomatic at the time of enrolment and required immediate therapy. These children were not randomized into treatment groups. These too were excluded from further analyses, leaving 62 Xhosa children (44 HIV-1 infected and 18 uninfected controls).

Analyses for the remaining confounders (sex, age at scan and birthweight) were recalculated for the remaining children.

2.3.3 Hypothesis Testing: Structural Volumes between Groups

Univariate analysis of variance (ANOVA) was used to test for any significant differences between the structural volumes of diagnostic groups (HIV-1 infected versus uninfected controls) and treatment groups (ART-Def vs ART-40W vs ART-96W vs uninfected controls). For a single categorical variable comparing more than two factors but less than four a Fisher's Least Significant Difference test (LSD) was used for post-hoc analyses.

Analysis of covariance (ANCOVA) was performed to control for effects of covariates found to have significant association with structural volumes (sex and age at scan).

2.3.4 Hypothesis Testing: Structural Volume across Clinical Measures

Associations of structural volumes with clinical continuous variables were assessed using Pearson or Spearman rank ordered correlations amongst infected children only. If a continuous independent variable was found to be not normally distributed, a Spearman Rank ordered correlation was used to test for a significant relationship between the predictor variable and the structural volumes of the areas measured.

Plasma Viral Load (PVL) values for 2 time points (enrolment and prescan) were transformed into categorical variables, with values below 399 copies RNA/mL denoted as suppressed "Suppressed", 400-750 000 copies RNA/mL as "Low", and greater than 750 001 as "High".

Associations of structural volumes with CD4+ percentage (CD4%) was investigated at 3 time points (enrolment, prescan and nadir), as a continuous variable, using Pearson correlation. As in the original CHER study (Cotton et al. 2013; Violari et al. 2008) on HIV-1 infection and effects of treatment outcomes of HAART, where a CD4% of less than 25% was considered immunocompromised and a CD4% greater than 25% as being within the normal range.

CD4/CD8 ratio was investigated in a similar way. Values less than 1 were considered immunocompromised, greater than 1 as healthy, and values greater than 2 indicated a strong immune system. Nadir CD4/CD8 ratio was not available for analyses. Associations of structural volumes with CD4/CD8 ratio and CD4% were compared and the variable most strongly related to volume was noted.

As no clinical data was available for the control group, a Factorial ANOVA could not be performed.

2.3.5 Regression Analyses

Covariates of sex and age at time of scanning were investigated for possible associations with volume, for each structure. Only covariates found to be weakly related (p<0.1) to volume were retained in the regression model.

The Bonferroni method was used to correct for multiple comparisons testing and possible Type I error. The Bonferroni adjusted P-values were generated by dividing 0.05 by the number of permutations present in each set of analyses.

(Eg. $\text{Adjusted } P \text{ cut off} = \frac{0.05}{(\text{Number of structures analyzed}) \times (\text{Number of independent variables})}$

2.3.6 Hypothesis Testing: Manual versus Automated Measures

The Bland-Altman method for testing agreement between measures was used. A one-sample t-test was used to examine differences between the mean difference (automated volume deducted from manual volume) of structural volumes of manually traced structures compared to that of the automated FreeSurfer derived volumes, and how far they deviated from 0mm^3. Pearson and intraclass correlations were performed to show to what degree the automated measures accurately described the variability seen in manual tracing measures.

Finally, a univariate ANOVA was computed to assess volumetric difference using automated measures between HIV-1 infected and uninfected controls for each structure. This was to gauge the relative efficacy of automated measures in detecting possible pathology, and to assess agreement with results from manual segmentation analyses.

CHAPTER 3 RESULTS

3.1 Sample Characteristics

We present data for 62 Xhosa children (mean age ± s.e. = 5.43 ± 0.04; 25 male) comprising 18 uninfected controls, 17 ART-Def, 14 ART-40W, and 13 ART-96W. Sample characteristics are summarised in Table 3.1.

Table 3.1 Sample Demographics

Biographical Data		Uninfected Control (n=18)	HIV-1 Infected ART-Def (n=17)	HIV-1 Infected ART-40W (n=14)	HIV-1 Infected ART-96W (n=13)	TOTAL (N=62)	x^2 / *F*	*p*-value
Sex: Male	n(%)	8 (44%)	7 (41%)	4 (29%)	6 (46%)	25 (40%)	1.12	0.77
Age at Scan [Yrs][1]	Mean(SD)	5.6 (0.5)	5.3 (0.3)	5.4 (0.2)	5.4 (0.3)	5.4 (0.3)	**3.05**	**0.04**
	(Range)	(5.07-6.52)	(4.94-5.91)	(4.98-5.85)	(5.07-5.87)	(4.94-6.52)		
Birth weight [g]	Mean(SD)	3104 (641)	3126 (352)	3136 (462)	2999 (447)	3092 (483)	0.04	0.99

Values are Mean (SD), Range, or number(%) where specified.

Chi^2 for categorical Associations *F* statistic from Univariate ANOVA for parametric data.

Yrs=Years. g=Grams. SD=Standard deviation.

*Posthocs

1 Uninfected Controls>ART-Def,ART40W $p<0.05$

Uninfected Controls>ART-96W $p<0.1$

Demographic variables did not differ between groups except that uninfected children were slightly older than infected children. However, the age range of HIV-1 infected children fell within the range of uninfected controls. Although there was no significant sex difference between groups, the ART-40W group did have fewer males than all the other groups.

3.2 Reliability of Manual Segmentation

Table 3.2 shows inter- and intra-rater ICC, as well as Pearson's correlation, in each structure for a random selection of 10 brains that were retraced by an independent or the same observer, respectively.

Table 3.2 Inter- and Intra-observer Reliabilities for Manual Segmentation

		INTER-RATER		**INTRA-RATER**	
			ICC		**ICC**
		Pearson	Cronbach's	Pearson	Cronbach's
ROI		*r*	α	*r*	α
L Caudate+NA	Coeffiecient	**0.78**	**0.86**	**0.99**	**0.99**
	p -Value	**0.007**		**<0.001**	
R Caudate+NA	Coeffiecient	**0.72**	**0.84**	**0.98**	**0.99**
	p -Value	**0.019**		**<0.001**	
L Caudate	Coeffiecient	**0.71**	**0.83**	**0.99**	**0.99**
	p -Value	**0.020**		**<0.001**	
R Caudate	Coeffiecient	**0.74**	**0.85**	**0.98**	**0.99**
	p -Value	**0.015**		**<0.001**	
L NA	Coeffiecient	**0.78**	**0.87**	**0.95**	**0.96**
	p -Value	**0.008**		**<0.001**	
R NA	Coeffiecient	**0.86**	**0.90**	**0.82**	**0.83**
	p -Value	**0.001**		**0.003**	
CC	Coeffiecient	**0.93**	**0.94**	**0.89**	**0.94**
	p -Value	**<0.001**		**0.001**	
L Pu+GP	Coeffiecient	**0.89**	**0.88**	**0.98**	**0.99**
	p -Value	**0.001**		**<0.001**	
R Pu+GP	Coeffiecient	**0.8**	**0.86**	**0.99**	**0.99**
	p -Value	**0.006**		**<0.001**	
L Pu	Coeffiecient	**0.86**	**0.89**	**0.98**	**0.99**
	p -Value	**0.001**		**<0.001**	
R Pu	Coeffiecient	**0.77**	**0.85**	**0.98**	**0.93**
	p -Value	**0.009**		**<0.001**	
L GP	Coeffiecient	**0.78**	**0.80**	**0.88**	**0.93**
	p -Value	**0.008**		**0.001**	
R GP	Coeffiecient	**0.75**	**0.84**	**0.93**	**0.96**
	p -Value	**0.012**		**<0.001**	

All inter-rater Pearson correlations were highly significant and ranged from r=0.71 for the left caudate to r=0.93 for the corpus callosum. *Cronbach's α*'s were above 0.8 in all regions.

In all regions, intra-rater Pearson correlations were greater than r=0.82, and *Cronbach's α's* were all above 0.83.

3.3 Structural volumes between HIV-infected and uninfected children

Table 3.3 shows a comparison of structural volumes between uninfected and infected children both before and after controlling for potential confounders. Table 3.4 shows relations between volumes and potential confounders – sex, birthweight and age at scan.

Table 3.3 Comparison of structural volumes by diagnosis

	Uninfected Controls (n=18)	HIV-1 Infected (n=44)				
ROI (mm^3)	Mean (SD)	Mean (SD)	*F*	*p-value*	*F*[a]	*p-value*
L Caudate + NA	4564 (619)	4650 (472)	0.350	0.56	0.230	0.63
R Caudate + NA	4772 (583)	4867 (448)	0.486	0.49	0.305	0.58
L Caudate	4045 (551)	4060 (416)	0.014	0.91	0.003	0.95
R Caudate	4216 (527)	4247 (415)	0.061	0.81	0.000	0.99
L NA	520 (124)	591 (128)	**3.951**	**0.05**	**4.486**	**0.04**
R NA	556 (107)	621 (117)	**4.122**	**0.05**	**5.750**	**0.02**
CC	470 (71)	356 (64)	**38.009**	**<0.001**	**30.801**	**<0.001**
L Pu + GP	6696 (671)	7083 (679)	**4.187**	**0.05**	**5.525**	**0.02**
R Pu + GP	6715 (668)	7083 (691)	3.694	0.06	**5.074**	**0.03**
L Pu	4892 (578)	5237 (514)	**5.345**	**0.02**	**8.105**	**0.01**
R Pu	4897 (530)	5270 (512)	**6.665**	**0.01**	**9.280**	**0.01**
L GP	1804 (166)	1847 (210)	0.588	0.45	0.180	0.67
R GP	1818 (181)	1813 (214)	0.009	0.93	0.032	0.86

a After controlling for age at scan and sex

Table 3.4 Relations of structural volumes with sex, birthweight and age at scanning

	Sex		Birthweight		Age at Scan	
ROI	*r*	*p-value*	*r*	*p-value*	*r*	*p-value*
L Caudate+NA	-0.24	0.064	0.06	0.659	-0.08	0.518
R Caudate+NA	-0.24	0.064	0.08	0.555	-0.10	0.450
L Caudate	-0.24	0.061	0.08	0.545	-0.09	0.480
R Caudate	**-0.25**	**0.052**	0.09	0.478	-0.12	0.334
L NA	-0.10	0.431	-0.05	0.713	-0.01	0.928
R NA	-0.04	0.746	-0.03	0.808	0.07	0.600
CC	-0.11	0.391	0.17	0.174	**0.25**	**0.050**
L Pu + GP	**-0.31**	**0.015**	0.02	0.894	-0.02	0.883
R Pu + GP	-0.23	0.070	-0.01	0.960	0.02	0.885
L Pu	**-0.30**	**0.018**	0.02	0.853	0.04	0.781
R Pu	-0.17	0.176	-0.02	0.879	0.05	0.706
L GP	-0.24	0.059	-0.01	0.960	-0.17	0.194
R GP	**-0.34**	**0.008**	0.03	0.818	-0.07	0.615

Sex and age at scan were both retained in the model as the former was weakly ($p < 0.1$) related to structural volumes in all but four regions, and age at scan was related to CC volumes.

CC volumes were about 24% smaller in infected children compared to uninfected children. In contrast, nucleus accumbens and putamen were larger bilaterally in infected children compared to uninfected children. Left and right putamen were 7% and 8% larger, respectively, in infected children, and left and right nucleus accumbens, 14% and 12% larger, respectively. All volumetric differences remained significant after controlling for the potential confounding influences of sex and age at scan.

Table 3.5 Comparison of the association of age with structure volumes in uninfected and infected children.

	Correlation with Age at scanning			
	Uninfected Controls		HIV-1 Infected	
	(n=18)		(n=44)	
ROI	*r*	*p-value*	*r*	*p-value*
L Caudate+NA	0.263	0.292	**-0.373**	**0.013**
R Caudate+NA	0.265	0.287	**-0.393**	**0.008**
L Caudate	0.151	0.551	**-0.330**	**0.028**
R Caudate	0.172	0.494	**-0.399**	**0.007**
L NA	**0.642**	**0.004**	**-0.303**	**0.045**
R NA	**0.599**	**0.009**	-0.091	0.555
CC	0.267	0.285	-0.142	0.357
L Pu + GP	0.287	0.249	-0.064	0.681
R Pu + GP	0.375	0.125	-0.058	0.707
L Pu	0.345	0.161	0.006	0.971
R Pu	0.418	0.084	0.016	0.916
L GP	-0.041	0.871	-0.220	0.152
R GP	0.159	0.528	-0.228	0.136

Further analysis of the association of structure size with age revealed that, albeit over a very narrow age range, age was weakly associated with volume decreases bilaterally in the caudate and in the left NA amongst HIV-infected children only, compared to volume increases bilaterally in the NA amongst uninfected children (Table 3.5). The left NA was the only structure significantly associated with age in both groups. Figure 3.1 shows the opposite association of age with left NA volume amongst infected and uninfected children.

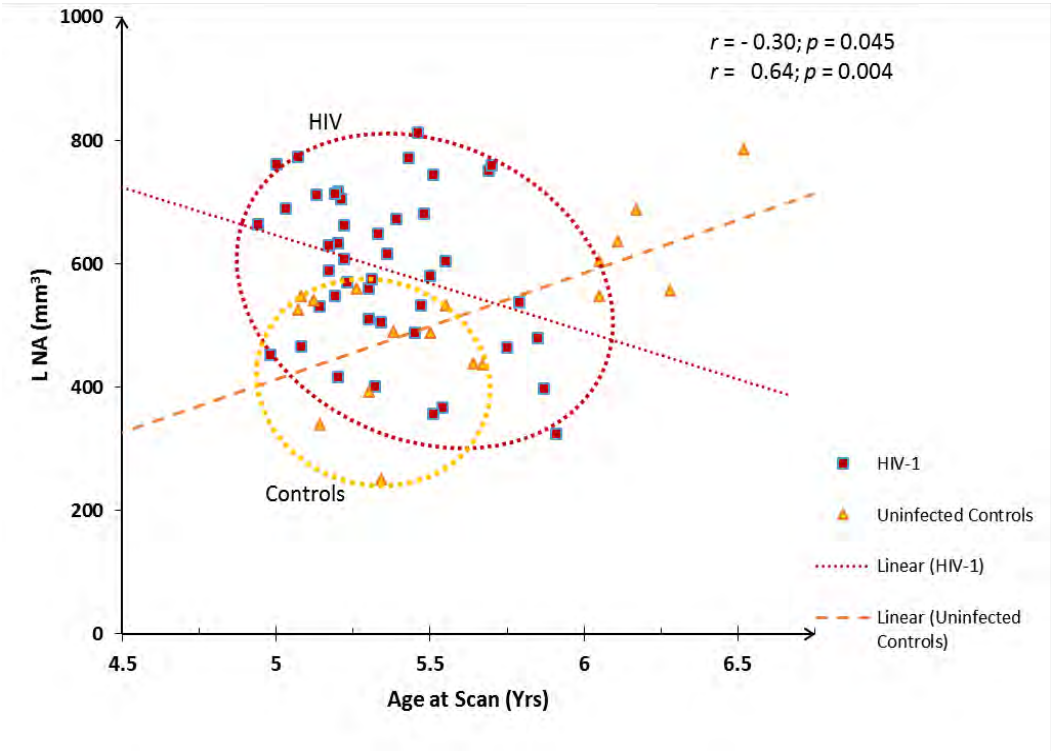

Figure 3.1 Association of age with left NA volume amongst infected and uninfected children

We observe that initially, as well as overall (Table 3.3), HIV-1 infected children had larger left NA than uninfected controls. However, with an increase in age the left NA of HIV-1 infected children decreases in size (156mm^3 p.a.), whilst that of the uninfected controls increases (172mm^3 p.a.).

3.4 Effects of Timing of HAART Initiation on Structural Volumes

In Table 3.6 we present a comparison of structural volumes between uninfected children and infected children that initiated ART at different times, both before and after controlling for potential confounders.

Table 3.6 Comparison of structural volumes by Treatment Group

			HIV-1 Infected						
		Uninfected Controls	ART-Def	ART-40W	ART-96W				
	ROI (mm^3)	(n=18)	(n=17)	(n=14)	(n=13)	*F*	*p-value*	F^a	*p-value*
1	L Caudate+NA	4564 (619)	4678 (415)	4635 (433)	4630 (603)	0.14	0.94	0.102	0.96
2	R Caudate+NA	4772 (583)	4894 (406)	4855 (406)	4846 (566)	0.184	0.91	0.128	0.94
3	L Caudate	4045 (551)	4051 (335)	4099 (385)	4028 (553)	0.059	0.98	0.135	0.94
4	R Caudate	4216 (527)	4252 (348)	4262 (396)	4222 (534)	0.038	0.99	0.062	0.98
5	L NA	520 (124)	627 (140)	536 (101)	601 (126)	**2.761**	**0.05**	**2.845**	**0.05**
6	R NA	556 (107)	641 (134)	593 (89)	623 (121)	1.824	0.15	2.395	0.08
7	CC	470 (71)	345 (47)	367 (80)	359 (68)	**12.7**	**<0.001**	**10.37**	**<0.001**
8	L Pu + GP	6696 (671)	7273 (822)	6963 (483)	6965 (645)	2.13	0.11	2.666	0.06
9	R Pu+GP	6715 (668)	7210 (796)	6963 (559)	7047 (698)	1.559	0.21	2.004	0.12
10	L Pu	4892 (578)	5368 (645)	5129 (327)	5181 (486)	2.354	0.08	**3.354**	**0.03**
11	R Pu	4897 (530)	5366 (624)	5169 (347)	5255 (514)	2.558	0.06	**3.438**	**0.02**
12	L GP	1804 (166)	1905 (222)	1833 (191)	1785 (209)	1.144	0.34	0.979	0.41
13	R GP	1818 (181)	1845 (192)	1794 (240)	1792 (222)	0.222	0.88	0.206	0.89

Values are mean(SD)

a After Controlling for Sex + Age at scan

Posthocs: Before controlling for confounders	Posthocs: After controlling for Sex and Age
5 L NA	5 L NA
ART-Def > Uninfected Controls p <0.05	ART-Def > Uninfected Controls p <0.05
ART-96W > Uninfected Controls p <0.10	ART-96W > Uninfected Controls p <0.10
6 R NA	6 R NA
ART-Def > Uninfected Controls p <0.05	ART-Def > Uninfected Controls p <0.05
	ART-96W > Uninfected Controls p <0.10
7 CC	7 CC
ART-Def, ART-40W,ART-96W < Uninfected Controls p <0.001	ART-Def, ART-40W,ART-96W < Uninfected Controls p <0.001
8 L Pu + GP	8 L Pu + GP
ART-Def > Uninfected Controls p <0.05	ART-Def > Uninfected Controls p <0.05
9 R Pu + GP	9 R Pu + GP
ART-Def > Uninfected Controls p <0.05	ART-Def > Uninfected Controls p <0.05
10 L Pu	10 L Pu
ART-Def > Uninfected Controls p <0.05	ART-Def > Uninfected Controls p <0.01
	ART-40W,ART-96W>Uninfected Controls p <0.1
11 R Pu	11 R Pu
ART-Def > Uninfected Controls p <0.05	ART-Def, ART-40W,ART-96W > Uninfected Controls p <0.05
ART-96W > Uninfected Controls p <0.10	
12 L GP	12 L GP
ART-Def > ART-96W p <0.10	ART-Def > ART-96W p <0.10

Before controlling for sex and age, only the CC and left NA differed between groups. These differences remained significant after controlling for the potential confounding influences of sex and age at scan and, in addition, differences in left and right Pu became significant. Post-hoc analyses revealed that in grey matter differences were typically due to volumes in the deferred treatment arm being larger than in uninfected children, while CC white matter volumes were smaller in children in each of the infected arms compared to uninfected control children. Only in the right Pu were volumes in each of the three treatment arms larger than in uninfected controls. There were no significant volume differences between infected children in the three treatment arms.

Figure 3.2 shows box-and-whisker plots for each structure that revealed a significant difference in volume between children in the different groups before controlling for potential confounders (left) and the accompanying estimated mean and standard error after controlling for confounders (right).

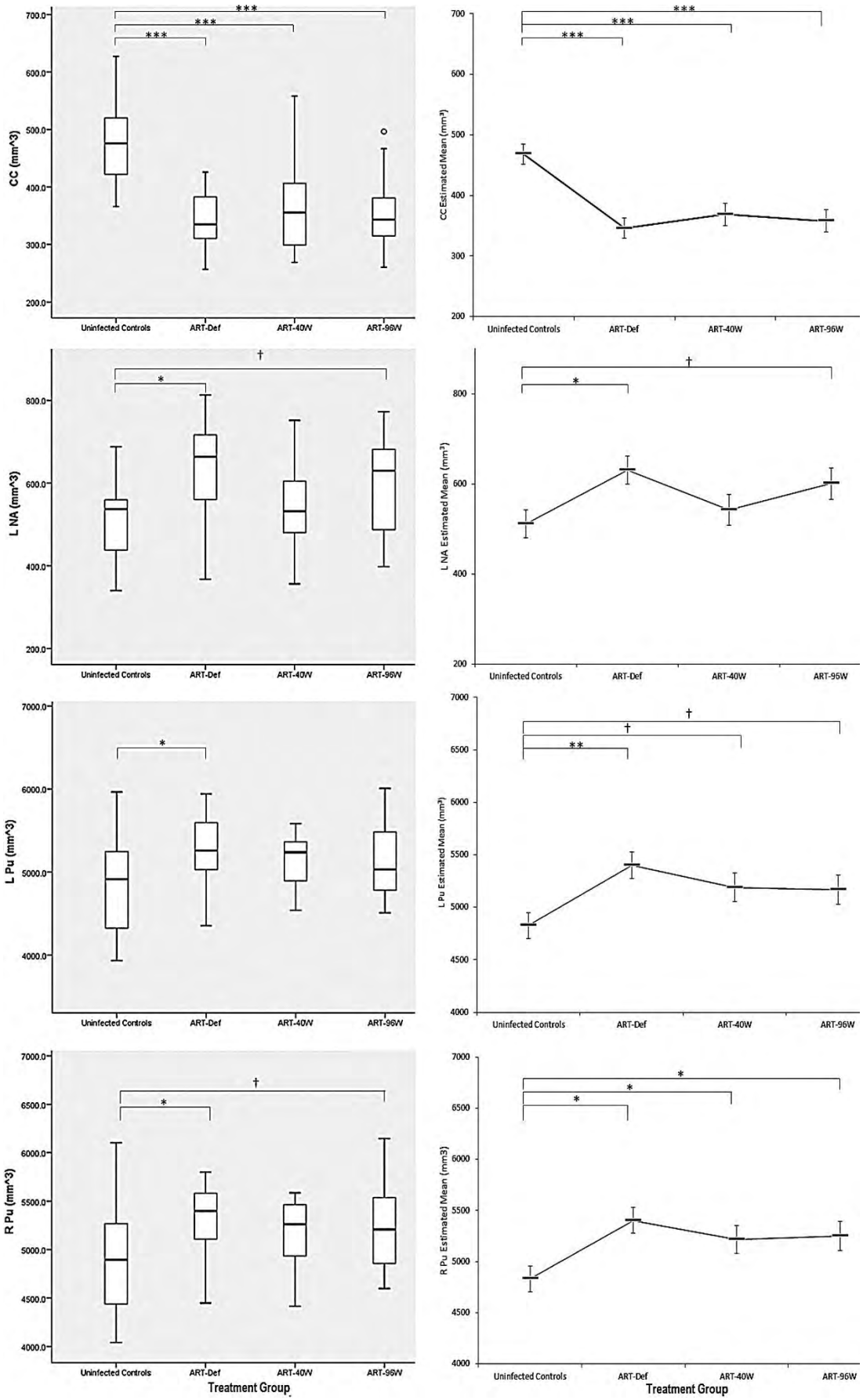

Figure 3.2 Box Plots of volumes for different groups in regions exhibiting group differences both before (left) and after (right) controlling for the potential confounding influences of sex and age at scan.

As there were no significant volume differences between infected children in the three treatment arms, the two early treatment arms (ART-40W, ART-96W) were combined for a separate analysis of early treatment versus deferred treatment. Results of this analysis are presented in Table 3.7.

Table 3.7 Comparison of Structure size by Treatment Initiation.

			HIV-1 Infected						
	ROI (mm3)	Uninfected Control (n=18)	ART-Def (n=17)	ART-Early (n=27)	TOTAL (N=62)	*F*	*p-value*	F^a	*p-value*
1	L Caudate+NA	4564 (619)	4678 (415)	4632 (511)	4625 (515)	0.213	0.81	0.129	0.88
2	R Caudate+NA	4772 (583)	4894 (406)	4850 (480)	4839 (488)	0.279	0.76	0.164	0.85
3	L Caudate	4045 (551)	4051 (335)	4065 (465)	4055 (454)	0.011	0.99	0.028	0.97
4	R Caudate	4216 (527)	4252 (348)	4243 (458)	4238 (446)	0.032	0.97	0.004	1.00
5	L NA	520 (124)	627 (140)	568 (116)	570 (130)	**3.19**	**0.05**	**3.512**	**0.04**
6	R NA	556 (107)	641 (134)	608 (105)	602 (117)	2.516	0.09	**3.46**	**0.04**
7	CC	470 (71)	345 (47)	363 (73)	389 (84)	**19.29**	**<0.001**	**15.694**	**<0.001**
8	L Pu + GP	6696 (671)	7273 (822)	6964 (555)	6971 (694)	**3.25**	**0.05**	**4.003**	**0.02**
9	R Pu+GP	6715 (668)	7210 (796)	7003 (619)	6976 (700)	2.323	0.11	3.058	0.06
10	L Pu	4892 (578)	5368 (645)	5154 (404)	5137 (552)	**3.557**	**0.04**	**5.114**	**0.01**
11	R Pu	4897 (530)	5366 (624)	5210 (429)	5162 (541)	**3.779**	**0.03**	**5.228**	**0.01**
12	L GP	1804 (166)	1905 (222)	1810 (198)	1834 (198)	1.527	0.23	1.118	0.33
13	R GP	1818 (181)	1845 (192)	1793 (227)	1814 (203)	0.339	0.71	0.265	0.77

Values are mean(SD)

a After Controlling for Sex + Age at scan

	Posthocs: Before controlling for confounders	Posthocs: After controlling for Sex and Age
5	L NA	L NA
	ART-Def > Uninfected Controls p <0.05	ART-Def > Uninfected Controls p <0.01
6	R NA	R NA
	ART-Def > Uninfected Controls p <0.05	ART-Def > Uninfected Controls p <0.01
7	CC	CC
	ART-Def, ART-Early < Uninfected Controls p<0.001	ART-Def, ART-Early < Uninfected Controls p<0.001
8	L Pu + GP	L Pu + GP
	ART-Def > Uninfected Controls p <0.05	ART-Def > Uninfected Controls p <0.01
9	R Pu + GP	R Pu + GP
	ART-Def > Uninfected Controls p <0.05	ART-Def > Uninfected Controls p <0.05
10	L Pu	L Pu
	ART-Def > Uninfected Controls p <0.05	ART-Def > Uninfected Controls p <0.01
		ART-Early>Uninfected Controls p<0.05
11	R Pu	R Pu
	ART-Def, ART-Early > Uninfected Controls p<0.05	ART-Def > Uninfected Controls p <0.01
		ART-Early>Uninfected Controls p<0.05

Both before and after controlling for sex and age there were no significant differences between deferred and early treatment groups. As before, ART-Def children had larger volumes than uninfected children bilaterally in the NA and Pu. Further, Pu volumes were larger bilaterally also in early treatment children than uninfected children. CC white matter volumes were smaller in both deferred and early treatment children compared to uninfected controls.

Figure 3.3 shows box-and-whisker plots of the left and right Pu volumes for each group, with estimated mean and standard error after controlling for age and sex alongside.

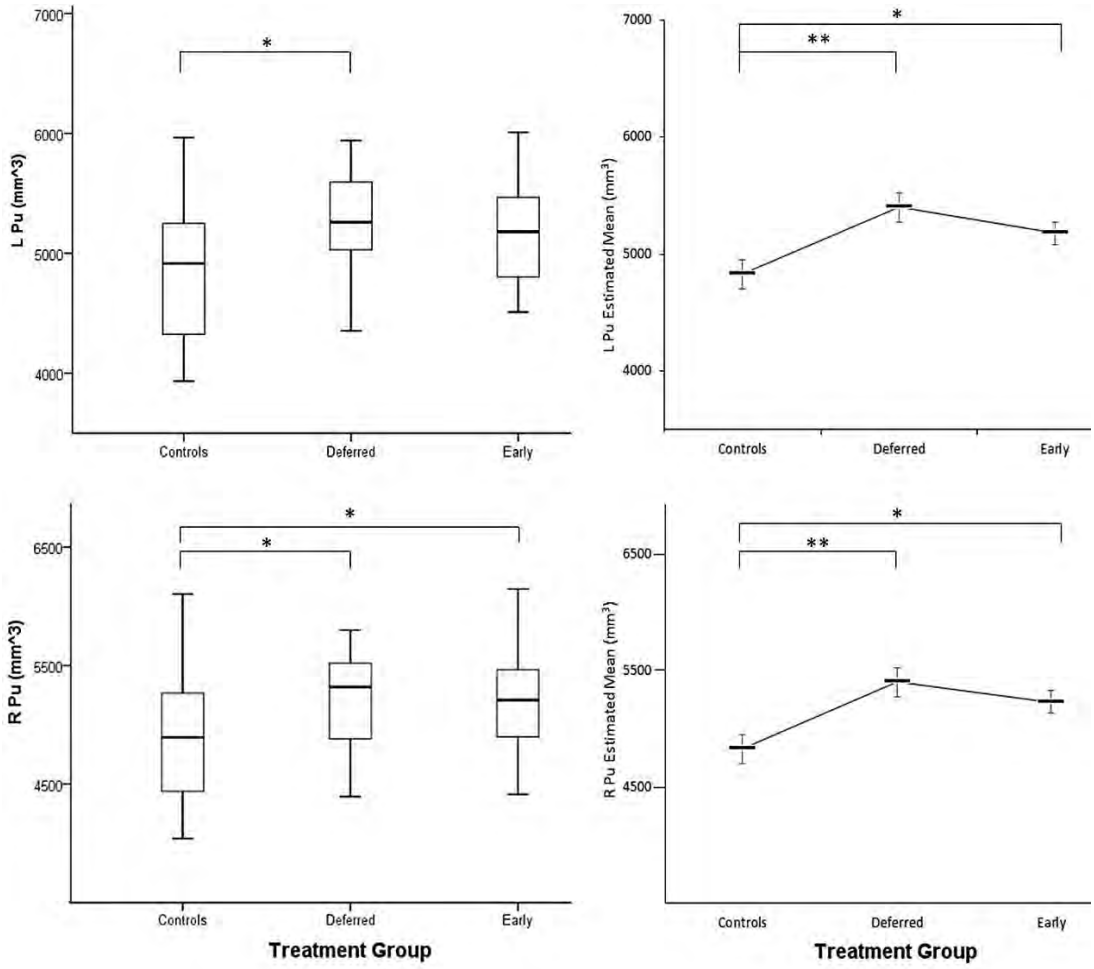

Figure 3.3 Plots showing differences in Pu volumes between uninfected children and infected children receiving either deferred or early treatment both before (left) and after (right) controlling for the potential confounding influences of sex and age at scan.

After controlling for age and sex, when compared to uninfected children, the left and right Pu were 12% larger in the deferred treatment group and 7% and 8%, respectively, in the early treatment group.

3.4.1 Clinical Measures amongst Infected Children

We examined associations of regional brain volumes with clinical measures amongst 44 HIV-1 infected children (17 male) comprising 17 ART-Def, 14 ART-40W, and 13 ART-96W. Clinical data for these children are summarised in Table 3.8.

Table 3.8 Sample Characteristics

		HIV-1 Infected					
Clinical Data[$]		ART-Def (n=17)	ART-40W (n=14)	ART-96W (n=13)	TOTAL (N=44)	χ^2 / *F*	*p*-value
Cumulative Treatment [Wks]	Median(IQR)	243.0 (25.0)	235.0 (42.0)	257.0 (110.0)	242.0 (40.0)	0.92	0.630
Age at ART initiation [Wks]	Mean(SD)	34.1 (16.9)	8.7 (1.6)	7.9 (1.6)	18.3 (16.4)	**30.67**	**<0.001**
Nadir							
CD4%	Mean(SD)	20 (6)	20 (5)	24 (7)	21 (6)	2.03	0.145
Enrolment[α]							
CD4%	Mean(SD)	36 (9)	36 (8)	36 (8)	36 (8)	<0.01	0.998
CD4/CD8 Ratio	Mean(SD)	1.37 (0.69)	1.56 (0.94)	1.35 (0.57)	1.43 (0.74)	0.33	0.724
CD4 Count (Cells/mL)	Median(IQR)	1889 (840)	1605 (1664)	1836 (1308)	1836 (1225)	0.22	0.895
CD8 Count (Cells/mL)	Median(IQR)	1406 (1455)	1293 (953)	1558 (1362)	1398 (1364)	0.86	0.650
Plasma Viral Load (RNA/ml)							
High (≥750001)	n(%)	11 (69%)	3 (21%)	9 (69%)	23 (53%)		
Low (400-750000)	n(%)	5 (31%)	11 (79%)	4 (31%)	20 (47%)	**8.58**	**0.014**
Suppressed (≤399)	n(%)	0 (0%)	0 (0%)	0 (0%)	0 (0%)		
Prescan[§]							
CD4%	Mean(SD)	40 (8)	34 (7)	38 (9)	38 (9)	1.89	0.165
CD4/CD8 Ratio	Mean(SD)	1.57 (0.58)	1.17 (0.52)	1.39 (0.83)	1.38 (0.66)	1.35	0.271
CD4 Count (Cells/mL)	Median(IQR)	1284 (608)	1087 (204)	960 (1251)	1125 (472)	2.46	0.292
CD8 Count (Cells/mL)	Median(IQR)	978 (554)	1107 (529)	1008 (734)	1010 (563)	0.08	0.962
Plasma Viral Load (RNA/ml)							
High (≥750001)	n(%)	0 (0%)	0 (0%)	0 (0%)	0 (0%)		
Low (400-750000)	n(%)	1 (7%)	1 (7%)	2 (15%)	4 (10%)	0.75	0.686
Suppressed (≤399)	n(%)	14 (93%)	13 (93%)	11 (85%)	38 (90%)		

Values are Mean (SD), Median (IQR), number(%)

χ^2 from Kruskal-Wallis ANOVA for non-normal data, *F* from Univariate ANOVA for parametric data.

$ Statistical tests in clinical data were performed for HIV-1 infected individuals only.

Nadir CD4/CD8 ratio was unavailable

α 1 ART-Def did not have clinical data at Enrolment. (Female)

§ 2 ART-Def did not have Clinical Data at Scanning. (1 Male)

Wks= Weeks. SD=Standard deviation. IQR=Interquartile Range

Groups did not differ on most of the clinical variables, except for age of ART initiation which was lower in the two early treatment arms than the deferred treatment arm as per the study design.

CD4/CD8 Ratio and CD4% showed no significant differences between groups at enrolment, or at time of scanning. Nadir CD4% also did not differ between groups.

Plasma Viral load in table 3.8 shows the distribution of children with high, low and suppressed viral loads in each of the three treatment arms both at enrolment and at time of scanning. A viral load of 400 RNA/ml or higher is considered clinically relevant. One

individual at enrolment and two at scanning did not have PVL data. At enrolment all cases were clinically relevant and none were suppressed. The proportion of subjects with high and low PVLs differed significantly between treatment groups at enrolment due to the fact that the ART-40W group had fewer children with high PVL compared to the other two groups. At the time of scanning, most (>85%) of the children in each of the arms had suppressed viral loads.

Table 3.9 presents a comparison of structure size between individuals who had high and low plasma viral loads at enrolment. Volumes in none of the regions differed between children with low and high PVLs at enrolment. This analysis could not be repeated at time of scanning as PVL was suppressed in most of the children.

Table 3.9 Comparison of Structure size by PVL severity at Enrolment

	PVL Severity at Enrolment				
	High (n=23)	Low (n=20)	Suppressed (n=0)		
ROI (mm^3)	Mean (SD)	Mean (SD)	Mean (SD)	*F*-stat	*p-value*
L Caudate + NA	4649 (499)	4670 (456)	- -	0.02	0.889
R Caudate + NA	4894 (525)	4851 (362)	- -	0.10	0.759
L Caudate	4045 (438)	4093 (402)	- -	0.14	0.714
R Caudate	4264 (479)	4247 (339)	- -	0.02	0.895
L NA	604 (135)	577 (124)	- -	0.46	0.499
R NA	630 (131)	604 (98)	- -	0.53	0.470
CC	342 (53)	373 (75)	- -	2.39	0.130
L Pu + GP	6991 (828)	7176 (477)	- -	0.77	0.385
R Pu + GP	7025 (820)	7127 (533)	- -	0.22	0.639
L Pu	5167 (631)	5299 (347)	- -	0.70	0.408
R Pu	5219 (616)	5303 (366)	- -	0.28	0.600
L GP	1824 (233)	1876 (188)	- -	0.64	0.428
R GP	1806 (223)	1824 (213)	- -	0.07	0.787

Figure 3.4 shows box-and-whisker plots of CD4% at enrolment, prescan and nadir values amongst all infected children. A CD4% of less than 25% is considered immunocompromised, and greater than 25% is in the normal range.

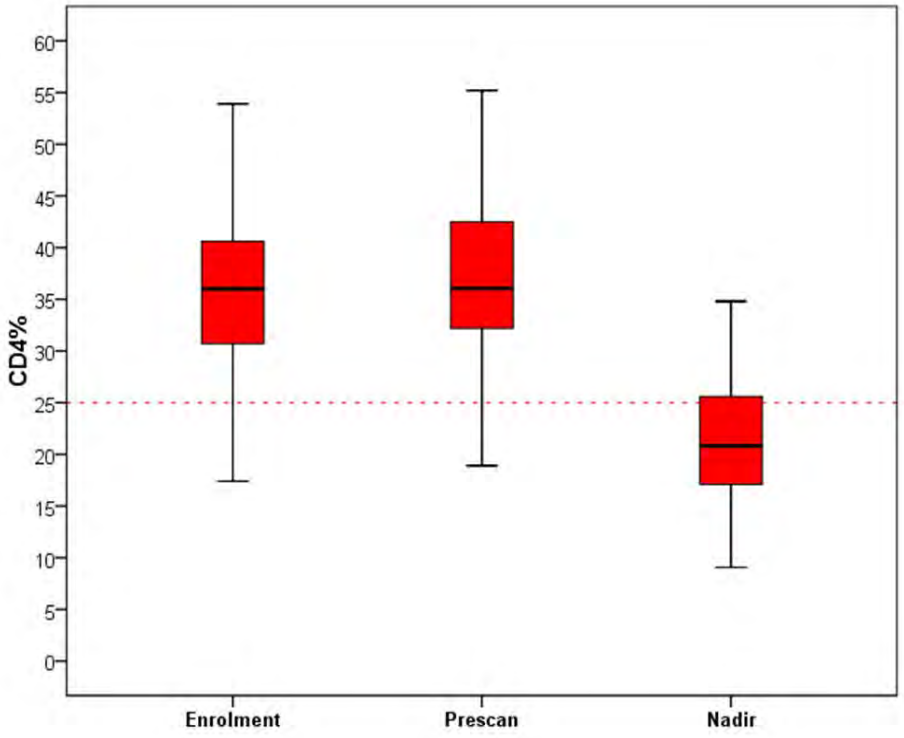

Figure 3.4 Box plot of CD4% at Enrolment, Prescan and Nadir values

Most children were stable on antiretroviral therapy at the time of scanning (CD4%>25%); only 1 child had a CD4% of less than 25%. At enrolment, 3 children were immunocompromised with CD4% less than 25%.

Nadir CD4% represents the lowest CD4% recorded between enrolment and the date of scanning. As seen in the nadir values, most of the children were immunocompromised at some point during the study; for 32 (73%) children CD4% values fell below 25% at some point while CD4% for 12 (27%) HIV-1 infected children never dropped below 25%.

In Figure 3.5, we present a box-and-whisker plot comparing CD4/CD8 ratios at enrolment and prescan amongst the infected children. Reference lines indicate ratios of 1 (red) and 2 (orange), respectively. Values below 1 are indicative of HIV-1 infection or anaemia, between 1 and 2 is in the normal range for HIV-1 negative individuals or individuals stable on ART, values higher than 2 indicate a strong immune system.

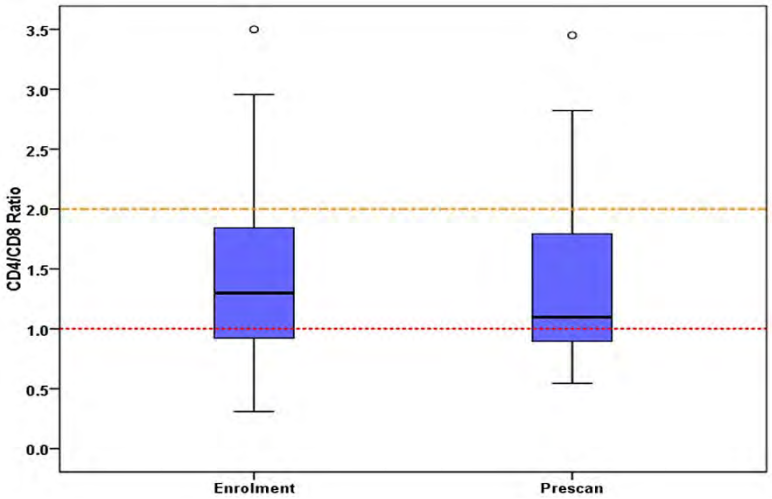

Figure 3.5 Box plot of CD4/CD8 Ratio at Enrolment and Prescan

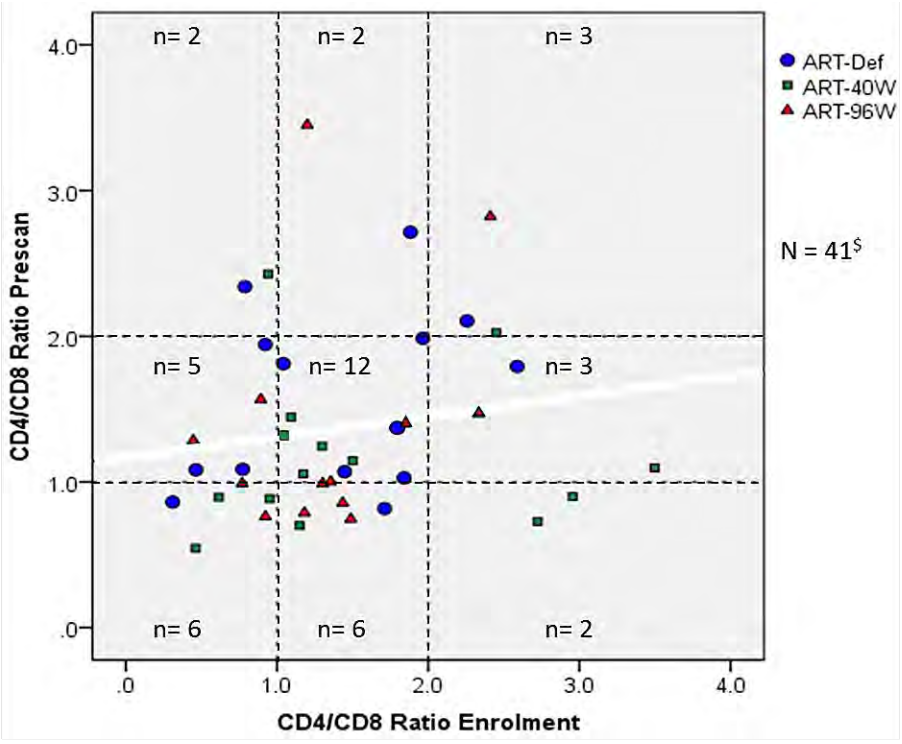

$Data is representative for clinical data available at both time points only. 3 ART-Def were unavailable.

Figure 3.6 Relationship of CD4/CD8 Ratio of each child at Enrolment with their value at Scanning

Figure 3.6 illustrates how CD4/CD8 ratios changed in each child from enrolment to time of scanning. At enrolment, 13 (32%) children had CD4/CD8 ratios below 1, 20 (49%) children between 1 and 2, and 8 (20%) children above 2. At time of scanning, 14 (34%) children had CD4/CD8 ratios below 1, 20 (49%) children between 1 and 2, and 7 (17%) children above 2. Six children had values below 1 at both enrolment and at scanning. Seven children with values below 1 at enrolment improved to above 1 at time of scanning, whilst 8 children with values above 1 at enrolment decreased to below 1 at time of scanning.

Further investigation of CD4 and CD8 cell counts separately (Figure 3.7) reveal that, as expected, mean CD4 count decreased from enrolment (mean ± s.e = 1996±133 Cells/mL) to time of scanning (mean ± s.e = 1307±97 Cells/mL) ($t(41) = 5.08$, $p < 0.001$). Similarly, mean CD8 count also dropped from enrolment (mean ± s.e = 1651±138 Cells/mL) to time of scanning (mean ± s.e = 1052±74 Cells/mL) ($t(41) = 4.20$, $p < 0.001$). The combined effect of these changes is that on average CD4/CD8 ratio does not change from enrolment to time of scanning.

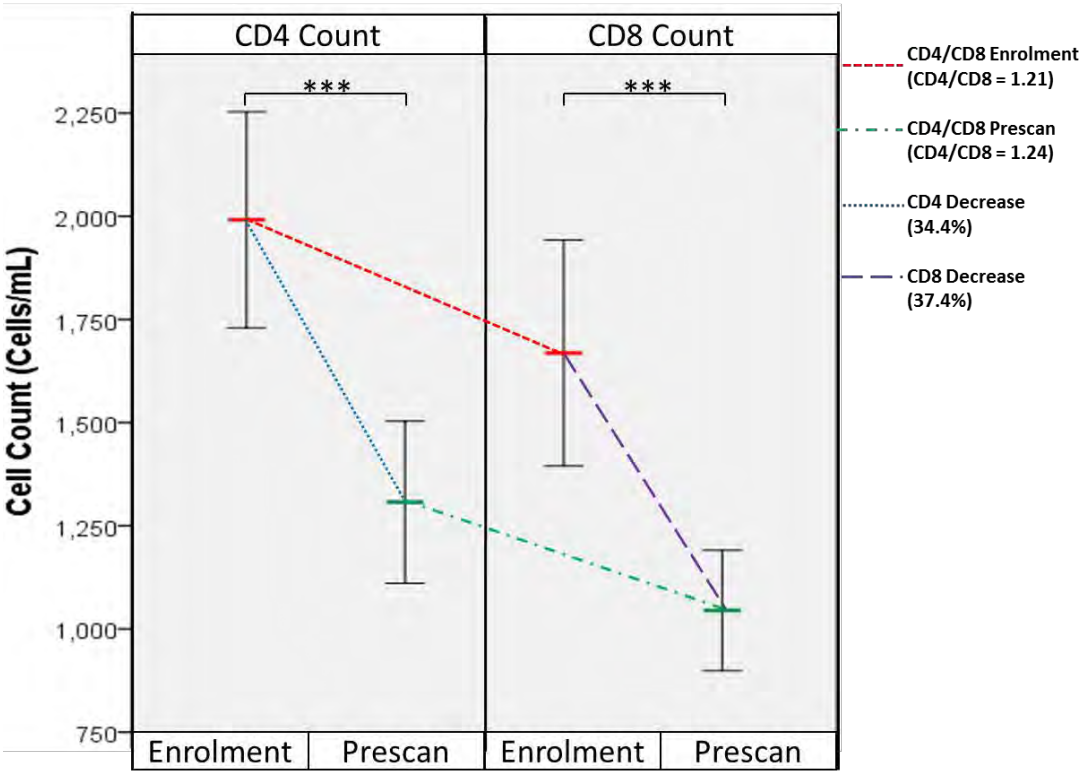

Figure 3.7 Comparison of CD4 and CD8 Cell Count at Enrolment and at Prescan

In Table 3.10 we present Pearson's or Spearman Rank Order correlations between structural volumes and T-Lymphocyte variables at time of enrolment and time of scanning.

Table 3.10 Associations of the T-Lymphocyte measures with structural volumes.

Enrolment

	CD4%		CD4/CD8 Ratio		CD4 Count		CD8 Count	
ROI	*Pearson r*	*p-value*	*Pearson r*	*p-value*	*Spearman Rho*	*p-value*	*Spearman Rho*	*p-value*
L Caudate+NA	-0.09	0.559	-0.26	0.093	-0.09	0.586	0.27	0.087
R Caudate+NA	-0.11	0.493	-0.26	0.094	-0.11	0.465	0.21	0.192
L Caudate	-0.09	0.559	-0.24	0.127	-0.01	0.935	**0.31**	**0.048**
R Caudate	-0.17	0.276	-0.28	0.069	-0.09	0.586	0.24	0.122
L NA	-0.04	0.798	-0.19	0.232	-0.17	0.283	0.09	0.578
R NA	0.19	0.225	-0.01	0.974	-0.14	0.367	-0.14	0.368
CC	-0.12	0.462	0.11	0.470	0.24	0.122	0.19	0.233
L Pu + GP	0.03	0.866	-0.11	0.488	-0.11	0.496	-0.05	0.730
R Pu + GP	0.06	0.721	-0.10	0.509	-0.10	0.508	-0.09	0.558
L Pu	0.07	0.675	-0.07	0.653	-0.09	0.570	-0.08	0.596
R Pu	0.05	0.749	-0.08	0.604	-0.15	0.325	-0.09	0.557
L GP	-0.07	0.636	-0.18	0.253	-0.08	0.617	0.10	0.510
R GP	0.06	0.694	-0.14	0.368	-0.06	0.681	-0.04	0.796

Prescan

	CD4%		CD4/CD8 Ratio		CD4 Count		CD8 Count	
ROI	*Pearson r*	*p-value*	*Pearson r*	*p-value*	*Spearman Rho*	*p-value*	*Spearman Rho*	*p-value*
L Caudate+NA	-0.27	0.083	**-0.36**	**0.018**	-0.05	0.740	0.14	0.393
R Caudate+NA	-0.23	0.148	**-0.34**	**0.026**	-0.05	0.737	0.06	0.712
L Caudate	-0.30	0.056	**-0.40**	**0.009**	0.02	0.882	0.24	0.127
R Caudate	-0.24	0.133	**-0.38**	**0.013**	-0.11	0.488	0.09	0.551
L NA	-0.03	0.847	-0.03	0.848	-0.22	0.157	-0.15	0.340
R NA	-0.04	0.824	0.04	0.821	-0.10	0.535	-0.14	0.389
CC	-0.04	0.811	-0.09	0.592	0.03	0.827	0.00	0.976
L Pu + GP	-0.02	0.895	0.01	0.943	-0.15	0.349	-0.15	0.356
R Pu + GP	-0.06	0.694	-0.02	0.877	-0.19	0.219	-0.19	0.220
L Pu	-0.01	0.973	0.03	0.867	-0.15	0.350	-0.14	0.391
R Pu	-0.05	0.767	0.00	0.995	-0.19	0.217	-0.21	0.188
L GP	-0.05	0.743	-0.03	0.872	-0.04	0.818	-0.11	0.488
R GP	-0.09	0.586	-0.08	0.628	-0.15	0.350	-0.13	0.399

At enrolment, higher CD8 count was associated with larger left caudal volumes, while lower CD4/CD8 ratios at time of scanning were associated with larger caudal volumes bilaterally (Figures 3.8 and 3.9). The box plot to the right of the scatter plots in figures 3.8 and 3.9, which show the mean volume (and 95% confidence interval) for 12 uninfected children whose ages fell within the age range of the HIV infected group, suggest that caudal volumes in children with low CD4/CD8 ratios at prescan are larger than those of uninfected control children.

Albeit CD4/CD8 ratio only showed weak trends at enrolment, enrolment and prescan CD4/CD8 ratios showed stronger and more significant associations with volumes of regions of interest than CD4% alone. CD4/CD8 ratio at prescan explained 8.7% and 8.9% more of the variability in the volumes of the left and right caudate, respectively, than CD4%.

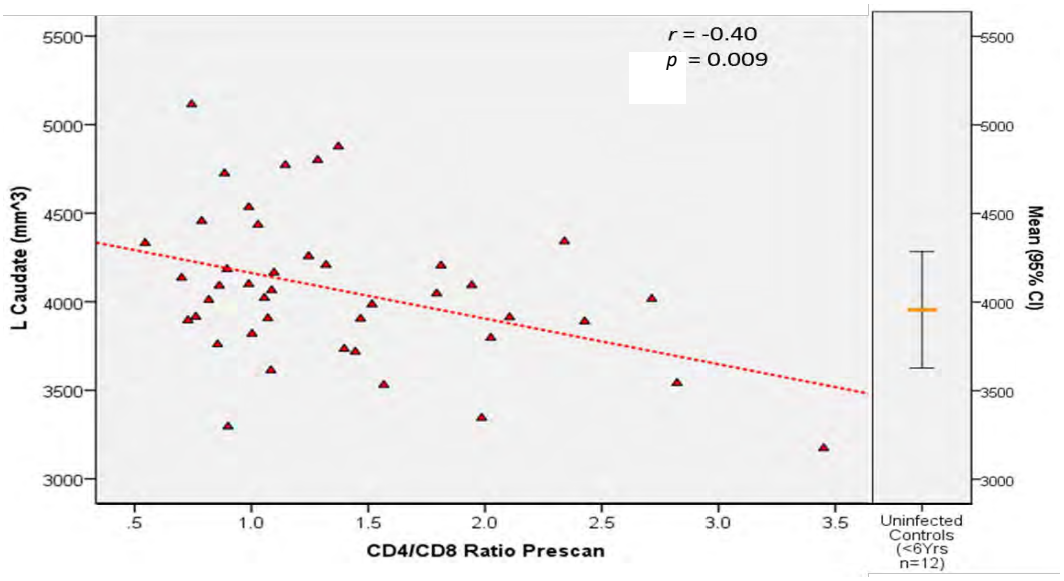

Figure 3.8 Scatter plot of the relation between left caudate volume and CD4/CD8 ratio at time of scanning

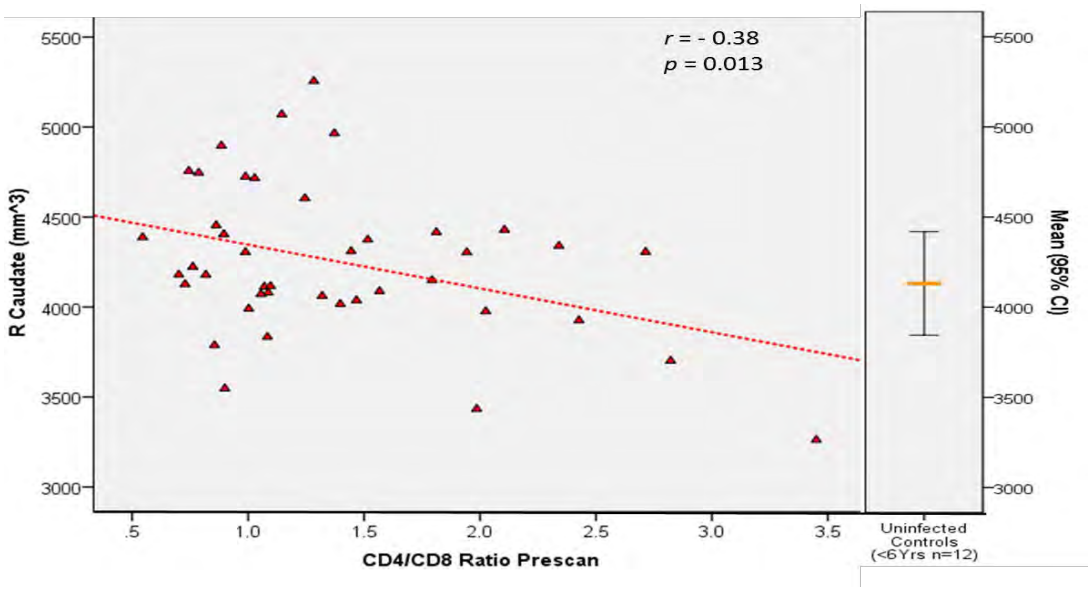

Figure 3.9 Scatter plot of the relation between right caudate volume and CD4/CD8 ratio at time of scanning

Table 3.11 indicates the association of regional volumes with potential confounders - sex and age - as well as how the association with age changes after controlling for sex. Only volumes in right caudate and left and right GP were associated with sex; only bilateral caudal and left NA volumes were associated with age.

Table 3.11 Associations of regional volumes with potential confounders

	Sex	Age at Scanning	
ROI Model	*r*	*r*	*β*
L Caudate	-0.185	**-0.330***	**-0.330***
R Caudate	-0.273†	**-0.399****	**-0.406****
L NA	-0.031	**-0.303***	**-0.303***
R NA	0.075	-0.091	-0.091
CC	-0.141	-0.142	-0.142
L Pu	-0.242	0.006	0.006
R Pu	-0.141	0.016	0.016
L GP	-0.276†	-0.220	-0.227
R GP	-0.283†	-0.228	-0.235

Values are Pearson *r* and *beta*. *Beta* is normalised regression coefficient after controlling for sex, where Sex has association (p <0.10).

†p <0.10, * p <0.05, **p <0.01

Table 3.12 shows how the association of the left and right caudal volumes with CD4/CD8 ratio at scanning changes when sex and age are included in the model in a stepwise manner.

Table 3.12 Stepwise Regression Models for the association of left and right caudal volumes with CD4/CD8 ratio at scanning

								CD4/CD8 at Prescan		+	Age at Scanning		+	Sex	
ROI Model		=	*F*	(*p*)	R^2	B	(*p*)	*β1*	(*p*)		*β2*	(*p*)		*β3*	(*p*)
L Caudate	Model 1	=	**7.63**	**(0.009)**	**0.16**	**4420**	**<0.001**	**-0.400**	**(0.009)**	+	-	-	+	-	-
	Model 2	=	**6.20**	**(0.005)**	**0.24**	**7035**	**<0.001**	**-0.374**	**(0.011)**	+	**-0.286**	**(0.048)**		-	-
	Model 3	=	**4.30**	**(0.021)**	**0.18**	**4611**	**<0.001**	**-0.392**	**(0.010)**	+				-0.143	(0.331)
	Model 4	=	**4.59**	**(0.008)**	**0.27**	**7312**	**<0.001**	**-0.364**	**(0.013)**	+	**-0.293**	**(0.043)**	+	-0.157	(0.268)
R Caudate	Model 1	=	**6.75**	**(0.013)**	**0.14**	**4590**	**<0.001**	**-0.380**	**(0.013)**						
	Model 2 [b]	=	**5.65**	**(0.007)**	**0.27**	**7790**	**<0.001**	**-0.348**	**(0.016)**	+	**-0.352**	**(0.015)**			
	Model 3 [b]	=	**4.85**	**(0.013)**	**0.20**	**4902**	**<0.001**	**-0.366**	**(0.015)**	+			+	-0.235	(0.110)
	Model 4 [c]	=	**6.24**	**(0.001)**	**0.33**	**8232**	**<0.001**	**-0.332**	**(0.018)**	+	**-0.364**	**(0.010)**	+	-0.252	(0.067)

Associations of CD4/CD8 ratio at scanning with left and right caudal volumes remained significant (β=-0.374, p=0.011 and β=-0.332, p=0.001) after controlling for the potential confounding influences of age (left caudate) and both age and sex (right caudate), respectively.

After Bonferroni correction for possible Type I error that may arise due to the fact that associations with CD4/CD8 ratio were repeated in 9 independent structures, none of the associations of lower CD4/CD8 ratio with greater regional volumes remained significant (all *p's*>0.006)

In Table 3.13 we show the association of regional volumes with age at ART initiation, both before and after controlling for sex and age at scan. The volumes of the left and right putamen showed a positive correlation with age at ART initiation (Figure 3.10).

Table 3.13 Associations of Volumes of Regions of Interest with Age at ART Initiation

		Age at ART Initiation	
ROI	Model	*r*	*β*
L Caudate	b	0.080	0.080
R Caudate	c	0.159	0.140
L NA	b	0.241	0.241
R NA		0.222	0.222
CC		-0.015	-0.015
L Pu		**0.406****	**0.406****
R Pu		**0.295***	**0.295***
L GP	a	0.269†	0.249†
R GP	a	0.219	0.199

Values are Pearson *r* and *β* from Linear Regression
Regression Model:
a - Regression modelled with Sex
b - Regression modelled with Age at scan
c - Regression modelled with Age at scan and Sex
Age/Time related variables are only modelled with Sex where applicable.
†p <0.10, * p <0.05, **p <0.01

The box plot to the right of the scatter plot in Figure 3.10 indicates the mean volume (and 95% confidence interval) for 12 uninfected controls whose ages fell within the age range of the HIV infected group, and suggests that volumes in the putamen region are enlarged in infected children with delayed ART compared to uninfected children, in whom volumes are typically smaller.

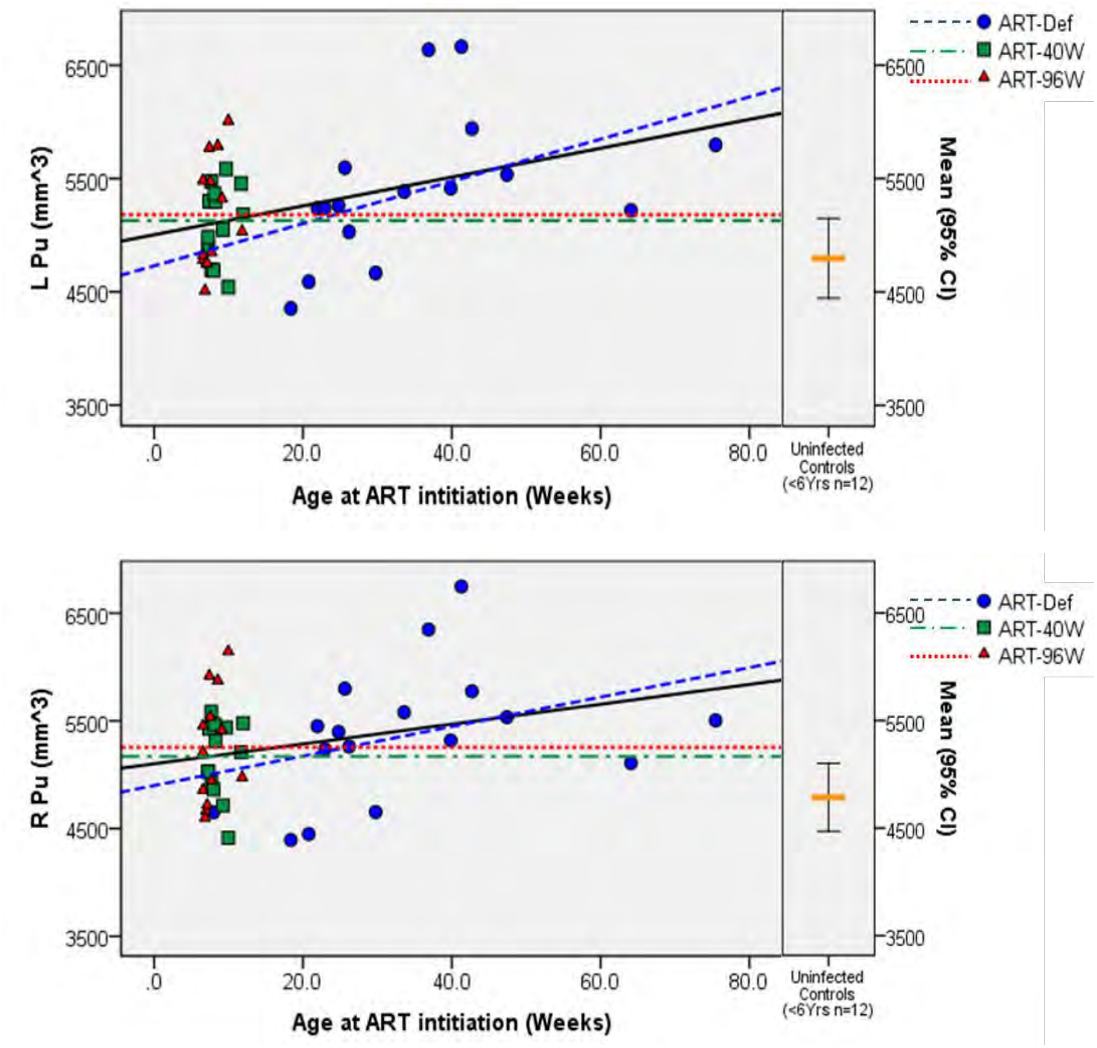

Figure 3.10 Scatter plots showing association of left and right Pu volumes with Age at ART Initiation

3.5 Manual tracing versus Automated FreeSurfer Measures

We compared volumes from manual tracing with those generated using automated FreeSurfer tools for both the full sample and for uninfected and infected children separately. Data for the uninfected children were analysed separately to assess whether results of manual and automated segmentation converge in the absence of possible pathology.

3.5.1 Bland Altman Analyses

Table 3.14 presents mean differences and percentage increase/decrease between manual and automated volumes. The volumes of certain structures were either over-estimated (larger) by automated FreeSurfer whilst others were underestimated (smaller) compared to manual tracing measures. Negative values indicate regions where the mean of the automated volume was larger than the manual.

Table 3.14 Summary of Paired T-test results for volumes obtained from FreeSurfer versus manual tracing

	Full Sample (n=62)				Uninfected Controls (n=18)				HIV-1 Infected (n=44)			
ROI	ΔMean (s.e.) (mm^3)	Δ%	*t*	*p-value*	ΔMean (s.e.) (mm^3)	Δ%	*t*	*p-value*	ΔMean (s.e.) (mm^3)	Δ%	*t*	*p-value*
L Caudate + NA	130 (48)	3%	2.737	0.008	-36 (105)	-1%	-0.341	0.737	**198 (49)**	**4%**	**4.063**	**<0.001**
R Caudate +NA	134 (42)	3%	3.223	0.002	-69 (86)	-1%	-0.803	0.433	**217 (41)**	**4%**	**5.264**	**<0.001**
L Caudate	**285 (42)**	**7%**	**6.724**	**<0.001**	205 (95)	5%	2.161	0.045	**318 (45)**	**8%**	**7.018**	**<0.001**
R Caudate	**287 (36)**	**7%**	**8.037**	**<0.001**	130 (72)	3%	1.824	0.086	**351 (37)**	**8%**	**9.407**	**<0.001**
L NA	**-155 (16)**	**-27%**	**-9.769**	**<0.001**	**-241 (30)**	**-46%**	**-8.170**	**<0.001**	**-120 (16)**	**-20%**	**-7.391**	**<0.001**
R NA	**-153 (15)**	**-25%**	**-10.194**	**<0.001**	**-200 (28)**	**-36%**	**-7.049**	**<0.001**	**-134 (17)**	**-22%**	**-7.845**	**<0.001**
CC	**-69 (13)**	**-18%**	**-5.174**	**<0.001**	39 (16)	8%	2.507	0.023	**-113 (12)**	**-32%**	**-9.017**	**<0.001**
L Pu + GP	**-599 (63)**	**-9%**	**-9.546**	**<0.001**	**-936 (139)**	**-14%**	**-6.742**	**<0.001**	**-461 (57)**	**-7%**	**-8.113**	**<0.001**
R Pu + GP	**-341 (55)**	**-5%**	**-6.235**	**<0.001**	**-598 (146)**	**-9%**	**-4.099**	**0.001**	**-235 (40)**	**-3%**	**-5.826**	**<0.001**
L Pu	**-608 (53)**	**-12%**	**-11.571**	**<0.001**	**-792 (129)**	**-16%**	**-6.115**	**<0.001**	**-533 (49)**	**-10%**	**-10.979**	**<0.001**
R Pu	**-485 (47)**	**-9%**	**-10.249**	**<0.001**	**-711 (127)**	**-15%**	**-5.619**	**<0.001**	**-392 (35)**	**-7%**	**-11.341**	**<0.001**
L GP	9 (27)	0%	0.326	0.745	-145 (54)	-8%	-2.664	0.016	72 (25)	4%	2.816	0.007
R GP	**144 (20)**	**8%**	**7.037**	**<0.001**	112 (47)	6%	2.395	0.028	**157 (22)**	**9%**	**7.257**	**<0.001**

ΔMean = Mean (Manual Measure - Automated Measure)

s.e. = Standard Error of mean

Δ% = Percentage difference from Manual

Adjusted *P*-Value cut-off $p<0.001$

Due to the large number of comparisons performed (39 tests), the threshold for statistical significance was adjusted by dividing 0.05 by 39, generating a critical *p*-value of 0.001.

Notably, automated and manual volumes differed in all regions except the left GP in HIV infected children, while there were no significant differences between manual and automated measures amongst uninfected children bilaterally in caudate+NA, caudate, GP, or CC, suggesting that subtle pathology may contribute to bias between manual and automated measures in infected children.

For example, in uninfected children, automated segmentation yielded marginally smaller corpus callosa than manual tracing (differences that were not significant), while in HIV-1 infected children automated segmentation resulted in volumes up to 30% larger in this region compared to manual tracing. The larger number of HIV-1 infected children and greater difference amongst these children explains the volume increases seen with automated segmentation in the full sample in this region.

As such, differences between automated and manual measures in the left and right caudate, CC, and right GP are due to differences amongst infected children only.

Figures 3.11, 3.12, 3.13 and 3.14 below are Bland Altman Plots showing the distribution of the differences between manual and automated volumes as a function of the mean of the two measures, for all structures that did not show significant differences in either the uninfected children or the overall sample. The red and yellow lines denote the mean differences for the infected and uninfected children, respectively, while the black line denotes the mean for the full sample. A mean near zero indicates the absence of a significant difference between manual and automated measures. Regression analysis of the mean difference between measures against the paired mean for each structure revealed no proportional bias in areas showing no significant difference.

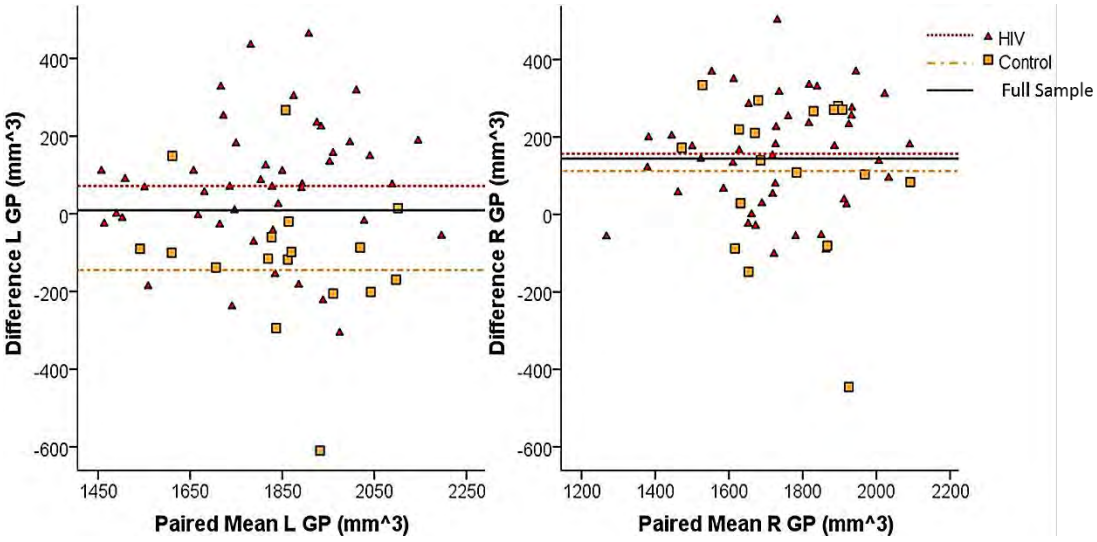

Figure 3.11 Bland-Altman Plot of Mean difference between Manual and Automated measures for left and right globus pallidus

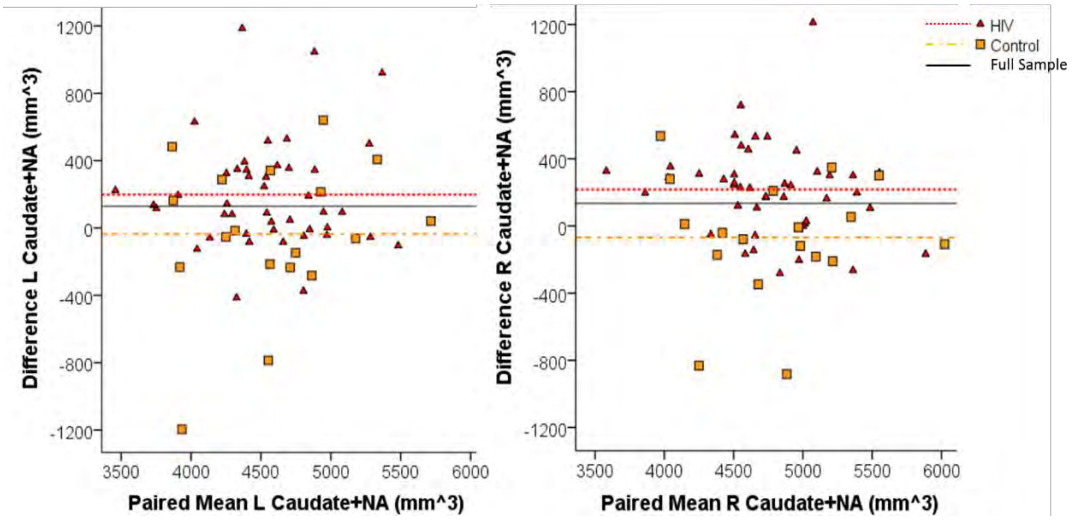

Figure 3.12 Bland Altman Plot of Mean difference between Manual and Automated for left and right Caudate +NA

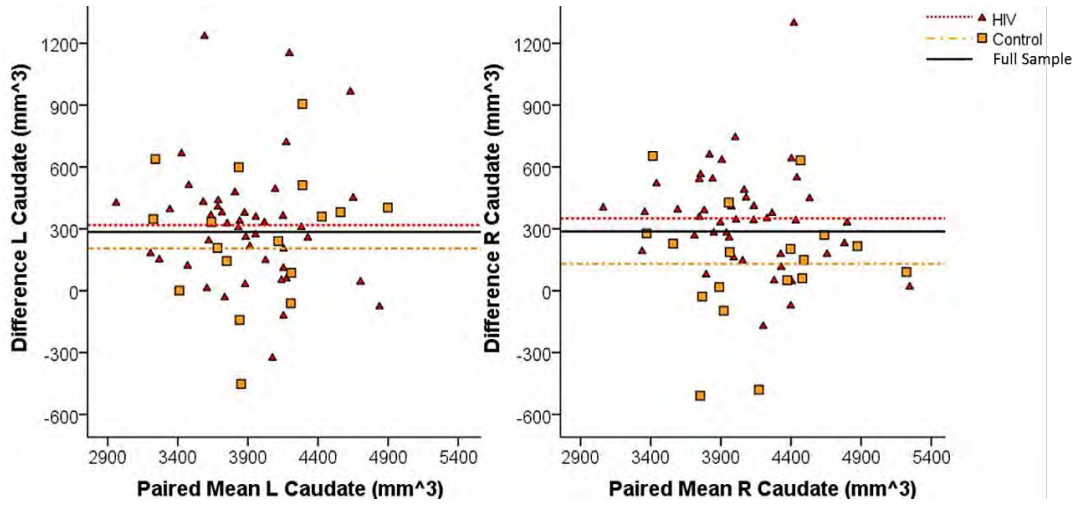

Figure 3.13 Bland-Altman Plot of Mean difference between Manual and Automated for left and right Caudate

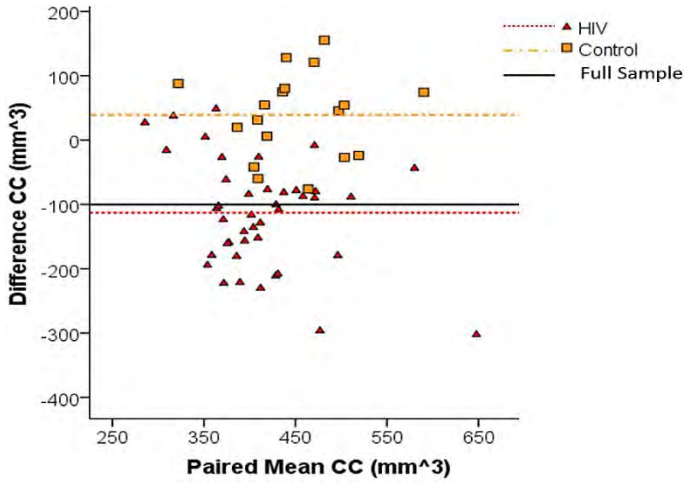

Figure 3.14 Bland-Altman Plot of Mean difference between Manual and Automated for CC

Table 3.15, below, is a summary of the correspondence / agreement between volumes from manual tracing and automated FreeSurfer segmentation.

Table 3.15 Comparison of volumes from manual and automated segmentation

	Full Sample (n=62)			
ROI	*r(X,Y)*	R^2	*p-value*	Cronbach's α
L Caudate + NA	**0.72**	**0.516**	**<0.001**	**0.84**
R Caudate +NA	**0.79**	**0.630**	**<0.001**	**0.88**
L Caudate	**0.75**	**0.568**	**<0.001**	**0.84**
R Caudate	**0.83**	**0.693**	**<0.001**	**0.90**
L NA	**0.48**	**0.227**	**<0.001**	**0.64**
R NA	**0.49**	**0.244**	**<0.001**	**0.64**
CC	0.23	0.053	0.071	0.38
L Pu + GP	**0.77**	**0.585**	**<0.001**	**0.87**
R Pu + GP	**0.81**	**0.653**	**<0.001**	**0.89**
L Pu	**0.76**	**0.575**	**<0.001**	**0.86**
R Pu	**0.76**	**0.582**	**<0.001**	**0.87**
L GP	**0.50**	**0.253**	**<0.001**	**0.67**
R GP	**0.62**	**0.389**	**<0.001**	**0.81**
	Uninfected Controls (n=18)			
ROI	*r(X,Y)*	R^2	*p-value*	Cronbach's α
L Caudate + NA	**0.71**	**0.503**	**0.001**	**0.82**
R Caudate +NA	**0.80**	**0.646**	**<0.001**	**0.89**
L Caudate	**0.69**	**0.483**	**0.001**	**0.81**
R Caudate	**0.83**	**0.697**	**<0.001**	**0.91**
L NA	0.44	0.194	0.067	0.61
R NA	0.43	0.186	0.074	0.60
CC	0.54	0.292	0.021	0.70
L Pu + GP	**0.76**	**0.582**	**<0.001**	**0.84**
R Pu + GP	**0.73**	**0.531**	**0.001**	**0.82**
L Pu	**0.70**	**0.484**	**0.001**	**0.80**
R Pu	0.68	0.469	0.002	0.79
L GP	0.47	0.218	0.050	0.60
R GP	0.48	0.233	0.043	0.64
	HIV-1 Infected (n=44)			
ROI	*r(X,Y)*	R^2	*p-value*	Cronbach's α
L Caudate + NA	**0.76**	**0.576**	**<0.001**	**0.86**
R Caudate +NA	**0.84**	**0.701**	**<0.001**	**0.91**
L Caudate	**0.79**	**0.629**	**<0.001**	**0.86**
R Caudate	**0.86**	**0.743**	**<0.001**	**0.91**
L NA	**0.60**	**0.357**	**<0.001**	**0.75**
R NA	**0.54**	**0.288**	**<0.001**	**0.68**
CC	0.45	0.204	0.002	0.60
L Pu + GP	**0.84**	**0.712**	**<0.001**	**0.92**
R Pu + GP	**0.93**	**0.856**	**<0.001**	**0.96**
L Pu	**0.81**	**0.663**	**<0.001**	**0.90**
R Pu	**0.86**	**0.738**	**<0.001**	**0.94**
L GP	**0.67**	**0.444**	**<0.001**	**0.65**
R GP	**0.69**	**0.475**	**<0.001**	**0.60**

Adjusted *P*-Value cut-off $p<0.001$

The strongest correlation observed between automated and manual segmentation was in the right lentiform nucleus of HIV-1 infected children, where 85.6% of the variability seen in manual segmentation was explained in the automated segmentation (*Cronbach's* α=0.96). The weakest correlation observed between automated and manual segmentation was in the corpus callosum for the whole sample where only 5.3% of the variability seen in manual segmentation was explained in the automated segmentation (*Cronbach's* α=0.38).

Overall, there were stronger correlations for grey matter structures amongst HIV-1 infected children (*Cronbach's* α=[0.60-0.96], R^2=[0.288-0.856]) as compared to the full sample (*Cronbach's* α=[0.64-0.90], R^2=[0.227-0.693]) and uninfected controls (*Cronbach's* α=*[*0.60-0.91], R^2=[0.186-0.697]). In uninfected controls associations between manual and automated volumes were not significant (after correction for multiple comparisons) in the left and right nucleus accumbens, left and right GP, and right putamen.

The corpus callosum had a stronger correlation with manual segmentation amongst the uninfected children (*Cronbach's* α=0.70, R^2=0.292) compared to HIV-1 infected children (*Cronbach's* α=0.60, R^2=0.204), however was not significant after correction for multiple comparisons in any of the 3 groups. Figure 3.15 is a scatter plot of manual against automated CC volumes, with reference line of perfect correlation (black). The red and yellow lines denote the relation in HIV-1 infected and uninfected controls, respectively. In infected children automated volumes are typically larger than manual volumes, while they are smaller than manual volumes amongst the uninfected children.

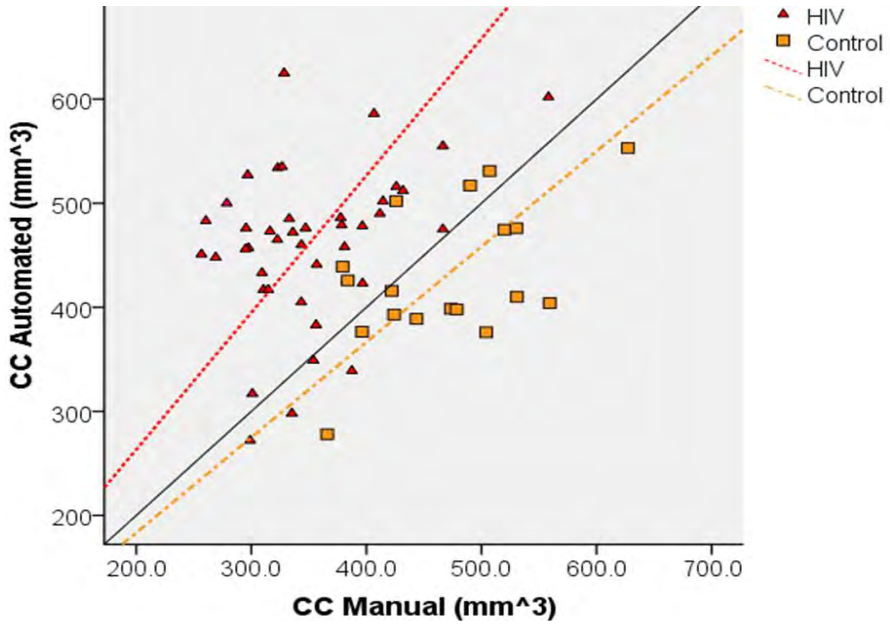

Figure 3.15 Scatter Plot of Manual versus Automated for CC

3.5.2 Group Differences using Automated FreeSurfer Measures

A central question to this thesis was whether regions where we observe volumetric differences between diagnostic groups would change if we use volumes obtained using automated measures compared to those obtained using manual tracing. Using volumes obtained from FreeSurfer, we found no significant differences between diagnostic groups, except for the left globus pallidus where HIV-1 infected children were found to have a significantly smaller left globus pallidus (mean±s.e.=1775±29mm^3) than uninfected controls (mean±s.e.=1949±60mm^3) ($F(1, 61) = 8.60$, $p = 0.005$). In contrast, it was shown previously (Table 3.3) that manual tracing revealed 5 different structures (bilateral NA, bilateral Pu, and CC) with significant differences in volume between infected and uninfected children.

CHAPTER 4 DISCUSSION

This discussion will focus on two main sets of findings, the effects of HIV and HAART on structure size and the congruence between manual and automated segmentation. This discussion will suggest possible explanations for the results that were obtained, as well as future avenues for research. This data could advance our understanding of the clinical and cognitive manifestations of HIV-1 in infected children, as well as elucidate upon segmentation measures that most accurately describe the neuroanatomy and pathology in children.

4.1 Effects of HIV-1 Infection and HAART on Regional brain volumes

In contrast to previous studies in HIV-infected adults that observed global atrophy (Becker et al. 2011; Chang et al. 2011; George et al. 2009; Sarma et al. 2014), the findings of this study suggest that pre- or postnatal HIV-1 infection and HAART result in localised subcortical volume increases in the brains of Xhosa children at or around 5 years of age, specifically in the nucleus accumbens (NA) and the putamen (Pu), effects that remained significant after controlling for the potential confounding influences of age and sex. Although there were no volumetric differences between children in the three different treatment arms, children in the ART-Def group showed the largest volume increases compared to uninfected control children. This result is consistent with the finding that increasing age at ART initiation was associated with greater volumes bilaterally in the Pu. In contrast, the corpus callosum (CC), which is the primary white matter structure responsible for inter-hemispheric connections, was reduced to the same extent in HIV-1 infected children from all three treatment arms compared to uninfected controls.

Notably, albeit over a small age range, increasing age was associated with volume decreases in the caudate and left NA amongst infected children, but with volume increases in the NA amongst the uninfected children. This volume decrease with increasing age amongst infected children could explain the atrophy associated with HIV in adults, although the reason for the observed volume increase in early childhood is unclear.

Amongst infected children, the mean CD4 and CD8 T-cell counts both decreased as expected with age from enrolment to scanning. Children have naturally high CD4 and CD8 T-cell counts, which decrease with age and thus differ greatly from that of adults (Paul et al.

2005; Shearer et al. 2007). The CD4/CD8 ratio remained constant from enrolment to scan date and within the normal range. We observed that CD4/CD8 ratio showed stronger associations with structure volumes than CD4%. Unexpectedly, amongst infected children, poorer immune health at the time of scanning, as evidenced by lower CD4/CD8 ratio, was associated with greater caudal volumes, effects that did not survive Bonferroni correction for multiple comparisons.

Thus, in three of four subcortical grey matter regions examined, we observe volume increases at age 5 years in infected children (effects that are strongest in children who initiated ART later in life) or children with poorer overall health, as evidenced by lower CD4/CD8 ratios. The globus pallidus (GP) is the only region where we did not observe volume increases associated with HIV infection.

The absence of volume reductions in our study may be due to current inflammation, reactive gliosis, apoptotic inhibition, and leukocyte infiltration in the areas of interest causing them to be abnormally larger (Ernst, Chang & Arnold 2003; George et al. 2009; Reid et al. 2001).

Reactive gliosis is described as the non-neoplastic proliferation of glia, most commonly astrocytes and occasionally microglia, in response to injury. This may exacerbate HIV infection in the brain as it has been shown that HIV preferentially targets astrocytes and microglia (Blumberg, Gelbard & Epstein 1994; Mitchell, Wendy 2001; van Rie et al. 2007; Tornatore et al. 1994). Astrocytes have functional HIV co-receptors (CCR5 and CXCR4) that could facilitate infection (Klein et al. 1999). Even in the absence of current acute inflammation and transient virologic increases, the engagement of these receptors by chemokine ligands (CCL3 and CCL5) that are increased in the brains of HIV-infected individuals, could alter astrocyte function and increase BBB permeability (Ivey, MacLean & Lackner 2009; Klein et al. 1999). Furthermore, once infected the release of CCL2 by astrocytes as a possible neuroprotective mechanism inhibits apoptosis in astrocytes and neurons against the toxic effects of Tat (from HIV) or glutamate (Ivey, MacLean & Lackner 2009). The lack of apoptosis and recruitment and activation of phagocytic cells could further exacerbate the inflammation and cause relative increases to structure size. This may explain why observed volume increases in our study were typically largest in children in the ART-Def arm who initiated ART only when they presented with certain clinical criteria, as one would expect effects of reactive gliosis and apoptotic inhibition to be more severe in these children in whom viral load was suppressed only later in life compared to children who initiated ART early (before 12 weeks of age).

The highest concentration of HIV is found in the caudate nuclei and CC (Ances et al. 2012; Thompson et al. 2006), possibly due to their close association with the ventricles, which may explain the association seen in the caudate with CD4/CD8 ratio as a measure of immune health. The proximity of these structures to the ventricles, and in turn the CSF, allows for easier penetration of HIV-infected mononuclear cells permitting higher concentrations of HIV toxins in these sites (Ances et al. 2012; Andronikou et al. 2014; McClernon et al. 2001; Oster et al. 1993; Thompson et al. 2006). This would in turn also apply to ARVs which more readily permeate through the BBB. The fact that the uninfected children who showed age-related volume increases in certain structures are marginally older and span a larger age range than the infected children who, in contrast, show age-related volume decreases, may conceal some subtle group differences. Controlling for sex and age at scan did not, however, alter the results of the group comparison.

Grey matter has larger numbers of glial cells, such as protoplasmic astrocytes to support the neuron's metabolic demands, than white matter, and comparatively larger microglia in the presence of pathology. The preferential targeting of astrocytes and microglia by HIV would thus naturally precipitate reactive gliosis and neuronal cell loss in these areas (Blumberg, Gelbard & Epstein 1994; Ernst, Chang & Arnold 2003; Hahn et al. 2013; Tornatore et al. 1994). Microglia are phagocytic antigen presenting cells that are mobilized after CNS injury or infection (Kandel, Schwartz & Jessell 2000). Since microglia are macrophage derived, they carry the presence of CD4 receptors making them vulnerable to HIV attack (Kandel, Schwartz & Jessell 2000). During inactivation/resting state these cells are relatively small and have undulating processes with spine-like projections. The function of microglia during resting state is unknown (Kandel, Schwartz & Jessell 2000). However, once activated and recruited upon the onset of infection or injury, the cells' processes become more protuberant and furcated than that of inactivated cells, making them difficult to distinguish from recruited phagocytes and perivascular cells. Microglia are thought to become activated in a number of diseases including multiple sclerosis and AIDS-related dementia, as well as more chronic neurodegenerative diseases, like Alzheimer's (Kandel, Schwartz & Jessell 2000).

These protoplasmic astrocytes and microglia cells are not as abundant in white matter. The CC, which contains mostly neuronal axon fibres with oligodendrocytes and myelin and fewer neuronal cell bodies than grey matter, requires fewer protoplasmic astrocytes due to decreased metabolic demands and are substituted with fibrous astrocytes. The effects of inflammation in white matter would thus not be as prevalent as in grey matter. Evidence of

cell loss in the CC has, however, been observed via MRS and immunohistochemically stained animal model studies (Chang et al. 2002; Hahn et al. 2013). Rat models have shown reduced oligodendrocyte populations and equivalent microglial increases in the presence of HIV within the CNS (Hahn et al. 2013). The loss of these support cells may result in perturbations to neuronal pathway function as well as facilitate further neuronal cell loss. Neuronal cell loss in affected grey matter would naturally cause repercussive thinning of the CC as axonal fibre tracts project via the CC from their cell bodies located in affected grey matter areas (DeLong 2000). This additive loss of neuronal axon tracts and accompanying oligodendrocytes may have an additive effect resulting in the smaller CC size we observe in HIV infected children. Therefore, decrease in structure size due to the summated loss of support cells and neuron tracts may greatly outweigh subtle hypertrophy, via proliferation and recruitment of phagocytic cells, such as microglia and fibrous astrocytes.

It has been shown that one defining pathological feature of HIV encephalopathy is diffuse white matter involvement that becomes more pronounced in the advanced stages of the disease (Pomara et al. 2001). In our study, the most significant difference between infected and uninfected individuals was observed within the CC. The CC of HIV infected children was found to be on average 24% smaller at age 5 years than in their uninfected counterparts. Numerous researchers have observed similar HIV-associated size reductions within the CC (Chiang et al. 2007; Dewey et al. 2010; Hasan et al. 2009). Thompson et al.(2006) reported a 25% decrease in the thickness of the CC in HIV infected adults compared to uninfected controls – an effect that was most prevalent within the anterior portions of the CC (Thompson et al. 2006). They also observed that the overall thickness of the CC is affected by loss of peripheral white matter, making this finding important for clinical settings. As, CC thickness, and volume may be used as a biomarker to test overall global white matter integrity (Andronikou et al. 2014; Thompson et al. 2006). Andronikou and colleagues examined CC volume and thickness as a biomarker of global white matter integrity in 33 South African children (age 7 – 49 months) diagnosed with HIV-related brain disease, all receiving ART. Since all children received MRI due to clinical indications, the study lacked uninfected controls (Andronikou et al. 2014). They observed that linear measurement and thickness of the motor segment of the CC associated with the degree of mental development. Although we did not analyse specific areas of the CC, this finding ties in with the subcortical grey matter areas (containing motor function domains) found to be affected in our study, as well as impairments to locomotor function described in our cohort (Laughton et al. 2012). Note should be taken that both African and mixed race individuals from low

socioeconomic background were included in Andronikou's (2014) study. In the present study, mixed race children (Cape Coloured) were excluded as volumes of subcortical structures significantly differed between Xhosa and Cape Coloured uninfected controls (Appendix A).

As the Pu and NA are located marginally further away from the ventricles than the caudate, these structures are perhaps not as readily penetrated by the HIV-infected mononuclear cells. However, once HIV invades the area and viral infection spreads, removal of metabolic waste and virions may be slower compared to that of the caudate. This may explain the larger Pu and NA observed in HIV infected children. Thus presence of inflammation in the form of reactive gliosis and leukocyte infiltration, resulting in slightly increased structure size, may be because of prolonged HIV exposure in the Pu and NA rather than present acute transient viral increases, as per the caudate.

The clinical manifestations of HIV-1 infection in these children do not paint a clear picture of causation. Plasma viral load (PVL) was suppressed (≤ 399 RNA/ml) in 90% of children at time of scanning. A previous study in 128 perinatally infected children found that 21% showed characteristic evidence of HIV infection induced encephalopathy, despite at least 74% of these children having viral load suppression at the time of diagnosis (Cooper et al. 1998). Findings of viral load suppression in the systemic blood supply may, however, not be representative of the compartmentalised and unique viral reservoirs in the CNS (Pillai et al. 2006; Strain et al. 2005).

Further, there could be ongoing effects from damage or delayed development arising during the initial phases of HIV invasion, prior to HAART initiation. In our study, all HIV infected treatment groups were clinically relevant with PVL ≥ 400 RNA/ml at enrolment. The PVL of the deferred group resembled that of the ART-96W group, where most children (69%) had PVL above 750000 RNA/ml, whilst PVLs were between 400 and 750000 RNA/ml in 79% of children in the ART-40W group. These differences in PVL at enrolment may explain why the L NA is less enlarged in the ART-40W group compared to uninfected children than in the ART-96W group, since viral penetration into the CNS occurs early on in infection (Ivey, MacLean & Lackner 2009). Neuroinvasion by HIV can occur as early as the initial 10 days post-infection (Lackner et al. 1994). The primary mode of neuroinvasion involves monocytes infected with HIV entering the brain during routine immune surveillance and replacement of perivascular macrophages (Annunziata 2003). Significant differences have been observed previously in a sample of vertically infected children between 6 months to 18 years of age, where disturbances to CNS were associated with VL within the CSF, whilst no associations

were found with PVL (Sei et al. 1996). Importantly though, those findings were reported cross-sectionally after the initial infection and viral insult from 6 months post-seroconversion. Thus observations in our study of fewer and less severe differences in structure size in the ART-40W group compared to the ART-96W group, which had more individuals with low PVL at enrolment, may indicate that even early HAART administered at around 8.3 ± 1.6 weeks of age is perhaps too late for individuals already experiencing high viral loads. Damage to the basal ganglia, and thus corpus striatum is dictated by the rate of initial insult (Becker et al. 2011). These findings suggest that early therapy before severe viral replication would be advantageous. The association of increased structure size of the left and right putamen with increased delay to initiate ART provides further evidence of the benefit of early ART. Unexpectedly though, we did not find any differences in regional volumes at age 5 years between children who had high or low PVLs at enrolment. A confounding issue here may be the duration of HAART itself, where one group received HAART for 40 weeks and the other for 96 weeks before interruption. It is possible that ART interruption negates some of the benefits of early ART. It has also been shown that HAART decreases motor and working memory performance in both children and adults (Chang et al. 2008; von Giesen et al. 2003), which suggests that there may be some complicated interplay between the benefits and risks associated with early ART.

Since associations between clinical variables and volumes differ in different brain regions, it appears that different structures are impacted in a unique way by HIV and/or ART, albeit bilaterally. The basal ganglia plays an integral role in motivation and learning, and movement related functions (DeLong 2000). Although the putamen is interconnected with many structures and as such is involved in many integrated functions, its two main functions are motor and learning (DeLong 2000; Packard & Knowlton 2002). It has also been hypothesized that the putamen plays a role in the selection of movement and the performance of previously learned movements (Griffiths, Perry & Crossman 1994). As such, damage to this area would present as deficits in motor function and learning. Deficits in motor function, presenting as spastic diplegia, have been reported amongst HIV-infected children in South Africa (Langerak et al. 2014). Other researchers have also noted these functional impairments in gross motor skill and function - mainly when comparing HIV-infected with uninfected children (Abubakar et al. 2008; Epstein et al. 1986; van Rie, Mupuala & Dow 2008). Perturbations in locomotor function have also been observed in children from our cohort via the Griffiths Mental Development Scales, albeit at an earlier age (10-16 months) (Laughton et al. 2009).

4.2 Automated versus Manual Segmentation

To our knowledge, this is the first study to manually segment structures of the basal ganglia in such a large cohort of children, especially in children with possible pathology linked to HIV infection with ART initiation at different times in infancy. Most studies investigating the reliability of manual versus automated segmentation have mainly assessed the hippocampus, with very few investigating individual structures of the basal ganglia (Barnes et al. 2008; Boccardi et al. 2011; Hsu et al. 2002; Morey et al. 2009; Mulder et al. 2014; Sánchez-Benavides et al. 2010; Shen et al. 2010; Tae et al. 2008).

Amongst uninfected children, we found that FreeSurfer overestimated both the left and right NA by 46% and 36%, respectively. Similarly, the left and right Pu were overestimated by 16% and 15%, respectively. No differences were found in the caudates, CC or GP. This suggests that similar overestimations may be expected in normal non-pathological Xhosa children around a similar age.

Amongst the HIV infected children, automated and manual volumes differed in all regions examined (all p's<0.001), except the left GP (p=0.007) where the difference did not survive Bonferroni correction for multiple comparisons. The largest difference between automated and manual measures was in the CC where automated volumes were 32% larger. The CC, bilateral NA and Pu were overestimated, whilst the bilateral caudates and right GP were underestimated.

Notably, the NA and Pu volumes from automated measures were larger than those obtained using manual tracing amongst both infected and uninfected children, and in the sample as a whole. These are also the areas that were larger in infected children compared to uninfected children via manual segmentation. It is possible that the overestimation of volumes using automated segmentation in these areas is due to different conventions for selecting boundaries, introducing bias into the measures. The fact that manual and automated measures were correlated in these areas amongst both infected and uninfected children (albeit more strongly so amongst infected children), suggests that different conventions may be the source of the discrepancy and that group differences arising from pathology may be preserved despite these differences. Unfortunately, group comparisons using volumes obtained from automated segmentation showed no differences in the NA and Pu, suggesting that differences arising from subtle pathology may be lost during automated segmentation.

Morey et al. in their study in 20 adults comparing manual tracing with FreeSurfer and FIRST, observed overestimation of volumes obtained using the two automated methods compared to manual tracing in both hippocampal and amygdala regions (Morey et al. 2009). This is consistent with our findings in uninfected children, where all the significant differences were due to overestimation of volumes by FreeSurfer, albeit in different brain regions.

Dewey and colleagues conducted a study involving 120 HIV infected patients, mean age 47.3±7.2 years (Dewey et al. 2010). Although they did not strictly use manual segmentation, except for reliability testing of a subset, they did test various automated segmentation packages against one another and with auto-assisted manual segmentation (AAM). They observed that FreeSurfer exhibited statistical differences in 3 of the 8 areas examined, with all structures being overestimated by FreeSurfer. Unfortunately, the only regions investigated that were in common with ours were the caudate and putamen. They reported mean differences in the left caudate and left putamen of 6.76% and 13.99%, respectively (Dewey et al. 2010). Although the overestimation of the Pu volumes by FreeSurfer amongst infected children in our study were similar, caudal volumes by FreeSurfer were smaller by roughly 8% in our study.

4.2.1 Association of Structure Size Between Segmentation Techniques

Following correction for multiple comparisons the automated measurements of the CC had no association with manual segmentation in any of the groups. Amongst the uninfected children, the Cronbach's alpha Intraclass Correlation Coefficient (ICC) in the CC was 0.70, whilst only 29% of the variability in the data from manual segmentation could be described by the automated volumes of this structure. Similarly, in the infected group with a Cronbach's alpha of 0.60 in the CC, only 20% of the variability in the manual data could be explained by the automated measures.

After Bonferroni correction for multiple comparisons, the uninfected group's automated measures showed no association with manual measures bilaterally in the NA, GP and right Pu. Except for the GP, differences between manual and automated measures were significant in these regions. Caudal manual and automated volumes were correlated and did not differ significantly.

In contrast, amongst infected children, despite the fact that automated volumes were correlated with manual volumes in all grey matter ROIs, all the regions (except the left GP) showed significant differences between manual and automated volumes. Also, NA and Pu

volumes were typically larger by automated segmentation, while caudal and GP volumes were smaller. These results demonstrate that automated segmentation may not be able to accurately segment regions in the presence of subtle pathology. The enlarged subcortical grey matter regions observed in the brains of the HIV infected children, resulting possibly in more vivid definition of structure outlines, as well as mimicking better an adult brain, for which the aseg+aparc 2009 training atlas was derived, may account for the high number of associations between automated and manual segmentation within the HIV-1 infected group.

Fischl et al. (2002) assessed the reliability of their automated segmentation methods. The overall outcome of their study was convincing. However, their training atlas was generated using only 12 manually labelled datasets (the age range is not mentioned in the paper) (Fischl et al. 2002). The study assessing the reliability of this atlas mentions study participants with normal cognition (controls) and subjects with increasing cognitive decline in the presence of Alzheimer's Disease (Fischl et al. 2002). These study participants ranged upwards of 67 years of age and resulted in extremely favourable association between their automated and manually segmented measures.

The relatively inflated Cronbach's alpha coefficients are a problematic outcome. While some studies assess the congruence between various segmentation measures using multiple statistical analyses (Bendersky et al. 2006; Dewey et al. 2010; Morey et al. 2009), many use Cronbach's alpha to gauge the agreement between manual segmentation of a subset of the data and automated segmentation protocols (Dewey et al. 2010; Knickmeyer et al. 2008; Shen et al. 2010; Tae et al. 2008). Cronbach's alpha is not sensitive enough to be used as a standalone measure for gauging reliability. Observation of the Pearson's coefficient of determination between automated and manual measures revealed consistently low association between measures as compared to Cronbach's alpha. This is expected as Pearson correlation is a more sensitive statistical test.

Since our results demonstrated differences between volumes obtained using automated segmentation and those obtained using manual tracing, and since these differences differed between infected and uninfected children, we were interested in assessing whether group differences obtained using manual tracing would be preserved using automated measures. Using automated measures only one group difference was found – a smaller left GP in infected children compared to uninfected controls. In contrast, manual segmentation revealed group differences in 4 grey matter regions (bilateral NA and bilateral Pu), all of which were larger in infected children compared to uninfected children, as well as a smaller CC in infected children.

4.2.2 Disagreement of Automated Structure Delineation

The exact boundaries of the NA on MR images are a contentious issue, even between expert manual tracers, since this structure can only truly be delineated from surrounding structures cytoarchitectonically (Makris et al. 2004; Neuromorphometrics Inc. 2007). The manual tracer draws upon knowledge of surrounding tissues and structures in delineating the structure of interest. Although manual tracing is inherently subjective, the tracer relies upon intuition and subjectivity to elicit more reliable segmentation of subcortical areas of interest. Since FreeSurfer segmentation relies upon voxel intensity and contrast to delineate structures, the naturally low contrast between white matter and arteries, pose a problem that is known to affect segmentation accuracy.

Three-dimensional image acquisition, such as 3D MEMPRAGE sequences, require repetition of all phase encoding steps in the slab direction. The inversion pulse is thus placed before the partition encoding loop (Runge, Nitz & Schmeets 2009). Within the partition encoding loop, the recovery of the longitudinal magnetisation causes the signal change. T1 weighted imaging benefits from the 3D MEMPRAGE sequences. The partition encoding loops used in 3D acquisitions allow for continuous coverage with thin slices in a reasonable measure of time, unlike that of multi-slice 2D imaging (Runge, Nitz & Schmeets 2009). The use of inversion pulse allows for better control over T1-weighting, allowing higher levels of contrast, compared to spin echo and 2D gradient echo imaging (van der Kouwe et al. 2008; Runge, Nitz & Schmeets 2009). The first pitfall with the 3D MEMPRAGE is the flow sensitivity of this sequence and is based on time-of-flight effects. This occurs when the blood flowing into the imaged volume causes changes to the amplitude of the signal. The second is phase effects, where, during applied gradients, there is a phase change due to the motion of the blood (Kim & Parker 2012). Therefore, the playoff of increased contrast between grey and white matter, using MEMPRAGE sequences in our sample, has had the effect of decreasing the amount of contrast between white matter and arterial supply. Voxels arising from closely associated arteries with white matter would thus appear with similar signal intensity and would introduce bias to the automated segmentation results, especially in the case of the CC and anterior cerebral artery.

Figure 4.2 shows a sagittal slice from an MR image of an HIV-1 infected child in our study. The light purple area is the CC. The image has been segmented using FreeSurfer and shows to what extent automated segmentation would overestimate the CC as a result of this lack of contrast between the arteries and the white matter (above the red dashed line). The red dashed line indicates where the manual tracer does not agree with the automated delineation of the CC, as arterial branches off of the anterior cerebral artery are clearly visible (indicated with green arrows).

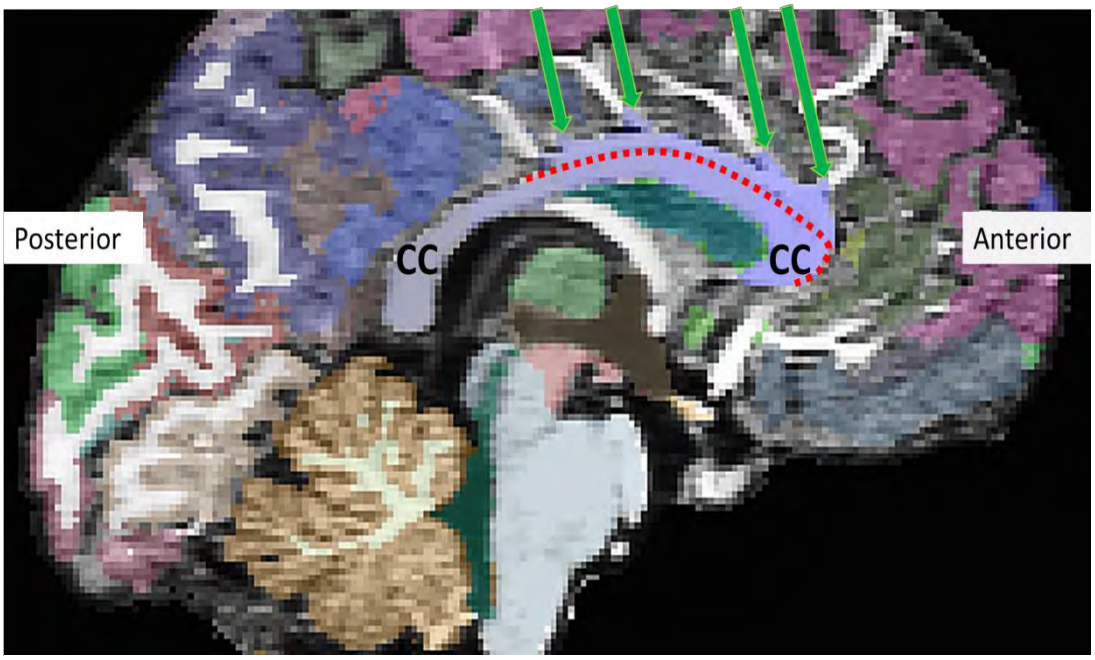

Figure 4.1 Sagittal view of corpus callosum (CC) with areas of disagreement between manual and automated measures indicated. The red dashed line indicates the boundary drawn by the manual tracer. The green arrows indicate arterial branches of the cerebral artery.

Figure 4.3 illustrates a coronal view from the same MR image. The areas of the basal ganglia have been labelled, and areas of disagreement are indicated by arrows A to D.

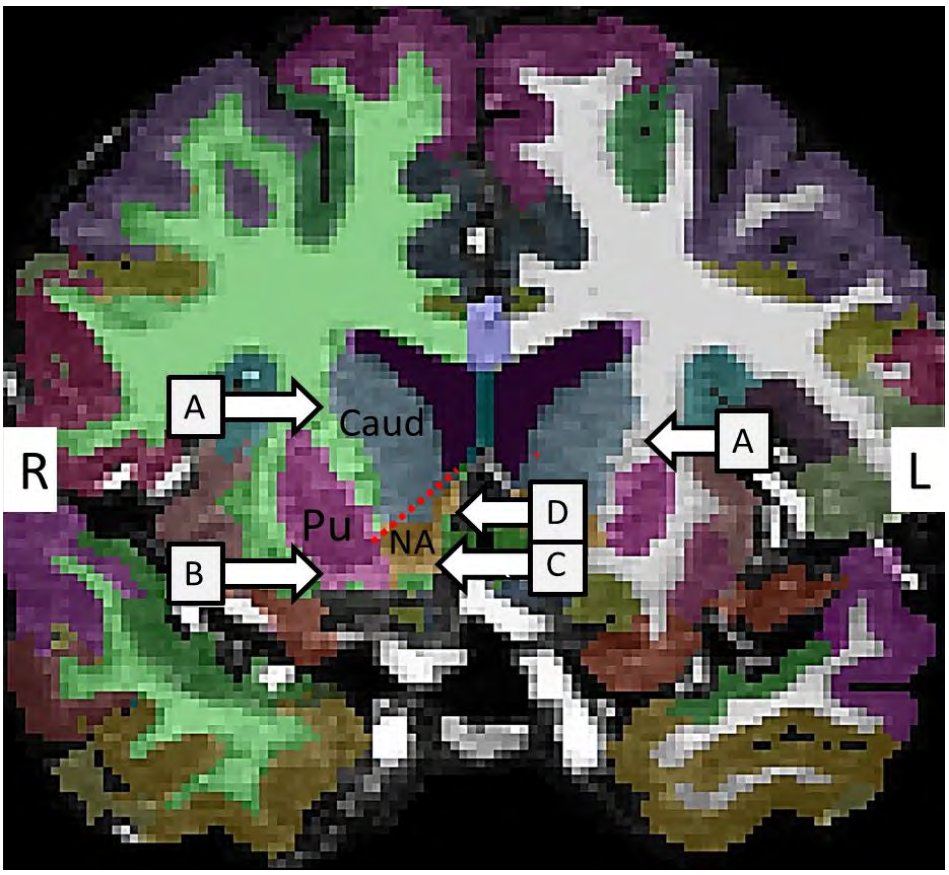

Figure 4.2 Coronal view of FreeSurfer delineation with areas of disagreement indicated with arrows A to D. (Caud = caudate, Pu = putamen, NA = nucleus accumbens)

Label A indicates areas where grey matter projections between the caudate and putamen have been labelled as white matter by FreeSurfer (in green and white). The discolouration of voxels can be seen projecting between the two structures.

Labels B and C indicate a discoloured band toward the inferior border of the putamen (B) and nucleus accumbens (C). This area consists of white matter. It extends downward from the septum pellucidum and forms the inferior border of both the putamen and NA, and separates them from the straight gyrus, anterior olfactory cortex, and olfactory tubercle.

Label D indicates the incongruence in the delineation of the border between the NA and caudate. This delineation can only truly be made cytoarchitectonically, it is generally accepted amongst neuroanatomists that a straight line from the inferior most point of the ventricle to the inferior most border of the internal capsule is sufficient in separating these two structures (Makris et al. 2004; Neuromorphometrics Inc. 2007). This instance of disagreement is merely protocol related which may differ between measures. As even within

manual tracing between tracers, specific delineation may differ depending on the protocol used within the training datasets.

It is important to note that much of the existent literature comparing automated and manual tracing has been compiled by researchers from various disciplines such as neuroscience, physics, and biomedical engineering. However, these studies are often field specific. Given the various fields, abilities in understanding and specialized knowledge would naturally differ between disciplines. However, the organic nature of the brain renders it subject to human variation that is unique to the individual. This makes the knowledge of a neuroanatomist a valuable addition to this field of research. Thus, a multidisciplinary approach, incorporating the specialist knowledge of such disciplines as anatomy, biomedical engineering, neurophysiology, and physics would enrich the nature of the literature surrounding this topic and aid assimilation of knowledge of the dynamic, organic nature of the brain in addition to reliable and valid ways to measure such an organ reproducibly. It is for this reason that the AAM method for delineating structures of interest, posed by Dewey et al. is perhaps the most parsimonious approach. The AAM method allows for the relative decreases to cost and time whilst still maintaining and incorporating the specialized knowledge-guided alterations to computer generated segmentations of a neurobiologist/neuroanatomist.

4.3 Limitations

Detailed statistical analyses were only performed on volumes in native space. The structures were not standardised for intracranial volume (ICV). However, as the group contained only children originating from a Xhosa ancestry, biological variation was assumed to be fairly low. Data from automated measures were also derived in native space, without standardising for ICV. Both male and female children were included in this study, however possible confounding influences of sex were investigated and controlled. Age at time of scanning proved to be more important than originally anticipated, considering that all children were between 5 and 6 years old at the time of scanning. Since children in this age range may be undergoing dynamic developmental changes, and children in the uninfected group were marginally older than HIV-1 infected children, it was important to control for age. Furthermore, HIV-1 infected children had been infected since birth, so that their period of infection corresponded with their age.

Due to the sheer number of structures as well as the large number of independent variables considered within this study, it was necessary to control for multiple comparisons. Use of Bonferroni and False discovery rate (FDR), in the form of Benjamini-Hochberg FDR analyses, were investigated as possible solutions to this problem. It was chosen to err on the side of caution and apply the more conservative Bonferroni correction.

Both Bonferroni correction and Benjamini-Hochberg FDR apply the assumption that individual tests, and thus independent variables, are mutually exclusive from one another (McDonald 2014). In our dataset this is not the case. Age and sex are naturally associated with body size, even in children. Our clinical independent variables PVL, CD4%, CD4/CD8 ratio, CD4 count and CD8 count are also not mutually exclusive variables as they all somewhat describe the relative state of current infection. Similarly, it would be amiss if our dependent variables of structure size were completely independent of each other, at least in terms of the size with surrounding structures within each child's basal ganglia, as they share boundaries and ICV. Using Bonferroni it was thus necessary to define the "family" of statistical tests for which the corrections would be applied. We chose this as being the total number of permutations being investigated within a defined statistical test, disregarding the lack of mutual exclusivity between variables in neighbouring analyses. This was to further our stance in erring on the side of caution in attempting to lessen the degree of Type-I error.

Correlating CD4 count, CD8 count and plasma viral load with structural volume data may not be beneficial because of HIV-1 having unique cell preferences in the brain (macrophage, microglia, astrocytes etc.). Thus, studying these relationships of constituents in blood tests may not be a true representation of HIV and HAART's effects on the brain. Genetic differences in the compartmentalised populations of HIV within the CSF and brain differ remarkably from what is observed in the blood.

Guardians/parents with HIV infected children who participated in this study were committed to helping their children. These parents/guardians may have inadvertently given extra care, attention and nurturing to their children and perhaps aided in their neurocognitive development possibly skewing some results (Mellins et al. 2003). These children may also have received improved care compared to infected children receiving standard community care.

Adherence to treatment regimen both during pregnancy and throughout the trial was undefined. Intasan et al.'s comparison of adherence strategies showed self-reporting had a stronger association with virologic failure than VL monitoring (Intasan et al. 2014).

4.4 Future Studies

Use of an active rat/ humanised mouse model to simulate perinatal HIV infection and development of the CNS is needed. Firstly, to monitor the reactive gliosis and characteristics of inflammation in the brain. Secondly, to immunohistochemically track changes in cell types in white and grey matter separately. Thirdly, to monitor the unique viral populations and immunorecruitment within the CNS. This will aid in elucidating whether the increase in structure size observed in this study is as a result of inflammation unique in children compared to adults.

Assimilation of the findings of this study with concurrent studies involving the same cohort of children would be advantageous. This would include associating structure size with the neurological tests conducted at the time of scanning. This will provide insight into structural-functional relationships involving the basal ganglia. Comparing this data to results from Magnetic Resonance Spectroscopy (MRS) will help confirm the possible presence of ongoing infection and reactive gliosis in the areas investigated. Quantitative techniques such as MRS and relaxometry in conjunction with MRI analysis may be necessary to determine early diagnostic outcomes, especially if one wishes to test the full impact and efficacy of HAART (Chang et al. 2004; Prado et al. 2011). Repeated scanning and manual segmentation of this same cohort and different ages will help track the ongoing processes occurring. In addition, 3D analysis comparing changes in shape with increasing age, using the manually segmented data, will help track which regions within each of these structures are most affected by HIV, as opposed to merely comparing the whole volume of each structure. Similarly, 3D analysis could be used to identify the regional boundaries where automated and manual segmentation differ the most.

Development of a childhood brain atlas to be used in the segmentation and parcellation protocol in FreeSurfer would be advantageous. Also given the amount of variation between sexes, as well as variation between individuals from differing ethnic origins, it should perhaps be posed that, although extremely costly and time consuming, unique atlases should be generated for these biological variations.

CHAPTER 5 CONCLUSION

Our results are in good agreement with results from other studies. Overall findings of this study suggest that perinatal HIV-1 infection targets select structures of the basal ganglia in Xhosa children at age 5 years. Both the NA and Pu are enlarged bilaterally in infected children. In contrast, the CC is smaller compared to uninfected children. Global atrophy may be masked by current ongoing infection and processes within the CNS. Although the odds of escaping the adverse effects linked to HIV-1 infection are low, our results suggest that earlier treatment aids in mitigating disease progression in the brains of 5-year-old Xhosa children. It appears that treatment should occur before plasma viral load reaches high levels to decrease the associated pathology to the basal ganglia. Damage to the corpus striatum that occurs despite treatment is possibly dictated by the rate of the initial insult (Andronikou et al. 2014; Becker et al. 2011). Although PVL was suppressed in all infected children at the time of scanning in our study, poorer immune health, as evidenced by lower CD4/CD8 ratios, was associated with larger caudal volumes.

Although there may be no group differences in the volumes of some brain structures, there may still exist differences in functional cognitive abilities which may only present in neurocognitive testing (Depas et al. 1995). Further studies of this nature would assist in developing efficient methods for management of HAART administration protocols in the hopes of alleviating some of the CNS damage in response to HIV infection.

Finally, our results demonstrate that automated segmentation using FreeSurfer may introduce bias into subcortical structure volumes in Xhosa children at, or around, 5 years of age. In view of these findings, caution should be employed when using automated measures to assess the effects of pathology on brain regions, especially in populations different to those in whom the atlases and automated methods were developed. We observed that reliability and validity differed between the pathological and normal brains in our study, and demonstrated that some statistical tests of reliability may be too lenient thus eliciting false confidence in the results. Thus, the efficacy of the intended automated measure should be compared to manually segmented data in a subset of the sample via multiple reliability tests. This would assure that the study measure portrays a truthful image of the pathology, without losing possibly valuable findings or producing inaccurate conclusions.

BIBLIOGRAPHY

Abubakar, A, van Baar, A, van de Vijver, FJR, Holding, P & Newton, CRJC 2008, 'Paediatric HIV and neurodevelopment in sub-Saharan Africa: a systematic review.', *Tropical medicine & international health : TM & IH*, vol. 13, no. 7, pp. 880–7.

Ammassari, A, Murri, R, Pezzotti, P, Trotta, MP, Ravasio, L, De Longis, P, Lo Caputo, S, Narciso, P, Pauluzzi, S, Carosi, G, Nappa, S, Piano, P, Izzo, CM, Lichtner, M, Rezza, G, Monforte, A, Ippolito, G, d'Arminio Moroni, M, Wu, AW & Antinori, A 2001, 'Self-reported symptoms and medication side effects influence adherence to highly active antiretroviral therapy in persons with HIV infection.', *Journal of acquired immune deficiency syndromes (1999)*, vol. 28, no. 5, pp. 445–9.

Ances, BM, Ortega, M, Vaida, F, Heaps, J & Paul, R 2012, 'Independent effects of HIV, aging, and HAART on brain volumetric measures.', *Journal of acquired immune deficiency syndromes (1999)*, vol. 59, no. 5, pp. 469–77.

Andronikou, S, Ackermann, C, Laughton, B, Cotton, M, Tomazos, N, Spottiswoode, B, Mauff, K & Pettifor, JM 2014, 'Correlating brain volume and callosal thickness with clinical and laboratory indicators of disease severity in children with HIV-related brain disease.', *Child's nervous system : ChNS : official journal of the International Society for Pediatric Neurosurgery*, vol. 30, no. 9, pp. 1549–57.

Annunziata, P 2003, 'Blood-brain barrier changes during invasion of the central nervous system by HIV-1. Old and new insights into the mechanism.', *Journal of neurology*, vol. 250, no. 8, pp. 901–6.

Aquaro, S, Calio, R, Balzarini, J, Bellocchi, C, Garaci, E & Federico, C 2002, 'Macrophages and HIV infection : therapeutical approaches toward this strategic virus reservoir', vol. 55, pp. 209–225.

Arendt, G, Hefter, H, Hilperath, F, von Giesen, H-J, Strohmeyer, G & Freund, H-J 1994, 'Motor analysis predicts progression in HIV-associated brain disease', *Journal of the Neurological Sciences*, vol. 123, no. 1-2, pp. 180–185.

Ashkenazi, A & Shai, Y 2011, 'Insights into the mechanism of HIV-1 envelope induced membrane fusion as revealed by its inhibitory peptides.', *European biophysics journal : EBJ*, vol. 40, no. 4, pp. 349–57.

Aylward, EH, Henderer, JD, McArthur, JC, Brettschneider, PD, Harris, GJ, Barta, PE & Pearlson, GD 1993, 'Reduced basal ganglia volume in HIV-1-associated dementia: results from quantitative neuroimaging.', *Neurology*, vol. 43, no. 10, pp. 2099–104.

Bachanas, PJ, Kullgren, KA, Schwartz, KS, Lanier, B, Mcdaniel, JS, Smith, J & Nesheim, S 2001, 'Predictors of Psychological Adjustment in School- Age Children Infected With HIV', vol. 26, no. 6, pp. 343–352.

Bagenda, D, Nassali, A, Kalyesubula, I, Sherman, B, Drotar, D, Boivin, MJ & Olness, K 2006, 'Health, neurologic, and cognitive status of HIV-infected, long-surviving, and antiretroviral-naive Ugandan children.', *Pediatrics*, vol. 117, no. 3, pp. 729–40.

Barnes, J, Foster, J, Boyes, RG, Pepple, T, Moore, EK, Schott, JM, Frost, C, Scahill, RI & Fox, NC 2008, 'A comparison of methods for the automated calculation of volumes and atrophy rates in the hippocampus.', *NeuroImage*, vol. 40, no. 4, pp. 1655–71.

Bazzoli, C, Jullien, V, Le Tiec, C, Rey, E, Mentré, F & Taburet, A-M 2010, 'Intracellular Pharmacokinetics of Antiretroviral Drugs in HIV-Infected Patients, and their Correlation with Drug Action.', *Clinical pharmacokinetics*, vol. 49, no. 1, pp. 17–45.

Becker, JT, Sanders, J, Madsen, SK, Ragin, A, Kingsley, L, Maruca, V, Cohen, B, Goodkin, K, Martin, E, Miller, EN, Sacktor, N, Alger, JR, Barker, PB, Saharan, P, Carmichael, OT & Thompson, PM 2011, 'Subcortical brain atrophy persists even in HAART-regulated HIV disease.', *Brain imaging and behavior*, vol. 5, no. 2, pp. 77–85.

Bendersky, M, Musolino, PL, Rugilo, C, Schuster, G & Sica, REP 2006, 'Normal anatomy of the developing fetal brain. Ex vivo anatomical-magnetic resonance imaging correlation.', *Journal of the neurological sciences*, vol. 250, no. 1-2, pp. 20–6.

Berger, E a, Murphy, PM & Farber, JM 1999, 'Chemokine receptors as HIV-1 coreceptors: roles in viral entry, tropism, and disease.', *Annual review of immunology*, vol. 17, pp. 657–700.

Berger, JR & Arendt, G 2000, 'HIV dementia: the role of the basal ganglia and dopaminergic systems', *Journal of Psychopharmacology*.

Bernier, BE, Whitaker, LR & Morikawa, H 2011, 'Predictive Reward Signal of Dopamine Neurons Predictive Reward Signal of Dopamine Neurons', pp. 1–27.

Berridge, KC 2007, 'The debate over dopamine's role in reward: the case for incentive salience.', *Psychopharmacology*, vol. 191, no. 3, pp. 391–431.

Blumberg, BM, Gelbard, HA & Epstein, LG 1994, 'HIV-1 infection of the developing nervous system: central role of astrocytes in pathogenesis.', *Virus research*, vol. 32, no. 2, pp. 253–67.

Boccardi, M, Ganzola, R, Bocchetta, M, Pievani, M, Redolfi, A, Bartzokis, G, Camicioli, R, Csernansky, JG, de Leon, MJ, DeToledo-Morrell, L, Killiany, RJ, Lehéricy, S, Pantel, J, Pruessner, JC, Soininen, H, Watson, C, Duchesne, S, Jack, CR & Frisoni, GB 2011, 'Survey of protocols for the manual segmentation of the hippocampus: preparatory steps towards a joint EADC-ADNI harmonized protocol.', *Journal of Alzheimer's disease : JAD*, vol. 26 Suppl 3, no. 0 3, pp. 61–75.

Bonner, K, Mezochow, A, Roberts, T, Ford, N & Cohn, J 2013, 'Viral Load Monitoring as a Tool to Reinforce Adherence : A Systematic Review', vol. 64, no. 1, pp. 74–78.

Brik, A & Wong, C-H 2003, 'HIV-1 protease: mechanism and drug discovery.', *Organic & biomolecular chemistry*, vol. 1, no. 1, pp. 5–14.

Brouwers, P, Tudor-Williams, G, DeCarli, C, Moss, HA, Wolters, PL, Civitello, LA & Pizzo, PA 1995, 'Relation between stage of disease and neurobehavioral measures in children with symptomatic HIV disease.', *AIDS (London, England)*, vol. 9, no. 7, pp. 713–20.

Cantó-nogués, C, Sánchez-ramón, S, Álvarez, S, Lacruz, C & Muñóz-fernández, MÁ 2005, 'HIV-1 Infection of Neurons Might Account for Progressive HIV-1-Associated Encephalopathy in Children', vol. 27.

Carr, A & Cooper, DA 2000, 'Adverse effects of antiretroviral therapy.', *Lancet*, vol. 356, no. 9239, pp. 1423–30.

Cavarelli, M & Scarlatti, G 2011, 'HIV-1 co-receptor usage: influence on mother-to-child transmission and pediatric infection.', *Journal of translational medicine*, vol. 9 Suppl 1, BioMed Central Ltd, no. Suppl 1, p. S10.

Caviness, VS, Kennedy, DN, Richelme, C, Rademacher, J & Filipek, P a 1996, 'The human brain age 7-11 years: a volumetric analysis based on magnetic resonance images.', *Cerebral cortex (New York, N.Y. : 1991)*, vol. 6, no. 5, pp. 726–36.

Chang, L, Andres, M, Sadino, J, Jiang, CS, Nakama, H, Miller, E & Ernst, T 2011, 'Impact of apolipoprotein E ε4 and HIV on cognition and brain atrophy: antagonistic pleiotropy and premature brain aging.', *NeuroImage*, vol. 58, no. 4, pp. 1017–27.

Chang, L, Ernst, T, Witt, MD, Ames, N, Gaiefsky, M & Miller, E 2002, 'Relationships among brain metabolites, cognitive function, and viral loads in antiretroviral-naïve HIV patients.', *NeuroImage*, vol. 17, no. 3, pp. 1638–48.

Chang, L, Lee, PL, Yiannoutsos, CT, Ernst, T, Marra, CM, Richards, T, Kolson, D, Schifitto, G, Jarvik, JG, Miller, EN, Lenkinski, R, Gonzalez, G & Navia, BA 2004, 'A multicenter in vivo proton-MRS study of HIV-associated dementia and its relationship to age', *NeuroImage*, vol. 23, pp. 1336 – 1347.

Chang, L, Yakupov, R, Nakama, H, Stokes, B & Ernst, T 2008, 'Antiretroviral treatment is associated with increased attentional load-dependent brain activation in HIV patients.', *Journal of neuroimmune pharmacology : the official journal of the Society on NeuroImmune Pharmacology*, vol. 3, no. 2, pp. 95–104.

Chiang, M-C, Dutton, R a, Hayashi, KM, Lopez, OL, Aizenstein, HJ, Toga, AW, Becker, JT & Thompson, PM 2007, '3D pattern of brain atrophy in HIV/AIDS visualized using tensor-based morphometry.', *NeuroImage*, vol. 34, no. 1, pp. 44–60.

Chiriboga, CA, Fleishman, S, Champion, S, Gaye-Robinson, L & Abrams, EJ 2005, 'Incidence and prevalence of HIV encephalopathy in children with HIV infection receiving highly active anti-retroviral therapy (HAART).', *The Journal of pediatrics*, vol. 146, no. 3, pp. 402–7.

Cohen, R a, Harezlak, J, Schifitto, G, Hana, G, Clark, U, Gongvatana, A, Paul, R, Taylor, M, Thompson, P, Alger, J, Brown, M, Zhong, J, Campbell, T, Singer, E, Daar, E, McMahon, D, Tso, Y, Yiannoutsos, CT & Navia, B 2010, 'Effects of nadir CD4 count and duration of human immunodeficiency virus infection on brain volumes in the highly active antiretroviral therapy era.', *Journal of neurovirology*, vol. 16, no. 1, pp. 25–32.

Cotton, MF, Violari, A, Otwombe, K, Panchia, R, Dobbels, E, Rabie, H, Josipovic, D, Liberty, A, Lazarus, E, Innes, S, van Rensburg, AJ, Pelser, W, Truter, H, Madhi, S a, Handelsman, E, Jean-Philippe, P, McIntyre, J a, Gibb, DM & Babiker, AG 2013, 'Early time-limited antiretroviral therapy versus deferred therapy in South African infants infected with HIV: results from the children with HIV early antiretroviral (CHER) randomised trial.', *Lancet*, vol. 382, Elsevier Ltd, no. 9904, pp. 1555–63.

Cullen, BR 1991, 'Regulation of HIV-1 gene expression.', *FASEB journal : official publication of the Federation of American Societies for Experimental Biology*, vol. 5, no. 10, pp. 2361–8.

Cullen, BR 1992, 'Mechanism of action of regulatory proteins encoded by complex retroviruses.', *Microbiological reviews*, vol. 56, no. 3, pp. 375–94.

Deeks, SG, Kitchen, CMR, Liu, L, Guo, H, Gascon, R, Narváez, AB, Hunt, P, Martin, JN, Kahn, JO, Levy, J, McGrath, MS & Hecht, FM 2004, 'Immune activation set point during early HIV infection predicts subsequent CD4+ T-cell changes independent of viral load.', *Blood*, vol. 104, no. 4, pp. 942–7.

DeLong, M 2000, 'The Basal Ganglia', in ER Kandel, JH Schwartz & TM Jessell (eds), *Principles of Neural Science*, 4th edn, McGraw-Hill Companies, Inc., New York, NY, pp. 730–741.

Depas, G, Chiron, C, Tardieu, M, Nuttin, C, Blanche, S, Raynaud, C & Syrota, a 1995, 'Functional brain imaging in HIV-1-infected children born to seropositive mothers.', *Journal of nuclear medicine : official publication, Society of Nuclear Medicine*, vol. 36, no. 12, pp. 2169–74.

Dewey, J, Hana, G, Russell, T, Price, J, McCaffrey, D, Harezlak, J, Sem, E, Anyanwu, JC, Guttmann, CR, Navia, B, Cohen, R & Tate, DF 2010, 'Reliability and validity of MRI-based automated volumetry software relative to auto-assisted manual measurement of subcortical structures in HIV-infected patients from a multisite study.', *NeuroImage*, vol. 51, Elsevier Inc., no. 4, pp. 1334–44.

Dowker, A 2006, 'What can functional brain imaging studies tell us about typical and atypical cognitive development in children?', *Journal of physiology, Paris*, vol. 99, no. 4-6, pp. 333–41.

Doya, K 2000, 'Complementary roles of basal ganglia and cerebellum in learning and motor control.', *Current opinion in neurobiology*, vol. 10, no. 6, pp. 732–9.

Duyckaerts, C & Litvan, I 2008, 'Transmissable diseases Neuropathology and HIV dementia', *Brain Pathology*, vol. 89.

Epstein, LG & Gelbard, H a 1999, 'HIV-1-induced neuronal injury in the developing brain.', *Journal of leukocyte biology*, vol. 65, no. 4, pp. 453–7.

Epstein, LG, Sharer, LR, Oleske, JM, Connor, EM, Goudsmit, J, Bagdon, L, Robert-guroff, M & Koenigsberger, MR 1986, 'Neurologic Manifestations of Human Immunodeficiency Virus Infection in Children', *Pediatrics*, vol. 78.

Ernst, T, Chang, L & Arnold, S 2003, 'Increased glial metabolites predict increased working memory network activation in HIV brain injury', *NeuroImage*, vol. 19, no. 4, pp. 1686–1693.

Esposito, F, Corona, A & Tramontano, E 2012, 'HIV-1 Reverse Transcriptase Still Remains a New Drug Target: Structure, Function, Classical Inhibitors, and New Inhibitors with Innovative Mechanisms of Actions.', *Molecular biology international*, vol. 2012, p. 586401.

Fan, Y, Shi, F, Smith, JK, Lin, W, Gilmore, JH & Shen, D 2011, 'Brain anatomical networks in early human brain development.', *NeuroImage*, vol. 54, Elsevier B.V., no. 3, pp. 1862–71.

Farquhar, C, Rowland-Jones, S, Mbori-Ngacha, D, Redman, M, Lohman, B, Slyker, J, Otieno, P, Obimbo, E, Rostron, T, Ochieng, J, Oyugi, J, Bosire, R & John-Stewart, G 2004, 'Human leukocyte antigen (HLA) B*18 and protection against mother-to-child HIV type 1 transmission.', *AIDS research and human retroviruses*, vol. 20, no. 7, pp. 692–7.

Fellay, J, Shianna, K V, Ge, D, Colombo, S, Ledergerber, B, Weale, M, Zhang, K, Gumbs, C, Castagna, A, Cossarizza, A, Cozzi-Lepri, A, De Luca, A, Easterbrook, P, Francioli, P, Mallal, S, Martinez-Picado, J, Miro, JM, Obel, N, Smith, JP, Wyniger, J, Descombes, P, Antonarakis, SE, Letvin, NL, McMichael, AJ, Haynes, BF, Telenti, A & Goldstein, DB 2007, 'A whole-genome association study of major determinants for host control of HIV-1.', *Science (New York, N.Y.)*, vol. 317, no. 5840, pp. 944–7.

Feng, Y, Broder, CC, Kennedy, PE & Berger, EA 2011, 'Pillars article: HIV-1 entry cofactor: functional cDNA cloning of a seven-transmembrane, G protein-coupled receptor. Science. 1996. 272: 872-877.', *Journal of immunology (Baltimore, Md. : 1950)*, vol. 186, no. 11, pp. 6076–81.

Fischer, U, Huber, J, Boelens, WC, Mattaj, IW & Lührmann, R 1995, 'The HIV-1 Rev activation domain is a nuclear export signal that accesses an export pathway used by specific cellular RNAs.', *Cell*, vol. 82, no. 3, pp. 475–83.

Fischl, B, Salat, DH, Busa, E, Albert, M, Dieterich, M, Haselgrove, C, van der Kouwe, A, Killiany, R, Kennedy, D, Klaveness, S, Montillo, A, Makris, N, Rosen, B & Dale, AM 2002, 'Whole brain segmentation: automated labeling of neuroanatomical structures in the human brain.', *Neuron*, vol. 33, no. 3, pp. 341–55.

Gale, HB, Gitterman, SR, Hoffman, HJ, Gordin, FM, Benator, D a, Labriola, AM & Kan, VL 2013, 'Is frequent CD4+ T-lymphocyte count monitoring necessary for persons with counts >=300 cells/μL and HIV-1 suppression?', *Clinical infectious diseases : an official publication of the Infectious Diseases Society of America*, vol. 56, no. 9, pp. 1340–3.

George, R, Andronikou, S, Plessis, J, Plessis, A, Toorn, R Van & Maydell, A 2009, 'Central nervous system manifestations of HIV infection in children', pp. 575–585.

Ghodke, Y, Anderson, PL, Sangkuhl, K, Lamba, J, Altman, RB & Klein, TE 2012, 'PharmGKB summary: zidovudine pathway.', *Pharmacogenetics and genomics*, vol. 22, no. 12, pp. 891–4.

Giedd, JN, Blumenthal, J, Jeffries, NO, Castellanos, FX, Liu, H, Zijdenbos, a, Paus, T, Evans, a C & Rapoport, JL 1999, 'Brain development during childhood and adolescence: a longitudinal MRI study.', *Nature neuroscience*, vol. 2, no. 10, pp. 861–3.

Von Giesen, HJ, Antke, C, Hefter, H, Wenserski, F, Seitz, RJ & Arendt, G 2000, 'Potential time course of human immunodeficiency virus type 1-associated minor motor deficits: electrophysiologic and positron emission tomography findings.', *Archives of neurology*, vol. 57, no. 11, pp. 1601–7.

Von Giesen, HJ, Köller, H, Theisen, A & Arendt, G 2002, 'Therapeutic effects of nonnucleoside reverse transcriptase inhibitors on the central nervous system in HIV-1-infected patients.', *Journal of acquired immune deficiency syndromes (1999)*, vol. 29, no. 4, pp. 363–7.

Von Giesen, HJ, Niehues, T, Reumel, J, Haslinger, B a, Ndagijimana, J & Arendt, G 2003, 'Delayed motor learning and psychomotor slowing in HIV-infected children.', *Neuropediatrics*, vol. 34, no. 4, pp. 177–81.

Girard, P-M, Nelson, M, Mohammed, P, Hill, A, van Delft, Y & Moecklinghoff, C 2013, 'Can we stop CD4+ testing in patients with HIV-1 RNA suppression on antiretroviral treatment?', *AIDS (London, England)*, vol. 27, no. 17, pp. 2759–63.

Govender, R, Eley, B, Walker, K, Petersen, R & Wilmshurst, JM 2011, 'Neurologic and neurobehavioral sequelae in children with human immunodeficiency virus (HIV-1) infection.', *Journal of child neurology*, vol. 26, no. 11, pp. 1355–64.

Gray, LR, Tachedjian, G, Ellett, AM, Roche, MJ, Cheng, W-J, Guillemin, GJ, Brew, BJ, Turville, SG, Wesselingh, SL, Gorry, PR & Churchill, MJ 2013, 'The NRTIs lamivudine, stavudine and zidovudine have reduced HIV-1 inhibitory activity in astrocytes.', *PloS one*, vol. 8, no. 4, p. e62196.

Griffiths, PD, Perry, RH & Crossman, AR 1994, 'A detailed anatomical analysis of neurotransmitter receptors in the putamen and caudate in Parkinson's disease and Alzheimer's disease.', *Neuroscience letters*, vol. 169, no. 1-2, pp. 68–72.

Gronenschild, EHBM, Habets, P, Jacobs, HIL, Mengelers, R, Rozendaal, N, van Os, J & Marcelis, M 2012, 'The effects of FreeSurfer version, workstation type, and Macintosh operating system version on anatomical volume and cortical thickness measurements.', *PloS one*, vol. 7, no. 6, p. e38234.

Grubbs, F 1969, 'Procedures for detecting outlying observations in samples', *Technometrics*, vol. 11, no. 1, pp. 1–21.

Hahn, YK, Podhaizer, EM, Farris, SP, Miles, MF, Hauser, KF & Knapp, PE 2013, 'Effects of chronic HIV-1 Tat exposure in the CNS: heightened vulnerability of males versus females to changes in cell numbers, synaptic integrity, and behavior.', *Brain structure & function*.

Han, X & Fischl, B 2007, 'Atlas renormalization for improved brain MR image segmentation across scanner platforms.', *IEEE transactions on medical imaging*, vol. 26, no. 4, pp. 479–86.

Hasan, KM, Kamali, A, Iftikhar, A, Kramer, L a, Papanicolaou, AC, Fletcher, JM & Ewing-Cobbs, L 2009, 'Diffusion tensor tractography quantification of the human corpus callosum fiber pathways across the lifespan.', *Brain research*, vol. 1249, Elsevier B.V., pp. 91–100.

Hasan, KM & Pedraza, O 2009, 'Improving the reliability of manual and automated methods for hippocampal and amygdala volume measurements.', *NeuroImage*, vol. 48, Elsevier Inc., no. 3, pp. 497–8.

Heaps, JM, Joska, J, Hoare, J, Ortega, M, Agrawal, A, Seedat, S, Ances, BM, Stein, DJ & Paul, R 2012, 'Neuroimaging markers of human immunodeficiency virus infection in South Africa.', *Journal of neurovirology*, vol. 18, no. 3, pp. 151–6.

Hoare, J, Fouche, J-P, Spottiswoode, B, Donald, K, Philipps, N, Bezuidenhout, H, Mulligan, C, Webster, V, Oduro, C, Schrieff, L, Paul, R, Zar, H, Thomas, K & Stein, D 2012, 'A diffusion tensor imaging and neurocognitive study of HIV-positive children who are HAART-naïve "slow progressors".', *Journal of neurovirology*, vol. 18, no. 3, pp. 205–12.

Hoare, J, Ransford, GL, Phillips, N, Amos, T, Donald, K & Stein, DJ 2013, 'Systematic review of neuroimaging studies in vertically transmitted HIV positive children and adolescents.', *Metabolic brain disease*.

Hsu, Y-Y, Schuff, N, Du, A-T, Mark, K, Zhu, X, Hardin, D & Weiner, MW 2002, 'Comparison of automated and manual MRI volumetry of hippocampus in normal aging and dementia.', *Journal of magnetic resonance imaging : JMRI*, vol. 16, no. 3, pp. 305–10.

IBM Corp. 2013, *IBM SPSS Statistics for Windows*, 22, IBM Corp, Armonk; NY.

Intasan, J, Bunupuradah, T, Vonthanak, S, Kosalaraksa, P, Hansudewechakul, R, Kanjanavanit, S, Ngampiyaskul, C, Wongsawat, J, Luesomboon, W, Apornpong, T, Kerr, S, Ananworanich, J & Puthanakit, T 2014, 'Comparison of adherence monitoring tools and correlation to virologic failure in a pediatric HIV clinical trial.', *AIDS patient care and STDs*, vol. 28, no. 6, pp. 296–302.

Ivey, NS, MacLean, AG & Lackner, AA 2009, 'Acquired immunodeficiency syndrome and the blood-brain barrier.', *Journal of neurovirology*, vol. 15, no. 2, pp. 111–22.

Johann-Liang, R, Lin, K, Cervia, J, Stavola, J & Noel, G 1998, 'Neuroimaging findings in children perinatally infected with the human immunodeficiency virus.', *The Pediatric infectious disease journal*, vol. 17, no. 8, pp. 753–4.

Kandel, ER, Schwartz, JH & Jessell, TM 2000, *Principles of Neural Science*, 4th edn, McGraw-Hill Medical Publishing Division, New York, NY, p. 1414.

Kiernan, J & Rajakumar, R 2013, 'Barr's The Human Nervous System: An Anatomical Viewpoint', 10th edn, Lippincott Williams & Wilkins, p. 448.

Kim, S-E & Parker, DL 2012, *Magnetic Resonance Angiography*, JC Carr & TJ Carroll (eds), Springer New York, New York, NY.

Kirchhoff, F 2010, 'Immune evasion and counteraction of restriction factors by HIV-1 and other primate lentiviruses.', *Cell host & microbe*, vol. 8, Elsevier Inc., no. 1, pp. 55–67.

Klein, RS, Williams, KC, Alvarez-Hernandez, X, Westmoreland, S, Force, T, Lackner, AA & Luster, AD 1999, 'Chemokine receptor expression and signaling in macaque and human fetal neurons and astrocytes: implications for the neuropathogenesis of AIDS.', *Journal of immunology (Baltimore, Md. : 1950)*, vol. 163, no. 3, pp. 1636–46.

Knickmeyer, RC, Gouttard, S, Kang, C, Evans, D, Wilber, K, Smith, JK, Hamer, RM, Lin, W, Gerig, G & Gilmore, JH 2008, 'A structural MRI study of human brain development from birth to 2 years.', *The Journal of neuroscience : the official journal of the Society for Neuroscience*, vol. 28, no. 47, pp. 12176–82.

Koekkoek, S, Eggermont, L, De Sonneville, L, Jupimai, T, Wicharuk, S, Apateerapong, W, Chuenyam, T, Lange, J, Wit, F, Pancharoen, C, Phanuphak, P & Ananworanich, J 2006, 'Effects of highly active antiretroviral therapy (HAART) on psychomotor performance in children with HIV disease.', *Journal of neurology*, vol. 253, no. 12, pp. 1615–24.

Van der Kouwe, AJW, Benner, T, Salat, DH & Fischl, B 2008, 'Brain morphometry with multiecho MPRAGE.', *NeuroImage*, vol. 40, no. 2, pp. 559–69.

Lackner, AA, Vogel, P, Ramos, RA, Kluge, JD & Marthas, M 1994, 'Early events in tissues during infection with pathogenic (SIVmac239) and nonpathogenic (SIVmac1A11) molecular clones of simian immunodeficiency virus.', *The American journal of pathology*, vol. 145, no. 2, pp. 428–39.

Langerak, NG, du Toit, J, Burger, M, Cotton, MF, Springer, PE & Laughton, B 2014, 'Spastic diplegia in children with HIV encephalopathy: first description of gait and physical status.', *Developmental medicine and child neurology*, vol. 56, no. 7, pp. 686–94.

Lanier, ER, Sturge, G, McClernon, D, Brown, S, Halman, M, Sacktor, N, McArthur, J, Atkinson, JH, Clifford, D, Price, RW, Simpson, D, Torres, G, Catalan, J, Marder, K, Power, C, Hall, C, Romero, C & Brew, B 2001, 'HIV-1 reverse transcriptase sequence in plasma and cerebrospinal fluid of patients with AIDS dementia complex treated with Abacavir.', *AIDS (London, England)*, vol. 15, no. 6, pp. 747–51.

Laughton, B, Cornell, M, Boivin, M & Rie, A Van 2013, 'Review article Neurodevelopment in perinatally HIV-infected children : a concern for adolescence'.

Laughton, B, Cornell, M, Grove, D, Kidd, M, Springer, PE, Dobbels, E, van Rensburg, AJ, Violari, A, Babiker, AG, Madhi, S a, Jean-Philippe, P, Gibb, DM & Cotton, MF 2012, 'Early antiretroviral therapy improves neurodevelopmental outcomes in infants.', *AIDS (London, England)*, vol. 26, no. 13, pp. 1685–90.

Laughton, B, Grove, D, Kidd, M, Springer, PE, Dobbels, E, van Rensburg, AJ, Violari, A, Babiker, AG, Madhi, SA, Gibb, DM & Cotton, MF 2009, 'Early Antiretroviral Therapy is Associated with Improved Neurodevelopmental Outcome in HIV-infected Infants: Evidence from the CHER (Children with HIV Early Antiretroviral Therapy) Trial', IAS 2009, Cape Town, p. 1.

Lawless, MK, Barney, S, Guthrie, KI, Bucy, TB, Petteway, SR & Merutka, G 1996, 'HIV-1 membrane fusion mechanism: structural studies of the interactions between biologically-active peptides from gp41.', *Biochemistry*, vol. 35, no. 42, pp. 13697–708.

Lawrence, DM & Major, EO 2002, 'HIV-1 and the brain: connections between HIV-1-associated dementia, neuropathology and neuroimmunology.', *Microbes and infection / Institut Pasteur*, vol. 4, no. 3, pp. 301–8.

Leon, MJ De, Convit, A, Wolf, OT, Tarshish, CY, Desanti, S, Rusinek, H, Tsui, W, Kandil, E, Scherer, AJ, Roche, A, Imossi, A, Thorn, E, Bobinski, M, Caraos, C, Lesbre, P, Schlyer, D, Poirier, J, Reisberg, B & Fowler, J 2001, 'Prediction of cognitive decline in normal elderly subjects with 2- [18 F] fluoro-2-deoxy- D -glucose positron-emission tomography (FDG PET)', vol. 98, no. 19.

Letendre, SL, McCutchan, JA, Childers, ME, Woods, SP, Lazzaretto, D, Heaton, RK, Grant, I & Ellis, RJ 2004, 'Enhancing antiretroviral therapy for human immunodeficiency virus cognitive disorders.', *Annals of neurology*, vol. 56, no. 3, pp. 416–23.

Lindsey, JC, Malee, KM, Brouwers, P & Hughes, MD 2007, 'Neurodevelopmental functioning in HIV-infected infants and young children before and after the introduction of protease inhibitor-based highly active antiretroviral therapy.', *Pediatrics*, vol. 119, no. 3, pp. e681–93.

MacDonald, KS, Embree, J, Njenga, S, Nagelkerke, NJ, Ngatia, I, Mohammed, Z, Barber, BH, Ndinya-Achola, J, Bwayo, J & Plummer, F a 1998, 'Mother-child class I HLA concordance increases perinatal human immunodeficiency virus type 1 transmission.', *The Journal of infectious diseases*, vol. 177, no. 3, pp. 551–6.

Mackelprang, RD, John-Stewart, G, Carrington, M, Richardson, B, Rowland-Jones, S, Gao, X, Mbori-Ngacha, D, Mabuka, J, Lohman-Payne, B & Farquhar, C 2008, 'Maternal HLA homozygosity and mother-child HLA concordance increase the risk of vertical transmission of HIV-1.', *The Journal of infectious diseases*, vol. 197, no. 8, pp. 1156–61.

Mahy, M 2003, 'Measuring child mortality in AIDS-affected countries', *UN/POP/MORT*, vol. 15, no. September, pp. 1–9.

Makris, N, Kennedy, DN, Meyer, J, Worth, A, Caviness, VS, Seidman, L, Goldstein, J, Goodman, J, Hoge, E, Macpherson, C, Tourville, J, Klaveness, S, Hodge, SM, Melrose, R, Rauch, S, Kim, H, Harris, G, Boehland, A, Glode, B, Koch, J, Segal, E, Sonricker, A, Dieterich, M, Papadimitriou, G, Normandin, JJ, Cullen, N, Boriel, D & Sanders, H 2004, *General Brain Segmentation - Method and Utilization - Version 3*, Charlestown MA.

Malim, MH & Bieniasz, PD 2012, 'HIV Restriction Factors and Mechanisms of Evasion.', *Cold Spring Harbor perspectives in medicine*, vol. 2, no. 5, p. a006940.

Mariani, S a, Brigida, I, Kajaste-Rudnitski, A, Ghezzi, S, Rocchi, A, Plebani, A, Vicenzi, E, Aiuti, A & Poli, G 2012, 'HIV-1 envelope-dependent restriction of CXCR4-using viruses in child but not adult untransformed CD4+ T-lymphocyte lines.', *Blood*, vol. 119, no. 9, pp. 2013–23.

McArthur, JC 2004, 'HIV dementia: an evolving disease.', *Journal of neuroimmunology*, vol. 157, no. 1-2, pp. 3–10.

McArthur, JC, Brew, BJ & Nath, A 2005, 'Neurological complications of HIV infection.', *The Lancet. Neurology*, vol. 4, no. 9, pp. 543–55.

McClernon, DR, Lanier, R, Gartner, S, Feaser, P, Pardo, C a, St Clair, M, Liao, Q & McArthur, JC 2001, 'HIV in the brain: RNA levels and patterns of zidovudine resistance.', *Neurology*, vol. 57, no. 8, pp. 1396–401.

McCoig, C, Castrejón, MM, Castaño, E, De Suman, O, Báez, C, Redondo, W, McClernon, D, Danehower, S, Lanier, ER, Richardson, C, Keller, A, Hetherington, S, Sáez-Llorens, X & Ramilo, O 2002, 'Effect of combination antiretroviral therapy on cerebrospinal fluid HIV RNA, HIV resistance, and clinical manifestations of encephalopathy.', *The Journal of pediatrics*, vol. 141, no. 1, pp. 36–44.

McDermott, DH, Zimmerman, P a, Guignard, F, Kleeberger, C a, Leitman, SF & Murphy, PM 1998, 'CCR5 promoter polymorphism and HIV-1 disease progression. Multicenter AIDS Cohort Study (MACS).', *Lancet*, vol. 352, no. 9131, pp. 866–70.

McDonald, JH 2014, *Handbook of Biological Statistics*, 3rd edn, Sparky House Publishing, Baltimore, Marland, p. 305.

Medders, KE & Kaul, M 2011, 'Mitogen-activated protein kinase p38 in HIV infection and associated brain injury.', *Journal of neuroimmune pharmacology : the official journal of the Society on NeuroImmune Pharmacology*, vol. 6, no. 2, pp. 202–15.

Mellins, C a., Smith, R, O'Driscoll, P, Magder, LS, Brouwers, P, Chase, C, Blasini, I, Hittleman, J, Llorente, a. & Matzen, E 2003, 'High Rates of Behavioral Problems in Perinatally HIV-Infected Children Are Not Linked to HIV Disease', *Pediatrics*, vol. 111, no. 2, pp. 384–393.

Misra, A, Ganesh, S, Shahiwala, A & Shah, SP 2003, 'Drug delivery to the central nervous system: a review.', *Journal of pharmacy & pharmaceutical sciences : a publication of the Canadian Society for Pharmaceutical Sciences, Société canadienne des sciences pharmaceutiques*, vol. 6, no. 2, pp. 252–73.

Mitchell, W 2001, 'Neurological and developmental effects of HIV and AIDS in children and adolescents', *Mental retardation and developmental disabilities …*, vol. 216, pp. 211–216.

Mitchell, W 2001, 'Neurological and developmental effects of HIV and AIDS in children and adolescents.', *Mental retardation and developmental disabilities research reviews*, vol. 7, no. 3, pp. 211–6.

Mlcochova, P, Watters, S a, Towers, GJ, Noursadeghi, M & Gupta, RK 2014, 'Vpx complementation of "non-macrophage tropic" R5 viruses reveals robust entry of infectious HIV-1 cores into macrophages.', *Retrovirology*, vol. 11, Retrovirology, no. 1, p. 25.

Morey, RA, Petty, CM, Xu, Y, Hayes, JP, Wagner, HR, Lewis, D V, LaBar, KS, Styner, M & McCarthy, G 2009, 'A comparison of automated segmentation and manual tracing for quantifying hippocampal and amygdala volumes.', *NeuroImage*, vol. 45, Elsevier B.V., no. 3, pp. 855–66.

Mulder, ER, de Jong, R a, Knol, DL, van Schijndel, R a, Cover, KS, Visser, PJ, Barkhof, F & Vrenken, H 2014, 'Hippocampal volume change measurement: quantitative assessment of the reproducibility of expert manual outlining and the automated methods FreeSurfer and FIRST.', *NeuroImage*, vol. 92, Elsevier Inc., pp. 169–81.

Musich, T, Peters, PJ, Duenas-Decamp, MJ, Gonzalez-Perez, MP, Robinson, J, Zolla-Pazner, S, Ball, JK, Luzuriaga, K & Clapham, PR 2011, 'A conserved determinant in the V1 loop of HIV-1 modulates the V3 loop to prime low CD4 use and macrophage infection.', *Journal of virology*, vol. 85, no. 5, pp. 2397–405.

Netter, FH 2002, 'Neuroanatomy: Basal Nuclei (Ganglia)', in *Atlas of Neuroanatomy and Neurophysiology*, Icon Custom Communications, Teterboro, p. 4.

Neuromorphometrics Inc. 2007, *Segmentation Protocols - Version 1.1*, viewed 5 March 2012, <http://neuromorphometrics.org:8080/Seg/>.

Nozyce, ML, Lee, SS, Wiznia, A, Nachman, S, Mofenson, LM, Smith, ME, Yogev, R, McIntosh, K, Stanley, K & Pelton, S 2006, 'A behavioral and cognitive profile of clinically stable HIV-infected children.', *Pediatrics*, vol. 117, no. 3, pp. 763–70.

Ochsenbauer, C, Edmonds, TG, Ding, H, Keele, BF, Decker, J, Salazar, MG, Salazar-Gonzalez, JF, Shattock, R, Haynes, BF, Shaw, GM, Hahn, BH & Kappes, JC 2012, 'Generation of transmitted/founder HIV-1 infectious molecular clones and characterization of their replication capacity in CD4 T lymphocytes and monocyte-derived macrophages.', *Journal of virology*, vol. 86, no. 5, pp. 2715–28.

Oster, S, Christoffersen, P, Gundersen, HJG, Nielsen, JO, Pakkenberg, B & Pedersen, C 1993, 'Cerebral atrophy in AIDS: a stereological study', *Acta Neuropathologica*, vol. 85, no. 6, pp. 617–622.

Packard, MG & Knowlton, BJ 2002, 'Learning and memory functions of the Basal Ganglia.', *Annual review of neuroscience*, vol. 25, pp. 563–93.

Parks, RA & Danoff, J V 1999, 'Motor performance changes in children testing positive for HIV over 2 years.', *The American journal of occupational therapy : official publication of the American Occupational Therapy Association*, vol. 53, no. 5, pp. 524–8.

Paul, ME, Mao, C, Charurat, M, Serchuck, L, Foca, M, Hayani, K, Handelsman, EL, Diaz, C, McIntosh, K & Shearer, WT 2005, 'Predictors of immunologic long-term nonprogression in HIV-infected children: implications for initiating therapy.', *The Journal of allergy and clinical immunology*, vol. 115, no. 4, pp. 848–55.

Perelson, AS, Essunger, P, Cao, Y, Vesanen, M, Hurley, A, Saksela, K, Markowitz, M & Ho, DD 1997, 'Decay characteristics of HIV-1-infected compartments during combination therapy.', *Nature*, vol. 387, no. 6629, pp. 188–91.

Pillai, SK, Pond, SLK, Liu, Y, Good, BM, Strain, MC, Ellis, RJ, Letendre, S, Smith, DM, Günthard, HF, Grant, I, Marcotte, TD, McCutchan, JA, Richman, DD & Wong, JK 2006, 'Genetic attributes of cerebrospinal fluid-derived HIV-1 env.', *Brain : a journal of neurology*, vol. 129, no. Pt 7, pp. 1872–83.

Pollard, VW & Malim, MH 1998, 'The HIV-1 Rev protein.', *Annual review of microbiology*, vol. 52, pp. 491–532.

Pomara, N, Crandall, DT, Choi, SJ, Johnson, G & Lim, KO 2001, 'White matter abnormalities in HIV-1 infection: a diffusion tensor imaging study.', *Psychiatry research*, vol. 106, no. 1, pp. 15–24.

Powell, S, Magnotta, VA, Johnson, H, Jammalamadaka, VK, Pierson, R & Andreasen, NC 2008, 'Registration and machine learning-based automated segmentation of subcortical and cerebellar brain structures.', *NeuroImage*, vol. 39, no. 1, pp. 238–47.

Prado, PTC, Escorsi-Rosset, S, Cervi, MC & Santos, AC 2011, 'Image evaluation of HIV encephalopathy: a multimodal approach using quantitative MR techniques.', *Neuroradiology*, vol. 53, no. 11, pp. 899–908.

Ramos-Sanchez, EM, Goto, H, Rivero, DHRF, Mauad, T, de Souza, FN, Monteiro, AM & Gidlund, M 2014, 'In vivo assessment of antiretroviral therapy-associated side effects.', *Memórias do Instituto Oswaldo Cruz*, vol. 109, no. 4, pp. 484–7.

Rapoport, JL, Castellanos, FX, Gogate, N, Janson, K, Kohler, S & Nelson, P 2001, 'Imaging normal and abnormal brain development: new perspectives for child psychiatry.', *The Australian and New Zealand journal of psychiatry*, vol. 35, no. 3, pp. 272–81.

Raskino, C, Pearson, DA, Baker, CJ, Lifschitz, MH, O'Donnell, K, Mintz, M, Nozyce, M, Brouwers, P, McKinney, RE, Jimenez, E & Englund, JA 1999, 'Neurologic, neurocognitive, and brain growth outcomes in human immunodeficiency virus-infected children receiving different nucleoside antiretroviral regimens. Pediatric AIDS Clinical Trials Group 152 Study Team.', *Pediatrics*, vol. 104, no. 3, p. e32.

Reid, W, Sadowska, M, Denaro, F, Rao, S, Foulke, J, Hayes, N, Jones, O, Doodnauth, D, Davis, H, Sill, A, O'Driscoll, P, Huso, D, Fouts, T, Lewis, G, Hill, M, Kamin-Lewis, R, Wei, C, Ray, P, Gallo, RC, Reitz, M & Bryant, J 2001, 'An HIV-1 transgenic rat that develops HIV-related pathology and immunologic dysfunction.', *Proceedings of the National Academy of Sciences of the United States of America*, vol. 98, no. 16, pp. 9271–6.

Reynolds, SJ, Sempa, JB, Kiragga, AN, Newell, K, Nakigozi, G, Galiwango, R, Gray, R, Quinn, TC, Serwadda, D & Chang, L 2014, 'Is CD4 monitoring needed among ugandan clients achieving a virologic and immunologic response to treatment?', *AIDS patient care and STDs*, vol. 28, no. 11, pp. 575–8.

Van Rie, A, Harrington, PR, Dow, A & Robertson, K 2007, 'Review article Neurologic and neurodevelopmental manifestations of pediatric HIV / AIDS : A global perspective', *Neurology*, vol. 11, pp. 1 – 9.

Van Rie, A, Mupuala, A & Dow, A 2008, 'Impact of the HIV/AIDS epidemic on the neurodevelopment of preschool-aged children in Kinshasa, Democratic Republic of the Congo.', *Pediatrics*, vol. 122, no. 1, pp. e123–8.

Ritola, K, Robertson, K, Fiscus, SA, Hall, C & Swanstrom, R 2005, 'Increased human immunodeficiency virus type 1 (HIV-1) env compartmentalization in the presence of HIV-1-associated dementia.', *Journal of virology*, vol. 79, no. 16, pp. 10830–4.

Rosca, EC, Rosca, O, Chirileanu, RD & Simu, M 2011, 'HIV & AIDS Review Neurocognitive disorders due to HIV infection', *HIV & AIDS Review*, vol. 10, Polish AIDS Research Society., no. 2, pp. 33–37.

Rosenfeldt, V, Valerius, NH & Paerregaard, a 2000, 'Regression of HIV-associated progressive encephalopathy of childhood during HAART.', *Scandinavian journal of infectious diseases*, vol. 32, no. 5, pp. 571–4.

Runge, VM, Nitz, WR & Schmeets, SH 2009, *The Physics of Clinical MR Taught Through Images*, VM Runge, WR Nitz & SH Schmeets (eds), Georg Thieme Verlag, Stuttgart.

Sacktor, N, Haughey, N, Cutler, R, Tamara, A, Turchan, J, Pardo, C, Vargas, D & Nath, A 2004, 'Novel markers of oxidative stress in actively progressive HIV dementia', *Journal of Neuroimmunology*, vol. 157, pp. 176 – 184.

Sacktor, NC, Bacellar, H, Hoover, DR, Nance-Sproson, TE, Selnes, OA, Miller, EN, Dal Pan, GJ, Kleeberger, C, Brown, A, Saah, A & McArthur, JC 1996, 'Psychomotor slowing in HIV infection: a predictor of dementia, AIDS and death.', *Journal of neurovirology*, vol. 2, no. 6, pp. 404–10.

Safriel, YI, Haller, JO, Lefton, DR & Obedian, R 2000, 'Imaging of the brain in the HIV-positive child.', *Pediatric radiology*, vol. 30, no. 11, pp. 725–32.

Salimi, H, Roche, M, Webb, N, Gray, LR, Chikere, K, Sterjovski, J, Ellett, A, Wesselingh, SL, Ramsland, P a, Lee, B, Churchill, MJ & Gorry, PR 2013, 'Macrophage-tropic HIV-1 variants from brain demonstrate alterations in the way gp120 engages both CD4 and CCR5.', *Journal of leukocyte biology*, vol. 93, no. 1, pp. 113–26.

Sánchez-Benavides, G, Gómez-Ansón, B, Sainz, A, Vives, Y, Delfino, M & Peña-Casanova, J 2010, 'Manual validation of FreeSurfer's automated hippocampal segmentation in normal aging, mild cognitive impairment, and Alzheimer Disease subjects.', *Psychiatry research*, vol. 181, Elsevier Ireland Ltd, no. 3, pp. 219–25.

Sarma, MK, Nagarajan, R, Keller, M a, Kumar, R, Nielsen-Saines, K, Michalik, DE, Deville, J, Church, J a & Thomas, MA 2014, 'Regional brain gray and white matter changes in perinatally HIV-infected adolescents.', *NeuroImage. Clinical*, vol. 4, The Authors, pp. 29–34.

Schnell, G, Joseph, S, Spudich, S, Price, RW & Swanstrom, R 2011, 'HIV-1 replication in the central nervous system occurs in two distinct cell types.', *PLoS pathogens*, vol. 7, no. 10, p. e1002286.

Sei, S, Stewart, SK, Farley, M, Mueller, BU, Lane, JR, Robb, ML, Brouwers, P & Pizzo, PA 1996, 'Evaluation of human immunodeficiency virus (HIV) type 1 RNA levels in cerebrospinal fluid and viral resistance to zidovudine in children with HIV encephalopathy.', *The Journal of infectious diseases*, vol. 174, no. 6, pp. 1200–6.

Shah, SS, Zimmerman, R a, Rorke, LB & Vezina, LG 1996, 'Cerebrovascular complications of HIV in children.', *AJNR. American journal of neuroradiology*, vol. 17, no. 10, pp. 1913–7.

Shapiro, SS & Wilk, MB 1965, 'An analysis of variance test for normality (Complete samples)', *Biometrika*, vol. 52, no. 3/4, pp. 591–611.

Shearer, WT, Pahwa, S, Read, JS, Chen, J, Wijayawardana, SR, Palumbo, P, Abrams, EJ, Nesheim, SR, Yin, W, Thompson, B & Easley, K a 2007, 'CD4/CD8 T-cell ratio predicts HIV infection in infants: the National Heart, Lung, and Blood Institute P2C2 Study.', *The Journal of allergy and clinical immunology*, vol. 120, no. 6, pp. 1449–56.

Shearer, WT, Rosenblatt, HM, Gelman, RS, Oyomopito, R, Plaeger, S, Stiehm, ER, Wara, DW, Douglas, SD, Luzuriaga, K, McFarland, EJ, Yogev, R, Rathore, MH, Levy, W, Graham, BL & Spector, SA 2003, 'Lymphocyte subsets in healthy children from birth through 18 years of age: the Pediatric AIDS Clinical Trials Group P1009 study.', *The Journal of allergy and clinical immunology*, vol. 112, no. 5, pp. 973–80.

Shen, L, Saykin, AJ, Kim, S, Firpi, H a, West, JD, Risacher, SL, McDonald, BC, McHugh, TL, Wishart, H a & Flashman, L a 2010, 'Comparison of manual and automated determination of hippocampal volumes in MCI and early AD.', *Brain imaging and behavior*, vol. 4, no. 1, pp. 86–95.

Silverstein, PS & Kumar, A 2013, 'HIV-1 and Alcohol: Interactions in the Central Nervous System.', *Alcoholism, clinical and experimental research*.

StatSoft Inc. 2012, *STATISTICA 11*, 11.

Strain, MC, Letendre, S, Pillai, SK, Russell, T, Ignacio, CC, Günthard, HF, Good, B, Smith, DM, Wolinsky, SM, Furtado, M, Marquie-Beck, J, Durelle, J, Grant, I, Richman, DD, Marcotte, T, McCutchan, JA, Ellis, RJ & Wong, JK 2005, 'Genetic composition of human immunodeficiency virus type 1 in cerebrospinal fluid and blood without treatment and during failing antiretroviral therapy.', *Journal of virology*, vol. 79, no. 3, pp. 1772–88.

Tae, WS, Kim, SS, Lee, KU, Nam, E-C & Kim, KW 2008, 'Validation of hippocampal volumes measured using a manual method and two automated methods (FreeSurfer and IBASPM) in chronic major depressive disorder.', *Neuroradiology*, vol. 50, no. 7, pp. 569–81.

Tamula, MAT, Wolters, PL, Walsek, C, Zeichner, S & Civitello, L 2003, 'Cognitive decline with immunologic and virologic stability in four children with human immunodeficiency virus disease.', *Pediatrics*, vol. 112, no. 3 Pt 1, pp. 679–84.

Tardieu, M, Brunelle, F, Raybaud, C, Ball, W, Pautard, B, Lachassine, E & Mayaux, M 2005, 'Cerebral MR Imaging in Uninfected Children Born to HIV-Seropositive Mothers and Perinatally Exposed to Zidovudine', no. April, pp. 695–701.

Tardieu, M, Le Chenadec, J, Persoz, a., Meyer, L, Blanche, S & Mayaux, M-J 2000, 'HIV-1-related encephalopathy in infants compared with children and adults', *Neurology*, vol. 54, no. 5, pp. 1089–1095.

Tate, DF, Khedraki, R, McCaffrey, D, Branson, D & Dewey, J 2011, 'The role of medical imaging in defining CNS abnormalities associated with HIV-infection and opportunistic infections.', *Neurotherapeutics : the journal of the American Society for Experimental NeuroTherapeutics*, vol. 8, no. 1, pp. 103–16.

Thompson, PM, Dutton, R a, Hayashi, KM, Lu, A, Lee, SE, Lee, JY, Lopez, OL, Aizenstein, HJ, Toga, AW & Becker, JT 2006, '3D mapping of ventricular and corpus callosum abnormalities in HIV/AIDS.', *NeuroImage*, vol. 31, no. 1, pp. 12–23.

Timmermans, S, Tempelman, C, Godfried, MH, Nellen, J, Dieleman, J, Sprenger, H, Schneider, ME, de Wolf, F, Boer, K & van der Ende, ME 2005, 'Nelfinavir and nevirapine side effects during pregnancy.', *AIDS (London, England)*, vol. 19, no. 8, pp. 795–9.

Tisdall, MD, Hess, AT, Reuter, M, Meintjes, EM, Fischl, B & van der Kouwe, AJW 2012, 'Volumetric navigators for prospective motion correction and selective reacquisition in neuroanatomical MRI.', *Magnetic resonance in medicine : official journal of the Society of Magnetic Resonance in Medicine / Society of Magnetic Resonance in Medicine*, vol. 68, no. 2, pp. 389–99.

Tornatore, C, Chandra, R, Berger, JR & Major, EO 1994, 'HIV-1 infection of subcortical astrocytes in the pediatric central nervous system.', *Neurology*, vol. 44, no. 3 Pt 1, pp. 481–7.

Tozzi, V, Balestra, P, Galgani, S, Narciso, P, Ferri, F, Sebastiani, G, D'Amato, C, Affricano, C, Pigorini, F, Pau, FM, De Felici, A & Benedetto, A 1999, 'Positive and sustained effects of highly active antiretroviral therapy on HIV-1-associated neurocognitive impairment.', *AIDS (London, England)*, vol. 13, no. 14, pp. 1889–97.

Venerosi, A, Calamandrei, G & Alleva, E 2002, 'Animal models of anti-HIV drugs exposure during pregnancy Effects on neurobehavioral development', *Progress in Neuro-Psychopharmacology*, vol. 26, pp. 747 – 761.

Violari, A, Cotton, MF, Gibb, DM, Babiker, AG, Steyn, J, Madhi, SA, Jean-Philippe, P & McIntyre, JA 2008, 'Early antiretroviral therapy and mortality among HIV-infected infants.', *The New England journal of medicine*, vol. 359, no. 21, pp. 2233–44.

Walot, I, Miller, BL, Chang, L & Mehringer, CM 1996, 'Neuroimaging Findings in Patients with AIDS', *Clinical Infectious Diseases*, vol. 22, no. 6, pp. 906–919.

WHO-UNAIDS 2010, *GLOBAL REPORT ON THE GLOBAL AIDS EPIDEMIC 2010*, 2010th edn, WHO librarary.

— 2013, *GLOBAL REPORT*, 2013th edn, WHO librarary.

Wiley, C a, Schrier, RD, Nelson, J a, Lampert, PW & Oldstone, MB 1986, 'Cellular localization of human immunodeficiency virus infection within the brains of acquired immune deficiency syndrome patients.', *Proceedings of the National Academy of Sciences of the United States of America*, vol. 83, no. 18, pp. 7089–93.

Wolters, PL, Brouwers, P, Civitello, L & Moss, HA 1997, 'Receptive and expressive language function of children with symptomatic HIV infection and relationship with disease parameters : a longitudinal 24-month follow-up study', no. June 1996, pp. 1135–1144.

Woods, RP 2005, *Multitracer Software*, 1, UCLA Laboratory of Neuroimaging, California.

Wrzolek, MA, Brudkowska, J, Kozlowski, PB, Rao, C, Anzil, AP, Klein, EA, Del Rosario, C, Abdu, A, Kaufman, L & Chandler, FW 1995, *Opportunistic infections of the central nervous system in children*

with HIV infection: report of 9 autopsy cases and review of literature., *Clinical neuropathology*, vol. 14, Department of Pathology, State University of New York Health Science Center, Brooklyn 11203, USA., no. 4, pp. 187–196.

Xia, C, Luo, D, Yu, X, Jiang, S & Liu, S 2011, 'HIV-associated dementia in the era of highly active antiretroviral therapy (HAART).', *Microbes and infection / Institut Pasteur*, vol. 13, Elsevier Masson SAS, no. 5, pp. 419–25.

Yazdanian, M 1999, 'Blood-brain barrier properties of human immunodeficiency virus antiretrovirals.', *Journal of pharmaceutical sciences*, vol. 88, no. 10, pp. 950–4.

Zhang, L, Yu, W, He, T, Yu, J, Caffrey, RE, Dalmasso, E a, Fu, S, Pham, T, Mei, J, Ho, JJ, Zhang, W, Lopez, P & Ho, DD 2002, 'Contribution of human alpha-defensin 1, 2, and 3 to the anti-HIV-1 activity of CD8 antiviral factor.', *Science (New York, N.Y.)*, vol. 298, no. 5595, pp. 995–1000.

APPENDICES: Ethnic Group Analysis

A limitation of the present study relates to sampling. Upon reviewing the sample demographics, it became apparent that ethnicity and sex of participants needed further investigation to test for possible confounding effects.

Ethnicity as a possible confounding factor

Table A.1 Number of children per ethnic group in each diagnostic group

	Diagnostic Group				
	Uninfected	HIV-1 infected			
	controls	ART-Def	ART-40W	ART-96W	Total
Sample	n (%)	n (%)	n (%)	n (%)	n (%)
Cape Coloured	9 (11.5)	0 (0)	1 (1.3)	1 (1.3)	11 (14.1)
Xhosa	18 (23.1)	17 (21.8)	16 (20.5)	16 (20.5)	67 (85.9)
Total	27 (34.6)	17 (21.8)	17 (21.8)	17 (21.8)	78 (100)

There were only 11 (14.1%) Cape Coloured children within the sample. Most of these children were uninfected controls with only two being HIV-1 infected. There were no Cape Coloured children in the deferred treatment group and only one in each of the early treatment arms. In contrast, the representation of Xhosa children in each of the groups was nearly equal. The vast majority of the infected children were Xhosa. A Chi-square test revealed that the number of participants in each diagnostic group differed significantly between ethnic groups (χ^2 (one, N=78) =6.20, p=0.013).

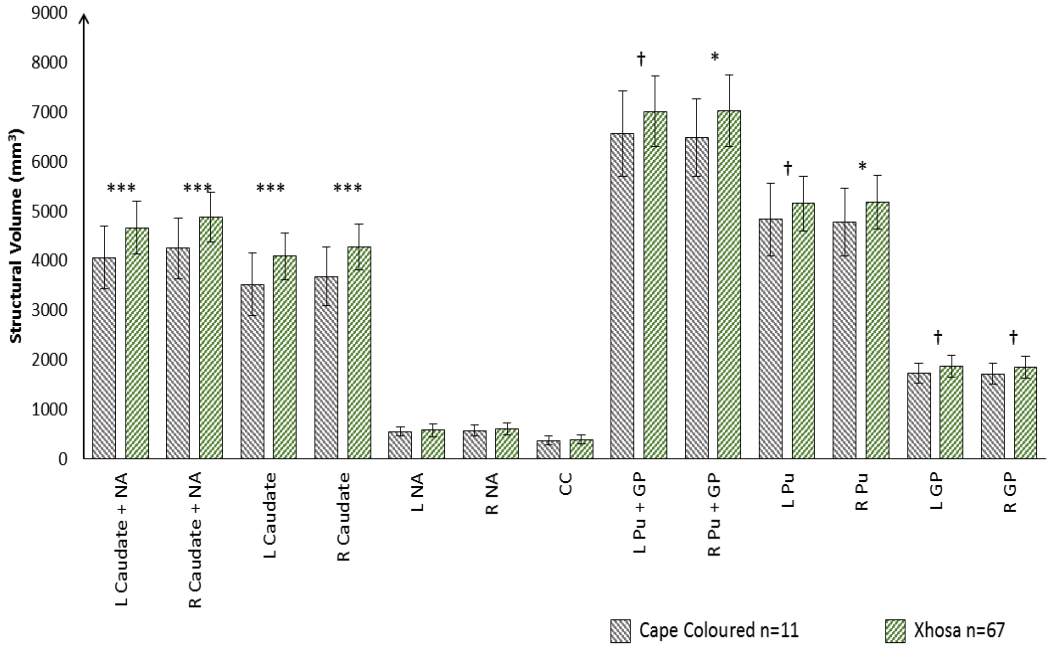

Figure A.1 Structural volumes between ethnic groups
† $p < 0.1$, * $p < 0.05$, *** $p < 0.001$

Figure A.1 shows means and standard deviations of structural volumes between children from different ethnic groups.

Volumes are larger in Xhosa children compared to Cape Coloured children bilaterally in the caudate and the right Pu, causing total volumes for the caudate + NA bilaterally and right lentiform nucleus to also be larger.

Comparisons for the volumes of structures between uninfected Cape Coloured and uninfected Xhosa control participants were investigated. Significant differences in structural volumes of the left caudate ($F(1,25)=10.19$; $p=0.004$) and right caudate ($F(1,25)=10.92$; $p=0.003$) and corpus callosum ($F(1,25)=13.06$; $p<0.001$) were observed.

Ethnicity meets the criteria of a confounding factor. Ethnicity has been shown to be associated with both the outcome and exposure variable. Ethnicity also does not occur as a direct result of the exposure variable. Due to the potential confounding effects of ethnicity on structural brain volumes, and the fact that the Treatment groups are not well matched for ethnicity, we removed the Cape Coloured children from all further analyses.